

Analysis of plasma chemokines and circulating tumour cells in
colorectal and breast cancer patient peripheral blood.

by

Deep Patel

A thesis
presented to the University of Waterloo
in fulfillment of the
thesis requirements for the degree of
Doctor of Philosophy
in
Pharmacy

Waterloo, Ontario, Canada, 2019

©Deep Patel 2019

Examining Committee Membership

The following members served on the Examining Committee for this thesis:

| | |
|--------------------------|---|
| External Examiner | Dr. Alison L. Allan Professor, Departments of Anatomy & Cell Biology and Oncology, Schulich School of Medicine and Dentistry, Western University |
| Supervisor | Dr. Jonathan Blay Professor, School of Pharmacy, University of Waterloo |
| Committee Member | Dr. Mariana Foldvari Professor, School of Pharmacy, University of Waterloo |
| Committee Member | Dr. Brenda L. Coomber Professor, Department of Biomedical Sciences, University of Guelph |
| Internal-External Member | Dr. Mungo Marsden Associate Professor, Department of Biology, University of Waterloo |

Author's declaration

I hereby declare that I am the sole author of this thesis. This is a true copy of the thesis, including any required final revisions, as accepted by my examiners.

I understand that my thesis may be made electronically available to the public.

Abstract

Circulating tumour cells (CTCs) provide a prognostic value in solid tumours including colorectal and breast. Enumeration of tumour cells from blood is becoming a common practice in informing prognosis and may guide therapy decisions. Enumeration alone does not capture heterogeneity of tumours and varying functional abilities of the CTCs to interact with the secondary microenvironment. Characterizing the isolated CTCs and assessing their functional abilities can track molecular changes in the disease progress. As a step toward identifying functional features of CTCs that could aid in clinical decisions, this study was aimed at analyzing chemokine release profile in drug resistance and developing a CTC isolation technique based on extracellular matrix interactions.

Cancer cells release different chemokines and express chemokine receptors which together work to direct cell infiltrates in the tumour microenvironment. This work examined changes in the profile of chemokine release using a model of drug resistance based on the colorectal cancer cell line HT29 and its counterpart HT29-R that is resistant to the late-stage chemotherapy drug irinotecan (SN-38). Following an initial screening of mRNA expression through PCR and qPCR, five of the chemokines (CCL2, CCL15, CXCL8, CXCL12, and CCL20) were analyzed further for their release patterns amongst cell lines and peripheral blood of healthy volunteers and stage IV colorectal and breast cancer patients. The release pattern of chemokines in patient samples differed from the results of the *in vitro* drug-resistance model. Specific tumour location, previous therapies, and genetic variability are all examples of the factors that may provide unique patterns and complicate modelling for chemokine release in late-stage cancer. A detailed analysis revealed an upward trend for midkine (NEGF2) when baseline and 12 months plasma samples were compared. Migration studies may further reveal the consequences of this expression profile. Migration assays were carried out with Transwell® chambers and HepG2 cells to partially mimic the hepatic microenvironment. Such studies can guide future functional studies for isolated CTCs.

We next sought to investigate extracellular matrix protein interactions, which might depend on a changing chemokine milieu. We utilized cancer cells' ability to adhere to extracellular matrix and created a platform to isolate CTCs from the peripheral blood samples. A total of 14 colorectal and 7 breast cancer patients donated blood samples. Adhesion assays were performed with a range of different ECM proteins. We identified an optimal ECM substratum composed of collagen and fibronectin at a mass coating ratio of 2:1. The isolated CTCs were identified through immunofluorescence with epithelial marker antibodies (EpCAM and pan-cytokeratin). Identification of CTCs was further confirmed by exclusion with a hematopoietic origin marker CD45. The captured number of cells ranged from 0 to 296, whereas the mean number was 26 and the median was 22 per patient sample (~8mL). This technique not only allows enumeration, but also isolates cells based on a functional approach. The isolated cells are successful in adhering to extracellular matrix proteins and can be further characterized through functional markers.

Overall, this study addresses two unique functional features of CTCs – their expression of certain chemokines and their ability to interact with both fibronectin and collagen - that form the basis to provide future clinical utility. Such an approach will help to inform clinicians about the aggressive nature of an individual tumour and guide treatment decisions toward best prognostic outcomes.

Acknowledgements

I would like to acknowledge the utmost support from my supervisor and mentor, Dr. Jonathan Blay who helped me throughout this program and provided many opportunities to understand the research world. None of this would have been possible without him. He is a great mentor not only for the academic world, but also in a personal and professional life.

My advisory committee members Dr. Mariana Foldvari, Dr. Brenda Coomber, and Dr. Paul Spagnuolo shared their wisdom in shaping my project and spending their precious time to address my progress on a routine basis. Dr. Allison Allan helped strengthened my thesis and served as an external committee member.

Dr. Murray Cutler trained me in the lab and I had further help from my colleague Spencer Berg. I have learned a great deal from both and their knowledge and passion in science drove me further. Elena Kreinin helped me in the beginning days to understand the lab routine.

My laboratory colleagues Julia Fux, Bogdan Diaconu, Alex Durocher, Heather Dekker, and Hayden Huh created a positive working environment, shared important feedback, and suggested interesting ideas that helped this project. I really appreciate all of your help, whether it is through donation of blood samples, picking up patient samples from the hospital, or just having conversations that kept us balanced. Outside of the Blay laboratory, I would like to acknowledge Anil, Lokesh, Roger, Monica, Gokul and Paul who provided advise and insight at different points in this journey, especially when I was lost and needed a second opinion. I am really grateful to Michael Collins, Mala Bahl, Mario Valdes, and the clinical trials team at Grand River Hospital.

I thank the two research organizations, Canadian Institutes of Health Research (CIHR), and NSERC (Natural Sciences and Engineering Research Council of Canada) who provided funding for this work.

My parents, and grandparents – I dedicate this work to you and bow down in respect. It was worth driving 150 km daily to catch a glimpse of you all. Last but not the least, a special shout out to my friend, my soulmate, and my life-partner Prachi Shah Patel who loved, and cared for me selflessly and stood by in an unwavering manner.

Table of Contents

| | |
|--|-------------|
| EXAMINING COMMITTEE MEMBERSHIP | ii |
| AUTHOR'S DECLARATION | iii |
| ABSTRACT | iv |
| ACKNOWLEDGEMENTS..... | v |
| LIST OF FIGURES | viii |
| LIST OF TABLES | ix |
| LIST OF ABBREVIATIONS..... | x |
| 1. INTRODUCTION | 1 |
| 1.1 COLORECTAL CANCER | 1 |
| 1.2 JOURNEY TO METASTASIS..... | 1 |
| 1.3 TREATMENT CHOICES AND DRUG RESISTANCE | 6 |
| 1.4 IMPORTANCE OF EXTRACELLULAR MATRIX | 7 |
| 1.5 MICROENVIRONMENT AT SECONDARY SITES..... | 8 |
| 1.6 RATIONALE OF THIS RESEARCH | 9 |
| 1.7 PURPOSE, GOAL AND HYPOTHESIS OF THIS RESEARCH | 10 |
| 1.8 SPECIFIC EXPERIMENTAL OBJECTIVES | 11 |
| 2. CHEMOKINES AND THEIR POTENTIAL ROLES IN COLORECTAL CANCER CELL LINES..... | 12 |
| 2.1 BACKGROUND..... | 12 |
| 2.1.1 Chemokines..... | 12 |
| 2.1.2 Functional considerations in migration | 22 |
| 2.2 MATERIALS AND METHODS | 26 |
| 2.2.1 Cell Culture..... | 26 |
| 2.2.2 Generation of Drug Resistant Cell Lines..... | 27 |
| 2.2.3 Polymerase Chain Reaction | 28 |
| 2.2.4 Chemokine Arrays..... | 34 |
| 2.2.5 Immunostaining Chemokines | 35 |
| 2.2.6 Migration assays: Transwell® | 36 |
| 2.2.6 Statistical Analysis | 38 |
| 2.3 RESULTS..... | 39 |
| 2.3.1 A panel of chemokines show definitive gene level changes in the drug-resistant cells | 39 |
| 2.3.2 Potential chemokine markers confirmed through qRT-PCR method | 42 |
| 2.3.3 Expression of CXCL12 identified on HT29 and HCT116 cells via immunofluorescence..... | 45 |
| 2.3.4 Secreted chemokines depict unique changes in drug-resistant HT29 cells. | 51 |
| 2.3.5 Preliminary migration studies that assess microenvironmental effects of chemokines | 55 |
| 2.4 DISCUSSION | 59 |
| 3. CHEMOKINES AND THEIR ANALYSIS IN PLASMA OF COLORECTAL AND BREAST CANCER PATIENTS . | 63 |
| 3.1 BACKGROUND | 63 |
| 3.2 MATERIALS AND METHODS | 65 |
| 3.2.1 Coordination of blood sample procurement..... | 65 |
| 3.2.2 Array Analysis | 66 |
| 3.2.3 Statistical analysis and patient characteristics..... | 66 |
| 3.3 RESULTS..... | 66 |

| | |
|---|------------|
| 3.4 DISCUSSION | 73 |
| 4. CAPTURING CIRCULATING TUMOUR CELLS FROM COLORECTAL AND BREAST CANCER PATIENTS.... | 76 |
| 4.1 BACKGROUND | 76 |
| 4.2 MATERIALS AND METHODS | 83 |
| 4.2.1 <i>Separating different components of the blood</i> | 83 |
| 4.2.2 <i>Adhesion Assays</i> | 85 |
| 4.2.3 <i>Optimizing the ECM composition for circulating tumour cell capture</i> | 87 |
| 4.2.4 <i>Spiking Experiments</i> | 87 |
| 4.2.5 <i>Immunostaining of CTCs</i> | 88 |
| 4.3 RESULTS..... | 91 |
| 4.3.1 <i>Technique development to capture circulating tumour cells</i> | 91 |
| 4.3.2 <i>Identification of the recovered circulating tumour cells from patient samples</i> | 111 |
| 4.4 DISCUSSION | 114 |
| 5. OVERALL DISCUSSION: CHALLENGES IN STUDYING CHEMOKINES AND THEIR RELEVANCE TO THE BEHAVIOUR OF CIRCULATING TUMOUR CELLS..... | 120 |
| 5.1 THE KEY FINDINGS OF THIS RESEARCH | 120 |
| 5.1.1 <i>Drug resistance, chemokines, and migration studies</i> | 120 |
| 5.1.2 <i>Linking chemokines in patient plasma with disease progression</i> | 120 |
| 5.1.3 <i>Capture platform for Circulating Tumour cells</i> | 121 |
| 5.2 CONSIDERATIONS IN INTERPRETATION AND FUTURE DIRECTIONS | 121 |
| 5.3 LIMITATIONS OF THIS RESEARCH | 123 |
| 6. REFERENCES | 125 |
| 7. APPENDICES | 140 |
| APPENDIX IA: COORDINATES AND NAMES OF CHEMOKINES FOR THE ARY017 – HUMAN CHEMOKINE ARRAY KIT ARY017..... | 140 |
| APPENDIX IB: COORDINATE GUIDE FOR CHEMOKINE ARRAY KIT ARY017 – R&D SYSTEMS. | 141 |
| APPENDIX II: RAW IMAGES OF THE RT-PCR RESULTS | 142 |
| APPENDIX III: COMPARISON OF DIFFERENT TRANSWELL CHAMBERS | 155 |
| APPENDIX IV: TRACKING FOR CHEMOKINE ARRAY SAMPLES | 156 |
| APPENDIX V: RAW ANALYSIS PLOTS OF INDIVIDUAL PATIENTS AT 0 AND 12 MONTHS | 157 |
| APPENDIX VI: COPY OF THE APPROVED ETHICS PROTOCOL CONFIRMATIONS..... | 159 |

List of Figures

| | |
|---|-----|
| FIGURE 1 GENERAL OVERVIEW OF THE METASTATIC PROCESS IN SOLID CANCERS. | 3 |
| FIGURE 2 ILLUSTRATION OF STEPWISE PROGRESS IN COLORECTAL CANCER AND INVASION THROUGH THE SUCCESSIVE LAYERS OF COLON WALL..... | 4 |
| FIGURE 3 STEPWISE CHANGES IN THE NORMAL COLON EPITHELIUM AS A RESULT OF GENETIC CHANGES. | 5 |
| FIGURE 4 THE COMPLEX NETWORK OF CHEMOKINE AND CHEMOKINE RECEPTORS. | 13 |
| FIGURE 5 PATHWAY FOR HOW CCL2 EXERTS ITS ACTION IN TRANSENDOTHELIAL MIGRATION..... | 16 |
| FIGURE 6 ILLUSTRATION OF THE ENTRY POINTS AND ARRANGEMENT OF LIVER MICROENVIRONMENT. | 23 |
| FIGURE 7 STEPWISE PROCESS DEPICTING THE GENERATION OF DRUG-RESISTANT CELL LINE SHOWING THE CONCENTRATIONS AND TIMES OF SUCCESSIVE INCREASING EXPOSURE TO THE DRUG SN-38..... | 27 |
| FIGURE 8 SET UP FOR MIGRATION EXPERIMENTS..... | 38 |
| FIGURE 9 COMPARISON OF CHANGES IN CHEMOKINE AND CHEMOKINE RECEPTOR GENE EXPRESSION WITHIN TWO PARENTAL AND RESISTANT CRC LINES..... | 40 |
| FIGURE 10 CHANGES IN CHEMOKINE GENE EXPRESSION BETWEEN HT29 AND HT29-R CELLS. | 43 |
| FIGURE 11 EXPRESSION OF EPITHELIAL MARKER EpCAM ON HT29 CELLS. | 46 |
| FIGURE 12 REPRESENTATIVE IMAGES SHOWING THE EXPRESSION OF EPITHELIAL MARKER EpCAM ON HCT116 CELLS. | 47 |
| FIGURE 13 IMMUNOFLUORESCENCE STAINING OF HT29 CELLS FOR CXCL12 CHEMOKINE. | 49 |
| FIGURE 14 IMMUNOFLUORESCENCE STAINING OF HCT116 CELLS FOR CXCL12 CHEMOKINE..... | 50 |
| FIGURE 15 REPRESENTATIVE IMAGE FOR CHEMOKINE ARRAY OF CONDITIONED MEDIA FROM HT29 AND HT29-R CELLS. | 52 |
| FIGURE 16 CC GROUP OF CHEMOKINES RELEASED IN THE CONDITIONED MEDIA OF CRC CELL LINE HT29 AND ITS DRUG-RESISTANT COUNTERPART HT29-R. | 53 |
| FIGURE 17 CXC GROUP OF CHEMOKINES RELEASED IN THE CONDITIONED MEDIA OF CRC CANCER CELL LINE HT29 AND ITS DRUG-RESISTANT COUNTERPART HT29-R. | 54 |
| FIGURE 18 REPRESENTATIVE FIGURES FROM 3 INDEPENDENT EXPERIMENTS SHOWING THE ABILITY OF CRC CELLS TO MIGRATE..... | 56 |
| FIGURE 19 A & B CHEMOKINE ARRAY OF HEPG2 CELLS' CONDITIONED MEDIA FROM THREE INDEPENDENT EXPERIMENTS..... | 58 |
| FIGURE 20 RELATIVE COMPARISON OF PLASMA CHEMOKINES AMONGST HEALTHY VOLUNTEERS, CRC AND BREAST CANCER PATIENTS. | 71 |
| FIGURE 21 CHANGES IN PLASMA MIDKINE LEVEL AMONG SIX PATIENTS WITH DISEASE PROGRESSION AT 12 MONTHS. | 72 |
| FIGURE 22 SEPARATION OF BLOOD COMPONENTS USING THE POLYSACCHARIDE MEDIUM FICOLL®..... | 84 |
| FIGURE 23 A REPRESENTATIVE SET OF PICTURES FROM A PATIENT BLOOD SAMPLE (GRCC014) PROCESSED THROUGH FICOLL®..... | 85 |
| FIGURE 24 SCHEMATIC OF THE ADHESION ASSAY SET-UP, VARIOUS ECM PROTEINS AND CONCENTRATIONS. | 86 |
| FIGURE 25 SCHEMATIC OF THE CELL-COUNTING PATTERN FOR SPIKING STUDIES AND PATIENT CTCs..... | 89 |
| FIGURE 26 ADHESION OF HT29 AND HT29-R CELLS ON COMMERCIAL ECM GEL..... | 93 |
| FIGURE 27 ADHESION OF HT29 AND HT29-R CELLS ON TWO TYPES OF COLLAGEN..... | 94 |
| FIGURE 28 ADHESION OF HT29 AND HT29-R CELLS ON TWO TYPES OF FIBRONECTIN..... | 95 |
| FIGURE 29 ADHESION OF HT29 AND HT29-R CELLS ON THE MURINE LAMININ..... | 96 |
| FIGURE 30 INCREASED ECM PROTEIN CONCENTRATIONS LEADS TO AN IMPROVED CAPTURE EFFICIENCY. | 98 |
| FIGURE 31 RECOVERY OF SPIKED CANCER CELLS FROM WHOLE BLOOD USING DENSITY GRADIENT MEDIUM FICOLL® AND OPTIPREP®..... | 100 |
| FIGURE 32 RECOVERY FROM SPIKED BLOOD SAMPLES USING FICOLL® MEDIUM. | 102 |
| FIGURE 33 SPIKED AND RECOVERED HCT116 CELLS FROM PERIPHERAL BLOOD SAMPLE..... | 104 |
| FIGURE 34 SPIKED AND RECOVERED HCT116 CELLS FROM PERIPHERAL BLOOD SAMPLE..... | 106 |
| FIGURE 35 CMFDA STAINED HCT116 CELLS SPIKED IN BLOOD AND RECOVERED..... | 107 |
| FIGURE 36 EXAMPLE OF A RECOVERED HT29 CELL SHOWING POSSIBLE SCREENING OF MULTIPLE MARKERS ON A SINGLE CELL..... | 108 |
| FIGURE 37 RECOVERED CTC EXAMPLE FROM PATIENT SAMPLE GRCC019..... | 111 |
| FIGURE 38 RECOVERED CTC EXAMPLE FROM PATIENT GRCC017..... | 112 |
| FIGURE 39 RECOVERED CTC FROM PATIENT GRCC016..... | 113 |

List of Tables

| | |
|--|-----|
| TABLE 1 LIST OF POTENTIAL CHEMOKINES AND CHEMOKINE RECEPTORS INVOLVED IN CRC METASTASIS AND DISEASE PROGRESSION..... | 21 |
| TABLE 2 REACTION SET-UP FOR THE ENDPOINT PCR WHERE THE FORWARD AND REVERSE PRIMERS ARE AT RESULTING CONCENTRATION OF 200NM EACH..... | 30 |
| TABLE 3 THERMOCYCLER PROGRAM SET UP FOR PCR..... | 30 |
| TABLE 4 THE PRIMERS FOR CHEMOKINES AND THEIR CORRESPONDING RECEPTOR PAIRS THAT WERE SCREENED WITH RT-PCR..... | 31 |
| TABLE 5 SUMMARY OF GENE EXPRESSION CHANGES FOR CHEMOKINES AND RECEPTORS BETWEEN HT29 AND HT29-R CELLS..... | 41 |
| TABLE 6 TRENDS OBSERVED FOR CHEMOKINE GENE EXPRESSION BETWEEN HT29 AND HT29-R CELLS..... | 42 |
| TABLE 7 HEPG2 CONDITIONED MEDIA ARRAY: TRENDS OBSERVED BASED ON THE VISUAL SPOT INTENSITY..... | 59 |
| TABLE 8 DISTRIBUTION OF PATIENTS BASED ON TUMOUR TYPE AND METASTATIC LOCATION..... | 66 |
| TABLE 9 INCREASED RECOVERY OF CTCs FROM PATIENT BLOOD USING A PROGRESSIVELY REFINED TECHNIQUE BASED UPON CAPTURE BY ADHERENCE TO ECM..... | 110 |

List of abbreviations

| | |
|----------------|---|
| ABC | ATP-binding cassette |
| APC | Adenomatous polyposis coli |
| BBB | Blood brain barrier |
| BCRP | Breast cancer resistance protein |
| C-Met | Tyrosine-protein kinase Met |
| cDNA | Complementary DNA |
| CEA | Carcinoembryonic antigen |
| CRC | Colorectal cancer |
| ctDNA | Circulating tumour DNA |
| DEPC | Diethylpyrocarbonate |
| DNA | Deoxyribonucleic acid |
| dNTP | Deoxynucleotide triphosphates |
| ECM | Extracellular matrix |
| EGFR | Epidermal growth factor receptor |
| EMT | Epithelial to mesenchymal transition |
| EtBr | Ethidium bromide |
| GPCR | G-protein coupled receptor |
| HER-2 | Human epidermal growth factor receptor 2 |
| HSC | Hepatic stellate cells |
| HSEC | Hepatic sinusoidal endothelial cells |
| KRAS | Kirsten rat sarcoma (oncogene) |
| LOH | Loss of heterozygosity |
| M-MLV | Moloney murine leukemia virus |
| MALT | Mucosa associated lymphoid tissue |
| MDSC | Myeloid derived suppressor cell |
| MET | Mesenchymal to epithelial transition |
| MMP | Matrix metalloproteinase |
| NF- κ B | Nuclear factor kappa B |
| P-gp | P-glycoprotein |
| PBMC | Peripheral blood mononuclear cell |
| PCR | Polymerase chain reaction |
| PFA | Paraformaldehyde |
| PI3KCA | Phosphatidylinositol 3-kinase |
| RANTES | Regulated on activation, normal T cell expressed and secreted |
| RBC | Red blood cell |
| RNA | Ribonucleic acid |
| SDF-1 | Stromal-cell derived factor 1 |
| STAT3 | Signal transducer and activator of transcription 3 |
| TAN | Tumour associated neutrophils |
| TEM8 | Tumour endothelial marker 8 |
| TNM | Tumour Node Metastases |
| TP53 | Tumour protein 53 |
| Trop2 | Trophoblast cell surface antigen 2 |
| VCAM-1 | Vascular cell adhesion molecule-1 |
| VGEF | Vascular endothelial growth factor |

1. Introduction

1.1 Colorectal Cancer

Globally, it is expected that colorectal cancer (CRC) will inflict 2.2 million new cases and 1.1 million deaths by 2030¹. The incidence and mortality vary in different countries, however, of the three groups divided based on temporal pattern, Canada falls in the group with increasing incidence and decreasing mortality¹. On average 73 Canadians were diagnosed with CRC every day in 2017². Colorectal cancer is the second leading cause of death from cancer in men and the third leading cause of death from cancer in women in Canada. About 20% of diagnosed CRC cases are at stage IV and this poses a significant challenge in terms of treatment². Ontario offers a free CRC screening program for adults between the age of 50 and 74 years³. Such screening programs help detect cases at an earlier stage and help reduce mortality rates. Factors such as family history, inflammatory bowel disease, and height are amongst the non-modifiable risk factors that affect many individuals⁴. However, consumption of red meat, alcohol and lack of fibre in the diet are examples of modifiable risk factors that increase the risk of CRC^{4,5}. From the pathological perspective, the disease presentation and location may vary between individuals. In the majority of patients, it occurs in the colon which is the longest part of the large intestine, however, 30% of the time, it occurs in the rectum². It is interesting to note that cancers originating in the colon have a higher chance of liver metastasis, whereas those originating in rectum have a higher incidence of lung metastasis^{6,7}.

1.2 Journey to Metastasis

It is estimated that 90% of human cancer deaths are caused by tumour invasion and metastasis^{8,9}. Acquisition of drug resistance and changes in the microenvironment can potentially help create a favourable niche for cells to develop an invasive phenotype^{10,11}. It is believed that

within the primary growth of a tumour, there might be localized invasive areas where certain tumour cells can undergo de-differentiation¹². During this process, the epithelial cells in the solid tumour lose their apical-basal polarity, detach from neighbouring cells, change morphologically to resemble fibroblasts and invade through the surrounding stroma (Figure 1). This is called epithelial to mesenchymal transition (EMT). As a result of the cells breaking through the different layers of the colon wall layers (Figure 2), they move closer to the blood vessels. The process of cells gaining entry into the blood circulation is defined as intravasation. The entry into the bloodstream poses a challenge of survival for tumour cells against attack by the immune system and shear forces in the general blood circulation. Those that succeed in surviving can initially be trapped physically in capillaries or blood vessels of distant secondary tissues such as the liver¹³. Here, they have numerous interactions with local vascular endothelium in an attempt to gain access into the tissue and this can lead to micrometastasis¹⁴. Exit into the secondary tissue space is known as extravasation. Tumour cell fate is also dependent on its specific interactions with endothelial cells and the surrounding microenvironment^{15,16}. Many groups have shown that during metastatic dissemination, cancer cells can extravasate into the surrounding tissues as single cells or collectively as a group¹⁷⁻²⁰.

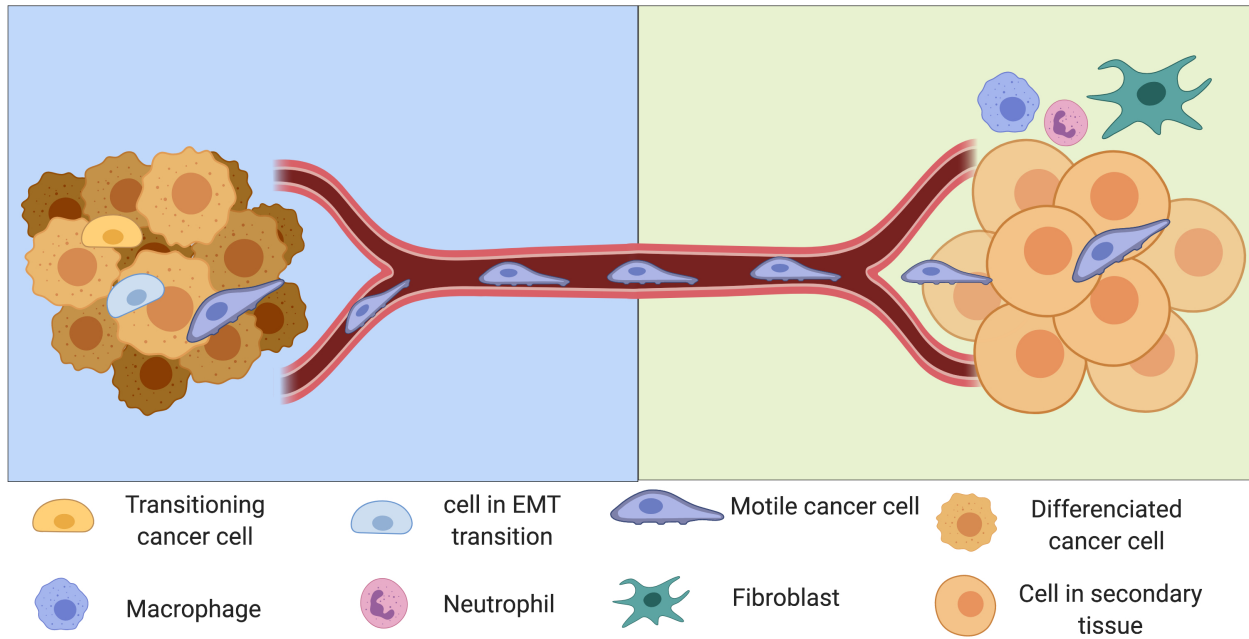


Figure 1 general overview of the metastatic process in solid cancers. A schematic diagram of cells undergoing epithelial to mesenchymal transition (EMT), circulation into the bloodstream and the reverse process of mesenchymal to epithelial transition (MET) required for distant site metastases (adapted from Friedlander et.al.)²¹ Created with Biorender[©].

Transformation of a normal epithelial cell into a cancerous cell is an extensive process through multiple genetic mutations over several years. Key driver genes that are associated with the development of this cancerous phenotype in CRC are APC²², KRAS²³, BRAF²⁴, PIK3CA²⁵, SMAD4²⁶, and p53^{27,28}. Figure 3 below demonstrate how colon cells from normal epithelium can be affected through different genetic changes leading to cancer.

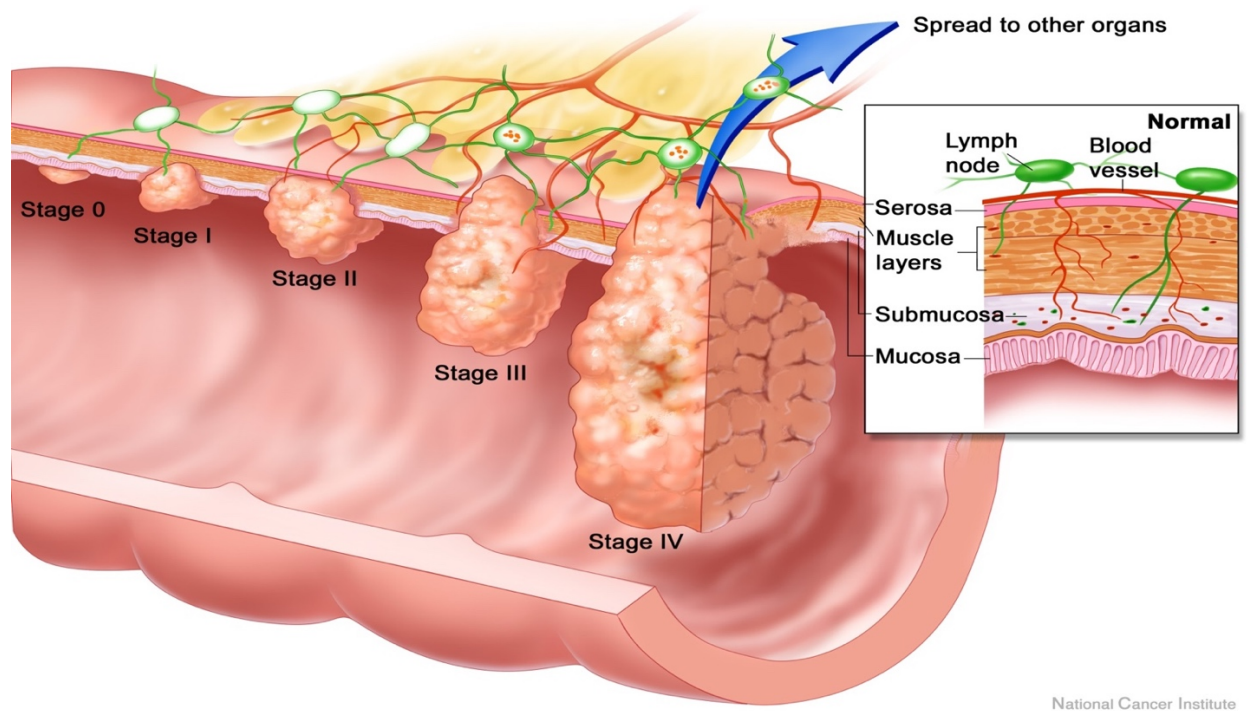


Figure 2 Illustration of stepwise progress in colorectal cancer and invasion through the successive layers of colon wall²⁹

Hanahan and Weinberg first defined the six hallmarks of cancer in 2000³⁰ followed by an addition of two new hallmarks³¹ to complete our understanding of what defines cancer. It is these unique characteristics that separate a cancerous cell from a normal cell – being able to resist cell death, induce proliferative signalling, gain immortal replication potential, reprogram energy metabolism, induce angiogenesis, evade the immune system and growth suppressors, and activate invasion and metastases³¹. A cell lineage that has gone through successive genotypic and phenotypic transformations can yield an immortal cancerous cell with the characteristics listed above³². As a result of the continuous replicative potential and other hallmark characteristics, colonies of a cancerous cell are able to grow in the local environment. Where a colony of cancerous cells is confined in a limited local area, it is referred to as carcinoma-in-situ³³. The confined boundary acts as a rate-limiting step in the transformation towards a malignant form of the disease.

It is possible that the capabilities to activate invasion and metastasize are gained in the later stage following various local environmental changes²⁰. Once these abilities are gained, cells can innervate different layers of the colon starting from the apical side.

The stepwise invasion through different layers of the colon is demonstrated in Figure 2 and the time period between each progressive step is illustrated by Figure 3. Cancerous cells from the abnormal growth or polyp that arises from the epithelium pass through the mucosa, submucosa, muscle layers, and serosa in order to spread to other organs or gain access to the lymphatic network or general circulation²⁹.

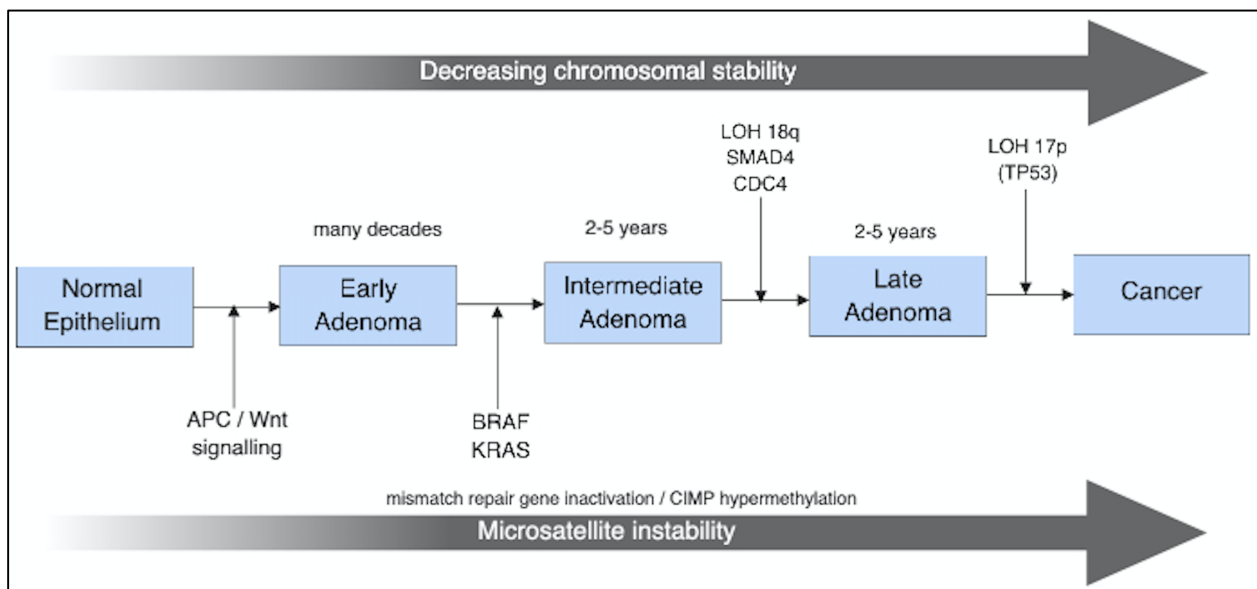


Figure 3 Stepwise changes in the normal colon epithelium as a result of genetic changes. (modified from ²⁸); APC: adenomatous polyposis coli; LOH: loss of heterozygosity. Created with Biorender[©]

1.3 Treatment choices and drug resistance

Chemotherapy, surgery, radiation, and targeted therapies are mainstays of CRC treatment³⁴. They are many times used in combination and the treatment approach varies depending on the ‘TNM’ staging of cancer. TNM stands for tumour, node, and metastasis, and is a system developed by the American Joint Committee on Cancer that is based on the depth of invasion in the bowel wall, the involvement of the surrounding lymph nodes, and presence of disease at distant sites³⁵.

Chemotherapy holds an important place in the treatment of CRC, and the three frontline chemotherapeutic drugs utilized in the treatment of CRC are 5-fluorouracil, oxaliplatin, and irinotecan^{36,37}. 5-fluorouracil was a drug discovered in the 1950s which was used as a monotherapy for a few decades until the advent of oxaliplatin and irinotecan³⁶. There have been significant improvements in the overall survival rates following the addition of these agents available for combination treatment³⁸. The availability of monoclonal antibody therapeutics bevacizumab (an antibody against vascular endothelial growth factor, VEGF) and Cetuximab (an antibody against the epidermal growth factor receptor, EGFR) marked a new era of targeted therapies and further improved survival rates in metastatic settings³⁹.

Cells have acquired various resistance mechanisms to cytotoxic therapies in CRC^{40,41}. The general mechanisms of resistance include decreased drug uptake, active efflux out of the cell, and changes in the enzymes involved in drug metabolism^{41,42}. For instance, a major mechanism for 5-fluorouracil resistance is believed to be increased expression of thymidylate synthase. Thymidylate synthase is an enzyme that mediates the conversion of deoxyuridine monophosphate to deoxythymidine monophosphate and plays an essential role in DNA biosynthesis^{43,44}. Whereas for irinotecan, overexpression of ATP-binding cassette (ABC) transmembrane transporters P-

glycoprotein (P-gp) and multi-drug resistance associated protein (MRP) are considered to be responsible for its resistance mechanism⁴⁵. These proteins are able to facilitate the efflux of irinotecan from the cells. There have been *in vivo* studies showing that the deletion of P-gp in mice decreased the biliary clearance of irinotecan by half⁴⁶. In addition, the breast cancer resistance protein (BCRP) is another common factor in the resistance mechanism for irinotecan. BCRP inhibitor GF120918 reversed the resistance effectively at 100nM in an *in vitro* breast cancer model⁴⁵. Similar to P-gp, BCRP is also a protein involved in the efflux of irinotecan out of the cells⁴⁷. Gradual changes in the genetic and epigenetic profile of originating cancer can also bring about drug resistance⁴⁸. A study by Lee *et.al.* demonstrated how the treatment of ovarian cancer cell lines with cisplatin, doxorubicin, and paclitaxel transiently increased CXCR4^{high}/CD24^{low} stem cell population and led to acquired drug resistance with sequential treatments⁴⁹. In clinical settings, drug resistance to chemotherapy as well as monoclonal antibody is commonly encountered and limits treatment options in the late stage therapy^{42,50,51}.

1.4 Importance of Extracellular Matrix

In order to progress along this pathway of metastasis, tumour cells first have to pass through a mesh-like proteinaceous network called the extracellular matrix (ECM)⁵². Some important molecules in the ECM are collagen, fibronectin, laminin, and hyaluronic acid⁵³. These structural and functional components of the ECM are recognized by receptors on the cell membrane such as integrins and CD44⁵⁴. Through modification of these interactions, and the phenomenon that tumour cells can restructure or degrade the ECM⁵⁵, invasive cells can proceed towards the site of intravasation. It is known that the breakdown and reorganization of ECM is an important factor for tumour cells to invade through the general tissue matrix and to cross basement membranes⁵⁶. Additionally, interactions of tumour cells with the endothelium are crucial at both steps during

intravasation⁵⁷ and extravasation⁵⁸. Consequently, changes in these processes may alter the overall rate of metastasis.

Increased ECM production and reduced ECM turnover rate are common in organ fibrosis during cancer progression⁵⁹. As well, a study by Barbazán *et.al.* demonstrated how interaction of colon cancer cells at the liver endothelium was facilitated by adhesion to vascular fibronectin⁶⁰. The ECM is thus a critical part of the process by which cancer progresses.

1.5 Microenvironment at Secondary Sites

Interactions at the secondary tissue microenvironment play a critical role in the establishment of metastases of solid tumours⁶¹. Principal sites of metastasis for a majority of solid tumours are lungs, liver, bones and brain⁶². Recent research has emphasized the importance of the interactions between the disseminated tumour cells and the cells of the microenvironment at these secondary sites⁶¹. There is heterogeneity in the microenvironment composition of these various tissues which may preferentially favour certain cells over others. Varying composition of extracellular matrices, the arrangement of endothelial cells and pericytes, a variety of immune system cells, and fenestrations within the endothelium provide different challenges and opportunities for tumour cells arriving at these locations. Tissue-specific cells such as astrocytes in the brain, alveolar cells in the lungs, and Kupffer cells in the liver also add to the complexity of microenvironment at these sites. It is believed that cells from late-stage disease adapt to the secondary microenvironment differently than those from the primary stage⁶³. They may be able to adhere, invade, survive and even proliferate better depending on the interactions that take place. It is these functional and behavioural differences that can be utilized in selectively trapping the invasive circulating tumour cells (CTCs) from peripheral blood.

The organ-specific interactions are complex and it is important to understand the microenvironmental processes that cancer cells encounter. It is evident from the literature that drug-resistance can affect the way cancer cells interact with their external environment – for example, the extracellular matrix. How these interactions differ between primary tumour cells and transformed or drug-resistant cells can provide an insight into crucial pathways and molecular targets. A model that studies drug-resistance and its implications in a disease process would help identify potential targets for drug therapy. Additionally, isolation of patient cells from late-stage cancers would allow analysis of these interactions *ex vivo* to guide decisions in clinical settings.

1.6 Rationale of this research

Cancer is often seen to become more aggressive as it develops drug resistance. The disease model of interest here is late-stage CRC. The Blay laboratory has previously developed drug-resistant CRC cell lines HT29-R and HCT116-R. These cell lines are resistant to SN-38 which is an active metabolite of the chemotherapy agent irinotecan – a topoisomerase I inhibitor used in late-stage CRC. It has been observed in the lab that both HT29-R and HCT116-R have a different morphologic phenotype compared to their corresponding parental cell lines.

The primary interest was in understanding the changes in chemokines that might correlate with the development of resistance in our paired cell lines. The differences in chemokine expression could reveal markers involved in migration during the late stage disease. Hence, I began first by screening for changes at the gene level amongst different chemokines and their receptors. Since the focus is on late-stage disease, we were also interested in understanding the journey of cells leaving the primary site, their ability to travel in the blood circulation, and interactions at the secondary site – liver being the primary location of interest. We first decided to exploit the extracellular matrix proteins in capturing CTCs from the peripheral blood samples of stage IV

colorectal and breast cancer patients. Utilizing the blood samples, there was also an opportunity to analyze the plasma chemokines between the two cancer types and healthy volunteers. In the end, we attempted to explore functional assays including the Transwell® and chick embryo model to understand implications of drug-resistance and invasive phenotype.

1.7 Purpose, goal and hypothesis of this research

The **overarching purpose** of this work was to examine the ways in which chemokine production and release may vary depending on the cellular populations and drug resistance, and how this may contribute to the tendency of cancer cells to migrate and metastasize, particularly due to altered interaction with the local extracellular matrix (ECM).

The **long-term goal** is to identify potential biomarkers related to chemokine activity and ECM interaction, that can be measured on circulating tumour cells (CTCs) and will provide information regarding the prognosis for individual cancer patients.

The research utilized established cell lines, and samples of blood (providing plasma and CTCs) from colorectal and breast cancer patients. Two related hypotheses were tested:

Hypothesis 1

The progression of disease in cancer patients, and the acquisition of drug resistance in the cancer cells, will alter the gene expression and release of chemokines in cancer.

Hypothesis 2

Circulating tumour cells can be isolated from the peripheral blood of cancer patients using an affinity substratum composed of the extracellular matrix upon which the cells migrate.

1.8 Specific experimental objectives

1. To assess changes in the production of chemokines between parental and drug-resistant cell lines.
2. To compare the plasma chemokine profiles of a range of colorectal and breast cancer patients and healthy volunteers.
3. To identify a reliable and consistent technique for recovery of CTCs from peripheral blood samples of colorectal and breast cancer patients, using a model ECM substratum.

2. Chemokines and their potential roles in colorectal cancer cell lines

2.1 Background

2.1.1 Chemokines

Chemokines are a subclass of the cytokine family and are low-molecular weight proteins with the ability to recruit leukocytes⁶⁴. There have been over 50 chemokines and 20 chemokine receptors identified in humans⁶⁵⁻⁶⁸. Chemokines are important due to their specificity in recruiting specific subsets of leukocytes depending on the microenvironmental need. However, as explained by Mantovani, “chemokines are redundant in their action on target cells and promiscuous in receptor usage”⁶⁵. This concept is depicted in Figure 4- one receptor can have multiple ligands and one ligand can activate more than one specific receptor. CCR6, CCR9, CX3CR1, CXCR4, CXCR5, and CXCR6 are the only receptors that each bind to one unique ligand. The nomenclature for chemokines is derived from the position of the cysteine residue where the CXC family has an amino acid positioned between two cysteines residues and CC family has two adjacent cysteines⁶⁴. Chemokine receptors have seven transmembrane domains and they are categorized in the G-protein-coupled receptor (GPCR) class.

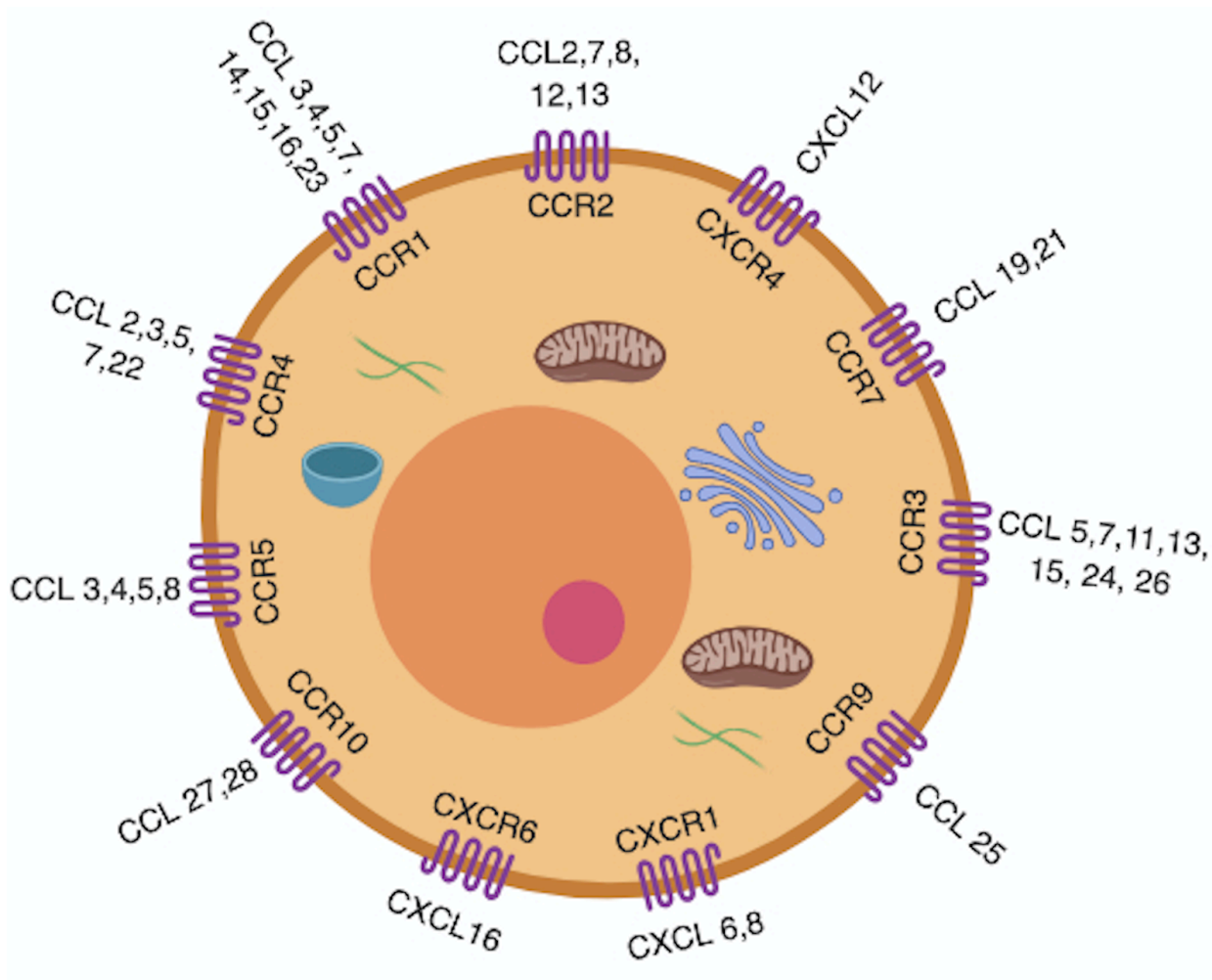


Figure 4 The complex network of chemokine and chemokine receptors.

Adapted from ⁶⁹ (Created with Biorender[®])

Modulating inflammation, host defense, immune surveillance, and directing the extravasation of leukocytes into tissue space are amongst the commonly known regular functions of chemokines^{70,71}. There is growing evidence to show that tumour cells are also able to release different chemokines and respond to chemokines via receptors on the surface of tumour cells⁶⁹. Müller *et.al.* initially presented the mechanism in which breast cancer cells with chemokine receptors CXCR4 and CCR7 were attracted to distant organs secreting their corresponding ligands CXCL12 and CCL21⁷². This supports the homing theory that distant organs are able to produce

chemotactic factors to attract receptor bearing cancer cells to migrate and settle at a new site⁷³, and implicates cancer cells in homing mechanisms. Studies have looked at the possibility of release of chemokines as a result of chemotherapy treatment⁶⁸. For instance, cancer cells exposed to anthracyclines release CXCL10 which is a potent chemotactic factor for T-cells⁷⁴. Sunitinib, a tyrosine kinase inhibitor has been shown to upregulate CXCL10 and CXCL11 in tumour vessels in murine melanomas⁷⁵.

Following the preliminary results, we became interested in 6 particular chemokines during the course of this research: CCL2, CCL5, CXCL12, CXCL8, CCL20 and CCL15.

2.1.1.1 CCL2

This member of the CC chemokine family is also known as monocyte chemotactic protein 1 (MCP1) and binds to CCR2 and CCR4 receptors. Monocytes and macrophages account for the majority of CCL2 production, however other cell types including endothelial cells, fibroblasts, epithelial cells, smooth muscle, and microglial cells are also capable of producing CCL2⁶⁷. The corresponding receptor CCR2 is expressed on T-cells, monocytes, epithelial and endothelial cells, whereas CCR4 is usually expressed primarily on T helper cells⁷⁶.

A role for CCL2 has been established in various types of cancer. For instance, CCL2 can induce macrophage accumulation and COX-2 expression in colorectal adenoma epithelium, promoting inflammation and leading to tumour progression in both an autocrine and a paracrine manner⁷⁷. Wolf *et.al.* investigated an additional unique feature of the CCL2/CCR2 interaction in the endothelium of capillaries that is initiated by CCL2 producing tumour cells⁷⁸. They showed a correlation between expression of CCL2 chemokine and enhanced metastasis, poor prognosis and recruitment of CCR2⁺Ly6C^{hi} monocytes⁷⁸. The role of CCL2 chemokine has been reported in transendothelial migration⁷⁹. CCL2 originating from tumour cells activates CCR2 receptors on

endothelium, and in turn, contributes to increased vascular permeability *in vivo* (Figure 5). This is supported by their results where CCR2 deficiency in mice was shown to prevent colon carcinoma extravasation and metastases in lungs⁷⁸. The interplay between cancer and the immune system is also important. The proposed mechanism of CCL2 highlights the ability of cancer cells to adapt what leukocytes do when they adhere to endothelium at an inflamed site. There is also growing evidence showing the contribution of CCL2 in fostering myeloid-derived suppressor cells (MDSCs)⁸⁰. The MDSCs can contribute to cancer immune evasion by suppressing T-cell anti-tumour functions⁸⁰. A recent study by Natsagdorj *et. al.* highlighted the involvement of CCL2 in drug resistance of prostate cancer cells against Cabazitaxel, a semisynthetic taxane⁸¹. A breast cancer study by Han *et. al.* demonstrated that estrogenic conditions were able to promote angiogenesis *in vitro* and *in vivo* through increased secretion of CCL2. In the same study, a knockdown of Twist in MCF-7 cells significantly reduced CCL2 production while under estrogenic conditions⁸².

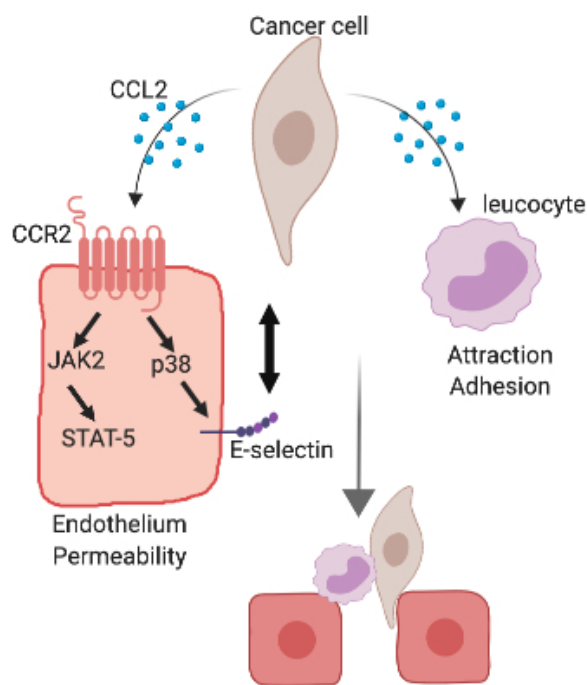


Figure 5 Pathway for how CCL2 exerts its action in transendothelial migration

Adapted from ⁷⁹ Created with Biorender©.

2.1.1.2 CCL5

Another chemokine of our interest is also from the C-C chemokine family and it is known as ‘Regulated upon Activation, Normal T-cell Expressed, and Secreted’ (RANTES) or CCL5. Normally, the expression and secretion of CCL5 are actively regulated in T-cells, and the corresponding receptor CCR5 is situated on T-cells, macrophages, and other leukocytes⁸³. Elevated tissue or plasma levels of CCL5 are markers of an unfavourable outcome in many types of cancer including gastric, breast, colorectal, and pancreatic cancer⁸⁴⁻⁸⁷. Activation of the CCL5/CCR5 pathway has been shown to induce angiogenesis, alter the extracellular matrix, and attract additional stromal and inflammatory cells to enhance the immune evasion mechanisms⁸⁸⁻⁹⁰. Different mechanisms and signalling pathways involving the CCL5/CCR5 axis are employed in the development of many solid cancers. It is known that CCL5 can work in an autocrine or

paracrine fashion and be released by cancer cells themselves or there can be indirect induction of the release of CCL5 from fibroblasts which will, in turn, recruit immune cells such as monocytes and regulatory T-cells to the tumour site⁸⁸. A study by Wang *et.al.* shows how CCL5 contributes to the activation of integrin $\alpha V\beta 3$, enhancing NF- κ B activity to result in an increase in MMP9 and enhancement of the invasive phenotype in osteosarcoma cell lines⁹¹. In a study by Cambien *et.al.* it was apparent through analysis of multiple CRC patient tissues that CCL5 and corresponding receptor CCR5 levels were upregulated⁸⁵. Additionally, systemic treatment with anti-CCL5 antibody in the BALB/c mouse model reduced the extent of liver metastasis⁸⁵. CCL5 signalling has shown to be involved in tamoxifen resistance in MCF-7 breast cancer cells, and cisplatin resistance in SKOV3 ovarian cancer cells through STAT-3 pathway^{92,93}. The study by Tsukishiro *et.al.* recruited patients with benign ovarian cysts and invasive carcinoma to measure plasma CCL5 levels using ELISA⁹⁴. It was found that patients with invasive ovarian cancer had elevated CCL5 levels compared to patients with benign ovarian cysts⁹⁴. However, the cells that secrete CCL5 in different tumour microenvironments varies based on the cancer type, and include fibroblasts, stromal cells or macrophages^{86,88,95}.

2.1.1.3 CXCL12

This is a chemokine from the CXC family and is also known as Stromal Derived Factor 1 (SDF-1)⁹⁶. This chemokine possesses two isoforms SDF-1 α and SDF-1 β , which differ in their last four amino acids⁹⁷. CXCL12 is expressed in various organs including heart, liver, brain, kidney, lymphoid organs, and skeletal muscle⁹⁷. The corresponding receptor is CXCR4. Extensive work has been carried out in the Blay laboratory to understand the CXCL12/CXCR4 axis in CRC. CXCR4 is upregulated by the energy metabolite adenosine⁹⁸ and downregulated by the eicosanoid 15dPGJ2⁹⁹. It is also downregulated by thiazolidinedione drugs through their action on PPAR γ ¹⁰⁰.

The study by Cutler *et.al.* examined the effect of chemotherapeutic agents on CXCL12-directed migration in CRC through changes in CXCR4 and CD26 expression¹⁰¹. Eradication of CXCR4-positive colon carcinoma cells following exposure to chemotherapeutic agents showcases the importance of this ligand-receptor couple in chemotherapeutic drug action¹⁰¹. CXCL12 has been known as the most potent angiogenic chemokine and it was shown that mice deficient in CXCL12 or its receptor CXCR4 have vascular malformations⁶⁸.

2.1.1.4 CXCL8

CXCL8, also known as interleukin-8, is a chemokine that traditionally has a role in inflammatory conditions caused by bacterial and chemical exposure¹⁰². It is produced by different cell types including monocytes, fibroblasts, endothelial cells, as well as tumour cells^{103,104}. It was the first chemokine that was shown to recruit neutrophils and a subset of T-cells^{103,105}. Under normal physiological circumstances, the receptor CXCR2 and all of its corresponding ligands CXCL1, CXCL2, CXCL3, CXCL5, CXCL7, and CXCL8 are responsible for mobilizing tumour-associated neutrophils (TANs)¹⁰⁶. CXCL8 is overexpressed in CRC and shown to promote disease progression through different mechanisms^{107,108}. In breast cancer populations, CXCL8 is found to be overexpressed in the estrogen-negative and HER2-positive subtypes¹⁰⁹. When plasma levels of CXCL8 were compared amongst healthy volunteers, early-stage, and late-stage solid cancer patients using ELISA, a stepwise increase in the levels was observed¹¹⁰. A study of patients with ulcerative colitis, colorectal adenomas, CRC, and colorectal liver metastasis compared the expression of CXCL8¹¹¹. It was found that patients in the CRC and liver metastasis group had significantly higher CXCL8 protein levels compared to the ulcerative colitis and colorectal adenoma subjects¹¹¹. There are also other CRC studies supporting the involvement of CXCL8 in the liver metastasis^{112,113}. CXCL8 released from other cell types can have implications for cancer

progression as well. For instance, a study by Khazali *et.al.* demonstrated that CXCL8 secreted by activated stellate cells and primary human non-parenchymal cells from the liver was able to activate dormancy in breast cancer cells¹¹⁴. Another study assessed the role of lactate formation in tumour environment and how that results in an activation of NF- κ B/IL-8 pathway leading to cell migration and angiogenesis *in vivo*¹¹⁵.

2.1.1.5 CCL20

In terms of intestinal physiology, it is known that CCL20 is produced by the follicle-associated epithelium that is over Peyer's patches, and mucosa-associated lymphatic tissue (MALT)^{73,116,117}. It is also secreted by the epithelial cells in the lungs and skin¹¹⁷. The corresponding receptor is CCR6, for which CCL20 is the sole ligand⁶⁹. CCR6 receptor is expressed on both naïve and memory β -cells¹¹⁷. The CCL20/CCR6 axis has an important role in a variety of cancer types including CRC. Specifically, the CCL20/CCR6 combination is involved in organ-selective liver metastasis of CRC^{73,118}. Within the liver, the expression of CCL20 is restricted to the periportal area, which is the entry point for blood draining from most of the lower gastrointestinal tract⁷³. A clinical study carried out by Frick *et.al.* compared CCL20 and CCR6 mRNA levels and protein concentrations in tissues of patients with ulcerative colitis, colorectal carcinomas (different stages), and primary colorectal tumours with liver metastases⁷². Significantly higher mRNA and protein levels of CCL20 were found in the colorectal adenomas and colorectal carcinomas⁷². In thyroid cancer, CCL20/CCR6 axis promotes migration and invasion through the NF- κ B pathway leading to MMP3 production¹¹⁹. The importance of CCL20 is not only due to its release from the tumour cells, but also a consequence of release from other cell types in the tumour microenvironment. For instance, a study by Liu *et.al.* demonstrated how

tumour-associated macrophages secreted CCL20 and promoted migration, epithelial to mesenchymal transition, and invasion of pancreatic cells¹²⁰.

2.1.1.6 CCL15

CCL15 is another member of CC family of chemokines and it has a known role for the recruitment of leukocytes and endothelial cells^{121,122}. In fact, one of the alternative names for CCL15 is leukotactin-1¹²¹. It is able to bind with both CCR1 and CCR3 receptor. However, it is mostly involved in the inflammatory conditions through its interaction with CCR1¹²³. CCR1 is normally expressed on monocytes, macrophages, dendritic cells, T cells, and B cells¹²³. This CCL15/CCR1 axis is implicated in many types of solid cancers where colorectal and hepatocellular carcinoma is most common^{124,125}. A study by Itatani *et.al.* demonstrated that knockdown of SMAD4 increased CCL15 expression on CRC cells which facilitated recruitment of CCR1 positive myeloid cells and promoted liver metastasis¹²⁶. There is a direct link showing that SMAD4 is able to bind the promoter region of CCL15 and negatively regulate its expression¹²⁶. SMAD proteins are important due to their involvement in the TGF- β signalling pathway¹²⁷. As shown in Figure 3, SMAD4 inactivation contributes towards a transition into a cancerous phenotype. In a study by Inamoto *et.al.*, CRC patients at stage II and III who were positive for serum CCL15 had a reduced relapse-free survival¹²⁸. In hepatocellular carcinoma, the serum CCL15 levels are found to be elevated and it was correlated with migration and invasion¹²⁹. It has also been a potential marker for breast cancer as per the cDNA microarray analysis from the METABRIC data, which comes from a Canada-UK project looking to sub-categorize breast cancer further based on its molecular signatures¹³⁰. A co-culture model studied by Yu *et.al.* showcased an interaction between mast cells and CRC cells where HT29 and Caco2 cells released CCL15 that was able to recruit mast cells, which in turn supported tumour cell growth¹³¹.

Table 1 List of potential chemokines and chemokine receptors involved in CRC metastasis and disease progression.

| Chemokine or receptor | Secreted by / expressed on | Relevance in colorectal cancer | Citations |
|------------------------|---|---|-----------|
| CCL2 | cancer cells | CCL2 secreted by CRC cells contributes to extravasation; receptor CCR2 found on endothelial cells | 33 28 78 |
| CXCL12 (SDF-1) / CXCR4 | distant organ stroma / cancer cells | CXCR4 expressed on CRC cells; Distant stromal environment release CXCL12 to prepare metastatic niche | 6,34 |
| CCL25 / CCR9 | cancer cells / MMP expressing stromal cells | highly expressed in primary stage; lost in late stages of CRC | 132 |
| CCL5 (RANTES) / CCR5 | cancer cells / leukocytes | overexpressed within primary as well as liver & pulmonary metastases of CRC patients | 36 |
| CCL9 / CCR1 | cancer cells / myeloid cells | Inactivation of CCR1 suppress liver metastasis by blocking immature myeloid cells accumulation in mouse model | 32 |
| CXCR3 | cancer cells | poor prognosis in CXCR3+ tumour patients and lymph node macrometastasis observed | 133 |
| CXCL8 | cancer cells | expression correlated with tumour associated macrophages | 33,38 |

2.1.2 Functional considerations in migration

One of the direct functional implications of chemokines is their effects on cell migration. Migration is an important aspect of the metastatic process as it allows the cancer cells to reach secondary sites where they can initiate colonization. Liver is one of the most common sites of metastasis for CRC. The process of cancer cells arriving at the secondary microenvironment and specific interactions they have decides their fate. The ECM at different organs vary tremendously and that too can contribute to the fate of tumour cells. For instance, The ECM represents only 3% of the relative area within a normal liver section, however, it is situated in a strategic location as a barrier between the blood flow and parenchyma¹³⁴. Therefore, it has many implications when its structure changes during the process of liver including carcinogenesis. Liver is readily accessible from the lower GI tract and cancers of the intestinal origin have a direct circulatory connection to the liver via the hepatic portal vein. Disseminated cells from other tissues will, in contrast, arrive into the liver via the hepatic artery.

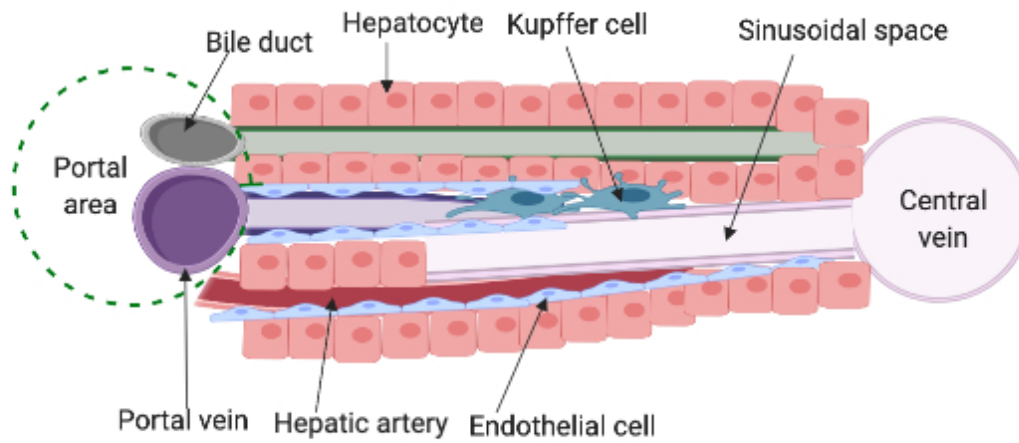


Figure 6 Illustration of the entry points and arrangement of liver microenvironment. The figure demonstrates various types of native liver cells that act as barriers to extravasation for arriving cancer cells. (Adapted from ¹³⁵) Created with Biorender[©]

Tumour cells arriving at the liver via both ports of entry first encounter the sinusoidal space (Figure 6). In this location, they are surrounded by a diverse population of native cells such as hepatic sinusoidal endothelial cells (HSECs), Kupffer cells, pit cells, stellate cells, and hepatocytes¹⁵. There are four stepwise phases of hepatic metastatic process: (i) a microvascular phase that involves initial infiltration of cancer cells, survival and adhesion to the microvasculature, extravasation into parenchyma, inflammatory responses and potential death of infiltrating cells; (ii) an intralobular micrometastatic phase which involves stromal cell recruitment, stellate cell activation, avascular growth and involvement of tumour-activated hepatocytes; (iii) an angiogenic micrometastatic phase which is when hypoxia and other tumour-derived factors lead to proangiogenic effects leading to replacement type or pushing type

metastasis; (iv) the established hepatic metastatic phase which is when the spread begins to affect the pathophysiology of deeper hepatic areas, effects of tumour-infiltrating stromal cells develop, and gene expression may also potentially alter as a result of the new hepatic microenvironment¹³⁶. Some studies show that the ability to adapt and grow into a secondary tissue microenvironment is already encoded within certain cells of the primary tumour¹³⁶, however, others conclude that depending on the organ microenvironment, gene-expression patterns of cancer cells can change significantly leading to the functional change and acquired growth ability¹³⁷. ECM components are quantitatively increased by almost 3 to 5 times in fibrotic liver conditions¹³⁴. Cells that play a major role in this transformation are hepatic stellate cells (HSCs). Once activated, HSCs can transform into myofibroblast phenotype and deposit large amounts of type I collagen¹⁵. Stellate cells have also been implicated in releasing growth factors and chemokines that may be beneficial to liver metastasis. A study by Matsusue *et.al.* showed that significant amounts of the chemokine SDF-1 is released by activated HSCs and can promote CXCR4-expressing CRC cells to invade and establish liver metastatic tumours in mice¹³⁸.

Similar to liver, another common site of metastasis is lungs. Tumours originating in rectum have a higher chance of lung metastasis compared to those from the colon. Lung is also a common site of metastasis in breast cancer patients. Due to direct anatomical access through the venous return, lungs are the most common and potential site of entrapment for cells dislodged from primary solid tumours around the body. For example, primary breast cancer cells that escape into the blood circulation will pass through the heart to the capillaries of the lungs¹³⁷. Lung tissue possesses non-fenestrated capillaries with loose junctions and the perfusion is comparable to the heart but relatively high compared to other organs¹³⁹. The upper limit of lung capillary pore size is around 5 nm¹⁴⁰. Five known mechanisms leading to pulmonary metastases are (i) spread through

the pulmonary or bronchial artery; (ii) spread via lymphatics; (iii) spread through the pleural space; (iv) spread via the airways; and (v) spread by direct neoplastic invasion¹⁴¹. However, the spread through general blood circulation is most common¹⁴¹. The interplay between local microenvironment and arriving tumour cells can support tumour initiation and growth or prevent it and result in tumour clearance¹⁴². The first point of contact within lung capillary is the layer of endothelial cells. Due to the gas exchange taking place here, type I alveolar cells are in very close vicinity. Between the endothelial and alveolar cells lies a fused basement membrane. The typical arrangement illustrates the barriers that a tumour cell has to cross through in order to reach into the lung parenchyma. Tumour cells also interact with the lung extracellular matrix, which is composed of keratin, fibronectin, and collagen¹⁴². Keratin is the predominant part of ECM in squamous cell carcinoma, whereas fibronectin predominates in desmoplastic lung adenocarcinomas¹⁴². The composition in the case of secondary lung metastasis might also vary. Two studies have shown that cells from small-cell lung cancer were able to withstand the chemotherapy-induced DNA damage as a result of the interaction between $\beta 1$ integrin and ECM proteins^{143,144}. Such tumour-specific differences in ECM composition and stromal environment can be exploited in understanding and designing a relevant platform to capture CTCs. Other cells in the alveolar surroundings include alveolar macrophages, septal cells, and monocytes which may also partake in promoting or hindering tumour cell invasion into lung parenchyma^{145,146}.

For *in vitro* studies, it becomes difficult to assess the holistic microenvironment and complex interactions. However, specific interactions can be studied by employing simpler models that answer specific questions.

With the interest in chemokines and their role in migration, we sought to design Transwell[®] experiments. This technique has benefits and drawbacks and careful assessment of results obtained

can help in answering specific questions related to cell migration. The assay using Transwell[®] is commonly referred to as the Boyden chamber assay¹⁴⁷. This assay uses a unique membrane (e.g. polycarbonate) with pores of varying sizes at the bottom surface. This surface can usually be coated with one of the ECM components like collagen type IV. Cancer cells are placed in the top chamber and the bottom chamber contains either a stimulus (e.g. chemokine) or another type of cell layer (Figure 8). As illustrated in the diagram, this assay holds the potential to study two different cell populations and their interactions. One of the drawbacks of this method is that it requires a large number of cells and single cell assays are difficult to carry out with Transwell[®] membranes. However, the utility of this assay has been studied using cells from different solid tumours¹⁴⁸. Here, we explored CRC cells HT29, HCT116, and their SN-38 resistant counterparts HT29-R and HCT116-R for their abilities to migrate toward HepG2 cells in the bottom chambers. HepG2 is an immortalized cell line from hepatocellular carcinoma and mimics many behaviours of normal differentiated hepatocytes¹⁴⁹. The purpose of using them in the Transwell[®] studies is to create an *in vitro* model of liver microenvironment with hepatocyte-like cells in the bottom chamber, and a layer of ECM proteins above. The cancer cells migrating through the ECM layer in response to the stimuli from HepG2 cells would reveal the functional characteristics of different cell lines.

2.2 Materials and Methods

2.2.1 Cell Culture

The cell lines HT29, HCT116, and HepG2 were obtained from American Type Culture Collection (ATCC). HT29-R and HCT116-R cell lines were produced in the laboratory (Figure 7). All of the cells were genotyped to confirm their identity and they were also tested periodically and found to be free of mycoplasma. These adherent cells were grown routinely in Nunc T-25 cell culture flasks (ThermoFisher). Hyclone Dulbecco's Modified Eagle Medium (DMEM) with 4mM

L-glutamine and 4500mg/L glucose, 1mM sodium pyruvate, and 5% v/v fetal bovine serum (FBS) was used for routine growth of cells. For the resistant counterparts HT29-R and HCT116-R, SN-38 (irinotecan metabolite from Sigma® CAS# 86639-52-3) at the final concentration of 30nM was added to the culture medium. When the cell culture reached near to confluence, cells were passaged. 1mL of 0.25% trypsin-EDTA (Gibco™) was added and spread through the monolayer of cells. If the cells were difficult to detach, the flask was kept in the incubator at 37°C for 1-2 min. Trypsin-EDTA was carefully removed and the flask was tapped onto the surface to fully detach the cells from the monolayer. Fresh 5mL of serum-containing media was used to wash the flask surface and prepare a cell suspension. 10% of the suspension volume was transferred to a new T25 flask (1:10 split ratio) and an additional 4.5 mL of media was added. SN-38 was added at a resulting concentration of 30nM for the resistant cell lines. The flasks were then stored in the incubator with 37°C and 5% CO₂

2.2.2 Generation of Drug Resistant Cell Lines

The SN-38 resistant cell lines were generated through a successively increasing drug exposure over a period of 12 weeks (Figure 7). Both of the resistant counterparts (HT29-R and HCT116-R) were generated by a previous post-doctoral fellow, Dr. Murray Cutler.

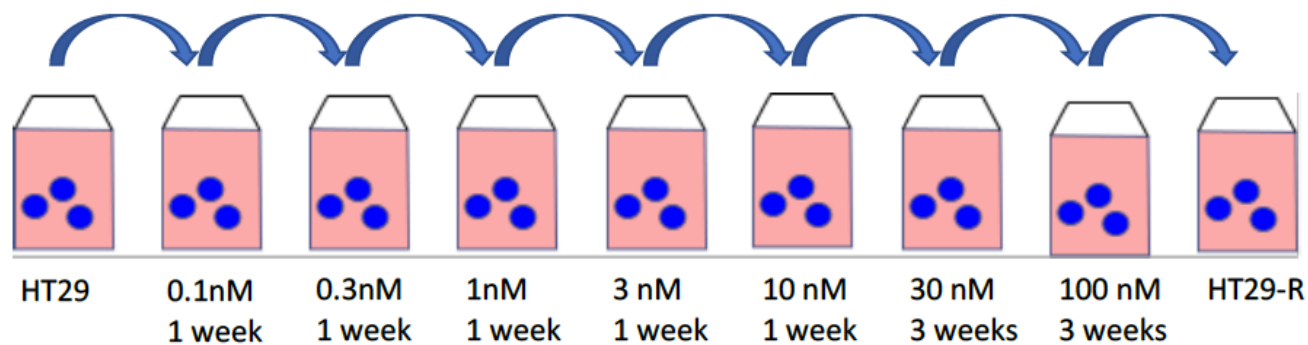


Figure 7 Stepwise process depicting the generation of drug-resistant cell line showing the concentrations and times of successive increasing exposure to the drug SN-38.

2.2.3 Polymerase Chain Reaction

2.2.3.1 RNA Extraction

The adherent colorectal cell lines were grown in T-25 flasks up to 80% confluence. The GenElute™ Total RNA miniprep Kit (Sigma Aldrich #RTN70) was utilized for the RNA extraction process. 2-mercaptoethanol (2-ME) was added to the provided lysis solution to a final concentration of 1% v/v. The culture medium was aspirated from the T-25 flasks and 1mL of the prepared lysis solution was added to cover the surface. Following 1 min incubation at room temperature, the cell lysate was collected from the flask, and centrifuged in the filtration column at 14000 x g for 2 min at room temperature in the minicentrifuge. This helped remove the cellular debris and shear the genomic DNA. A volume of 70% v/v ethanol equal to that of the lysate volume was then added to the supernatant and the solution was thoroughly mixed. This mixture was then added to the GenElute™ binding column for centrifugation at 14000 x g for 15 s. The desired RNA material was retained in the binding column and the supernatant was then discarded. 500µL of the wash solution 1 was then added to the binding column and put through centrifugation at 14000 x g for 15 s. The binding column was then transferred to the new collection tube and washed with the wash solution 2 (originally diluted with 100% ethanol). This tube was centrifuged at 14000 x g for 15 s and the filtrate was discarded. Another wash with 500µL of wash solution 2 was carried out at 14000 x g for 2 minutes. RNA was retained in the binding column which was then transferred to the new collection tube. The RNA was detached from the column using 50 µL of the provided elution buffer following centrifugation at 14000 x g for 1 min. Immediately after eluting the RNA into the solution, the collection tube was kept on ice to prevent degradation. The concentration and purity of the extracted RNA were measured using the NanoDrop® 2000c (Thermo Scientific). The RNA was stored at -80°C for future use.

2.2.3.2 Reverse Transcription

In order to perform the reverse transcription PCR (RT-PCR), the collected RNA was transformed into a complementary DNA (cDNA) through an amplification process. PCR hood (Airclean 600 PCR workstation) was utilized to set up the reverse transcription reaction. 2.5 µg of RNA was used as starting material for each reaction along with two master mixes. The first master mix contained 0.5µg/µL oligodT (Invitrogen) and 10nM deoxynucleotide triphosphates (dNTP, Invitrogen) in equal amounts. The second mastermix contained 10 µL of the 5x first strand buffer (Invitrogen), 5 µL of 0.1M DTT (Invitrogen), 2.5 µL Moloney murine leukemia virus (M-MLV, Life Technologies) reverse transcriptase enzyme. Each reaction also included a No-RT control where the reverse transcriptase enzyme was excluded to ensure that there was no contaminating genomic DNA in any reaction. A separate master mix was prepared for the No-RT control wells and diethylpyrocarbonate (DPEC) treated water was used instead of the reverse transcriptase enzyme. The samples were prepared by first mixing the RNA and master mix 1. Reaction tubes were set in the thermocycler Techne Genius[®] (LabX) and a program was set for reverse transcription. During the first part, tubes were incubated at 65°C for 5 min. Tubes were then kept on ice for 15 s. prior to addition of 20µL of master mix 2. The reaction tubes were then run at 37°C for 50 min followed by 70°C for 15 min in the thermocycler. Based on the ideal reaction condition, it was expected that the final product contained cDNA at 50ng/µL RNA-equivalent. Three tubes for each condition were pooled together and stored at -80°C.

2.2.3.3 Primer Design

The primer pairs that were used in polymerase chain reactions (PCR) and quantitative reverse-transcription PCR (qRT-PCR) experiments were designed through use of publicly available platforms including primerBLAST from National Center for Biotechnology Information

(NCBI), and OligoAnalyzer from Integrated DNA Technologies (IDT). All primers were ordered from Life Technologies.

2.2.3.4 Endpoint PCR

The cDNA was thawed on ice and all the reagents (Table 2) were set-up in the PCR hood (AirClean 600 PCR Workstation). The GoTaq green master mix (Promega) contained Taq DNA polymerase, dNTPs, MgCl₂, reaction buffers, and loading dye.

Table 2 Reaction set-up for the endpoint PCR where the forward and reverse primers are at resulting concentration of 200nM each.

| | |
|------|-----------------------------------|
| 12.5 | μL GoTaq green |
| 0.5 | μL Primer FWD |
| 0.5 | μL Primer REV |
| 9.5 | μL nuclease-free H ₂ O |
| 23 | μL total |
| + | |
| 2 | μL cDNA (100ng) |
| 25 | μL total reaction |

The reaction tubes for all the experimental groups were prepared in triplicate and run through the program as shown below in Table 3 and the primers used are listed in Table 4.

Table 3 Thermocycler program set up for PCR.

| | | | |
|-----------|------|--------|------------------|
| | 94°C | 75 s | initial denature |
| | 94°C | 45 s | denature |
| 36 cycles | 60°C | 45 s | anneal |
| | 72°C | 60 s | extension |
| | 72°C | 10 min | final extension |
| | 4°C | hold | hold |

Table 4 The primers for chemokines and their corresponding receptor pairs that were screened with RT-PCR.

| Gene | Primer sequence |
|-------------|---------------------------|
| CCL2 fwd | GCTGTGATCTTCAAGACCATTG |
| CCL2 rev | AAACAGGGTGTCTGGGGAAAG |
| CCR2 fwd | CTGTCCACATCTCGTTCTCGGTTTA |
| CCR2 rev | CCCAAAGACCCACTCATTTGCAGC |
| CCR4 fwd | ATCCTGAAGGACTTCAAGCTCCA |
| CCR4 rev | AGGTCTGTGCAAGATCGTTTCATGG |

| Gene | Primer sequence |
|-------------|------------------------|
| CCL25 fwd | TCTGCCTGCTGCGATATTCT |
| CCL25 rev | TTGGAAGGTCTGCGTGTTGT |
| CCR9 fwd | GTTCTCCTTGTTCTGTTCTGGG |
| CCR9 rev | ACTTTGGATGCCTTGTGGGT |

| Gene | Primer sequence |
|-------------|------------------------|
| CCL5 fwd | CTCATTGCTACTGCCCTCTGC |
| CCL5 rev | GCTCATCTCCAAGAGTTGAT |
| CCR5 fwd | TTGGGTTGGAAGTGAGGGTC |
| CCR5 rev | TGGGTGAGACTGTGTTCAAGC |

| Gene | Primer sequence |
|-------------|------------------------|
| CCL15 fwd | CCAAGCCAGGTGTCATATTCC |
| CCL15 rev | TCAGACCAAGAACTCACAGGA |
| CCR1 fwd | AGAGTTCCGACTGCCATCTTG |
| CCR1 rev | TAGACACTTTCCTCCCAACCC |

| Gene | Primer sequence |
|-------------|---------------------------|
| CXCL10 fwd | AAAGCAGTTAGCAAGGAAAGGTCTA |
| CXCL10 rev | TGTAGGGAAGTGATGGGAGAGG |
| CXCR3 fwd | GCCTACTGCTATGCCACAT |
| CXCR3 rev | CGTCTACCCTGCTTCTCGG |

| Gene | Primer sequence |
|-------------|---------------------------|
| CXCL8 fwd | TTGAATGGGTTTGCTAGAATGTGAT |
| CXCL8 rev | GGCACAGTGGAACAAGGACTT |
| CXCR1 fwd | GTGGCTCTGTGTGCTCTGA |
| CXCR1 rev | CTAAGGGCTGCTTGTCTCGT |

| Gene | Primer sequence |
|-------------|------------------------|
| CCL19 fwd | CTGGGTACATCGTGAGGAACTT |
| CCL19 rev | GGTGAACACTACAGCAGGCAC |

| | |
|-----------|------------------------|
| CCL21 fwd | GCAAGAGGACTGAGCGGT |
| CCL21 rev | AAAGCAGGAGAAAGAGTGTGGC |
| CCR7 fwd | TCCCACAGACTCAAATGCTCA |
| CCR7 rev | GCAGGAAACACCACACTCTC |

| Gene | Primer sequence |
|------------|------------------------|
| CXCL12 fwd | ACAGTCAGGTGGTGGCTTA |
| CXCL12 rev | AGGTTGAAAGAGGAGGTGAAGG |
| CXCR4 fwd | CTGTGACCGTTCTACCC |
| CXCR4 rev | AATACCAGGCAGGATAAGGC |

| Gene | Primer sequence |
|------------|--------------------------|
| CXCL13 fwd | GCTTGAGGTGTAGATGTGTCC |
| CXCL13 rev | ACTTGTTCTTCTTCCAGACTATGA |
| CXCR5 fwd | TCAGATGGAACCGCAGGAAG |
| CXCR5 rev | GCTTGGCTTGAGTGGGACAA |

| Gene | Primer sequence |
|-----------|-------------------------|
| CCL20 fwd | TTTGCTCCTGGCTGCTTTGAT |
| CCL20 rev | AGTTGCTTGCTGCTTCTGATTCG |
| CCR5 fwd | TTGGGTTGGAAGTGAGGGTC |
| CCR5 rev | TGGGTGAGACTGTGTTCAAGC |

Following the program, 5 μ L of each reaction product was loaded on a prepared 1% agarose gel that contained 0.2 μ g/ μ L ethidium bromide (EtBr). The gels were run at 94 volts for 30 min. Images were captured using the AlphaImager HP gel imaging system (Biotechne) for visualization of the bands under the UV light. The initial experiments also provided information on which primers worked well, and which primers did not. The negative controls were blank for all the genes tested and this confirmed that there was no contamination from the genomic DNA.

2.2.3.5 qRT-PCR

In order to confirm the preliminary results from the RT-PCR, five potential target genes were chosen to be fully quantified using the $\Delta\Delta$ CT method in a SYBR green based qRT-PCR. For all the reactions in quantitative PCR (qPCR), the primers were first tested with the end-point PCR to ensure that a single amplicon of the correct length was produced. Similar to the end-point PCR

experiments, qPCR reactions were also prepared in the dedicated PCR hood (Air Clean 600 PCR Workstation). qPCR was only carried out for the markers displaying a visually significant change between the parental and drug-resistant lines at the RT-PCR step. Rox reference dye (0.25 μ L) was used for the Agilent Master Mix in the qPCR reactions. The reactions were prepared in a 96-well plate (Thermo Scientific). 5 μ L of cDNA was diluted 10-fold using nuclease-free water prior to the addition in the reaction plate. Reaction plate was sealed using a clear adhesive film (Thermo Scientific).

The reaction plate was taken to the StepOnePlus Real-Time PCR system (Applied Biosystems) and run under these cycling conditions: hot-start with 95°C for 30 s. then 60°C for 60 s. and fluorescent readings were taken after each cycle up to 40 cycles. Following the 40 cycles, a melt-curve was generated in the machine which produced a curve in the associated software. A single unique curve provided confirmation of a single amplicon that was generated as a result of the reaction through 40 cycles. Numbers for the fluorescence value were recorded in the software after each cycle and these values were exported in excel. These values were fed into the LinRegPCR software to generate a window of linearity¹⁵⁰. The efficiency of the reaction was also calculated based on the fluorescence values as it is expected that every cycle will double the product under optimal conditions. Based on these data points and a minimum threshold value, this software was able to provide a relative initial mRNA concentration (N_0) value in arbitrary fluorescence units. As explained in Ruijter *et.al.*¹⁵¹, the formula for N_0 is:

$$N_0 = \frac{N_{cq}}{Eff^{cq}}$$

RPL27 was utilized as the control gene and the expression was consistent in both cell lines. It has been validated to act as a housekeeping gene in the past¹⁵². There are also other novel housekeeping genes that might have more evidence to be stable across different cancer types¹⁵³.

2.2.4 Chemokine Arrays

First, a new set of T-25 flasks were seeded with 40% initial density in the DMEM 5% FBS media. 30nM SN-38 was added for the resistant lines. After 36-48 hours, the existing media was aspirated followed by a wash with cold serum-free DMEM. Fresh media containing 1mg/mL BSA in DMEM was prepared and added to the flasks. The flasks were incubated overnight at 37°C in 5% CO₂. On the day of the assay, 5mL syringe and 0.45 µm filter were used to collect the media sample. Proteome Profiler Human Chemokine Array kit (R&D Systems) was used to process the collected samples. Please refer to the coordinates and the nomenclature guide in the Appendix I.

It was a pre-coated nitrocellulose membrane based assay yielding relative levels of selected human chemokines. Two mL of the collected sample media was mixed with 1mL of the array buffer 4. The provided detection antibody cocktail was diluted with filtered 100µL MilliQ® H₂O. Each array membrane was blocked using 2mL of the array buffer 6 in the provided 4-well chamber for 1 h on the rocker at room temperature. While the membranes were blocking, 20µL of the diluted antibody cocktail was added in each prepared sample and they were incubated at room temperature for 1 h. The blocking buffer was then aspirated and the prepared samples were added to each chamber. The 4-well chamber was incubated overnight at 4°C on a rocker.

Next day, each array membrane was carefully removed and washed three times with a 1x wash buffer at room temperature. Each wash was carried out on a rocker for 10 min. In the meanwhile, the provided streptavidin-HRP was diluted in the Array Buffer 6 at a 1 in 2000 dilution. Following the three washes, each array membrane was incubated with 2mL of the diluted streptavidin-HRP at room temperature for 30 min on a rocker. Another three washes as described

previously were carried out following the incubation. The membranes were then incubated with the 1:1 mixture of Chemi reagent 1 and Chemi reagent 2 provided for 1 min in a plastic protector sheet. The membranes were imaged using the Kodak© Image Station 4000mm Pro machine for 40, and 30 min.

The images were analyzed using the ImageJ® software and the dot blot analysis method 2 explained by National Institutes of Health (NIH)¹⁵⁴ was utilized for quantification. Briefly, the integrated density of each spot was measured by first turning the image in an 8-bit black and white image. The background was subtracted using the *Subtract Background* command. The image was then inverted to generate a black background with white array spots. Under the Analyze menu, and Set Measurements tab, integrated density was chosen and all the other parameters were left unchecked. A constant size circular section was created around each of the array spot, and the integrated density value was measured in this fashion with a *Measure* command by manually moving through each array spot. It was ensured that the size of the circular section remained the same when measuring different array images and this allows for a consistent approach allowing to make comparisons.

2.2.5 Immunostaining Chemokines

Expression of chemokines within the parental and drug-resistant cells was observed using immunofluorescence technique. Colorectal cancer cells were first seeded at 10% confluence in the four-chambered Nunc Lab Tek II chamber slides (Thermo Scientific) with DMEM 5% FBS media. Cells were allowed to grow in the incubator with 5% CO₂ at 37°C for 2 days. The slide was then placed on ice. The growth medium was carefully aspirated without disturbing the monolayer and it was replaced with 0.5mL DMEM 1mg/mL bovine serum albumin (BSA). The slide was kept in

the 5% CO₂ incubator for 30 min at 37°C. The slide was gently removed from the incubator and 1mL of freshly prepared 2% paraformaldehyde was added to the existing media. The slide was incubated at room temperature for 10 min and the solution was aspirated. The wells were washed with PBS Ca²⁺/Mg²⁺. 1mL of freshly prepared 5% FBS in PBS Ca²⁺/Mg²⁺ was added and incubated at room temperature for 30 min. In the meantime, primary antibody dilutions were prepared for CCL2 and CXCL12 in 1mg/mL BSA in PBS Ca²⁺/Mg²⁺. Mouse anti-human CCL2 was used at 1µg/mL and rabbit anti-human CXCL12 was used at 0.5 µg/mL concentration. The slide was covered with parafilm and incubated in the humidified chamber for 60 min. Following the incubation, the primary antibody solution was aspirated carefully and chambers were washed twice with cold PBS Ca²⁺/Mg²⁺ 1mg/mL BSA. The secondary antibody was prepared as 1 in 2000 (1µg/mL ending concentration). 750µL of the prepared secondary antibody was added into each chamber. The plate was covered with parafilm and aluminum foil to protect from drying and light. The slide was incubated in a humidified chamber for 60 min at room temperature. Two washes were carried out as earlier with cold 1mg/mL BSA in PBS Ca²⁺/Mg²⁺. The chamber on the slide was removed using the provided plastic slider. Two drops of Fluoroshield® aqueous gel mounting medium containing DAPI (Abcam) were added on top of each well surface. A rectangle 50mm coverslip (Fisher) was carefully placed onto the slide and allowed to dry for 60 min in dark. The fluorescence was observed using the Leica DM2000 microscope and the images were captured with Micropublisher 5.0 RTV camera and QCapture Pro 5 software.

2.2.6 Migration assays: Transwell®

The migration assays were carried out using 8 µM Transwell™ polycarbonate membrane inserts (Corning™). Each membrane was coated with 10 µg/mL collagen type I and 5µg/mL

human fibronectin for 2 hours at 37°C. HepG2 cells were grown in the bottom chambers with DMEM 5% FBS up to 75% confluence (Figure 8). On the day of the assay, existing media from the HepG2 cells was removed and chambers were filled with 700µL of 1mg/mL BSA in DMEM. Colorectal cancer cells were detached from T25 flasks and counted using a hemocytometer. 100µL of cell suspension containing 200,000 cells in DMEM 1mg/mL BSA were placed in the top chamber of the coated transwell membrane. For negative control, a coated membrane with cells was placed in a chamber without HepG2 cells at the bottom. The chambers with Transwell™ membranes were incubated overnight in 37°C with 5% CO₂. Next day, the membranes were washed with cold PBS Ca⁺²/Mg⁺² once and fixed with ice-cold methanol. Membranes were then stained with Mayer's hematoxylin (Sigma) for 20 min. Cotton swabs were used to remove cells from the upper chamber of the membrane and they were placed on a glass slide using an Fluroshield® aqueous mountant (Abcam). Cells that migrated on the other side of the membrane were imaged and counted using the inverted microscope (Motic AE21).

Analyzing the chemokines released by the cancer cells and identifying changes that come along with drug resistance is one aspect of understanding cancer progression. However, it is equally important to assess and see which secondary tissues are able to release chemokines that attract and harbour cancer cells. We decided to use the HepG2 cells (hepatocellular carcinoma) as a model to assess the interaction with CRC cells. Colorectal cancer cells HCT116, HCT116-R, HT29, and HT29-R were placed in the coated inserts following the 18 h incubation, cells migrated onto the other side of the membranes were fixed, stained, imaged, and counted.

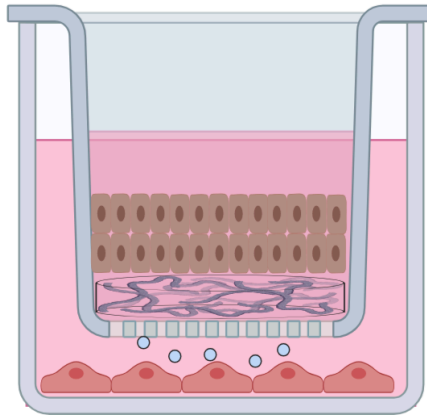


Figure 8 Set up for migration experiments. HepG2 cells (red) in the bottom chamber and CRC cells (brown) in the top chamber coated with human fibronectin and collagen type I (dark blue matrix). Chemokines released (light blue circles) from HepG2 cells travel upward to attract CRC cell migration through the 8 μ m membrane pores.

In addition to the Transwell[®] experiments, we wished to determine the relative expression of chemokines released from the HepG2 cells in this model. Identifying these chemokines would lead to potential candidates that drive the chemotactic gradient in order to attract CRC cells towards the bottom chamber. Same method described in section 2.3.4 was employed and HepG2 cell lines were used to collect the conditioned media.

2.2.6 Statistical Analysis

All experiments were carried out with three replicates or more. Prism[®] version 8 (GraphPad[®] – San Diego) software was used for the analysis of results from the migration assay and chemokine arrays.

2.3 Results

2.3.1 A panel of chemokines show definitive gene level changes in the drug-resistant cells

To examine the effect of established drug-resistance on the expression of chemokines and chemokine receptors in two human CRC lines (HT-29 and HCT116), endpoint PCR was carried out for mRNA expression in 22 targets. Eleven were chemokines and the remainder were their corresponding receptor pairs. Three independent sets of cDNA samples were prepared from different cell passages. More than one primer pair was tested for some targets with the design from NCBI Primer Blast. Primers that generated a single product on the gel electrophoresis were chosen to go further for replicate experiments. GAPDH was used as a positive control and it was equally expressed between all cell lines.

From the results, it was observed that CCL2 gene was upregulated in both the resistant cell lines HT29-R and HCT116-R when compared to the respective parental lines (Figure 9A). CXCL12 was upregulated in HT29-R (Figure 9G), however, there was no expression in either of the HCT116 cell-lines. The corresponding receptor CXCR4 had a very low expression and it was difficult to conclude an upward or downward trend from Figure 9D. CCL5, CCL15, CXCL8, and CCL20 genes (Figure 9B, C, F, and E respectively) were consistently downregulated in HT29-R counterpart when compared to HT29. CCR6 was the only receptor that had a strong expression and it was equal in all four cell lines as observed in Figure 9H. The trends observed between HT29 and HT29-R did not match what was observed between HCT116 and HCT116-R. For instance, the expression of CXCL8 stayed unchanged between HCT116 and HCT116-R. From Figure 9B, it is observed that the trend is similar for both parental and drug-resistant lines. However, the relative gene expression of CCL5 in HCT116 is visually less when compared to HT29.

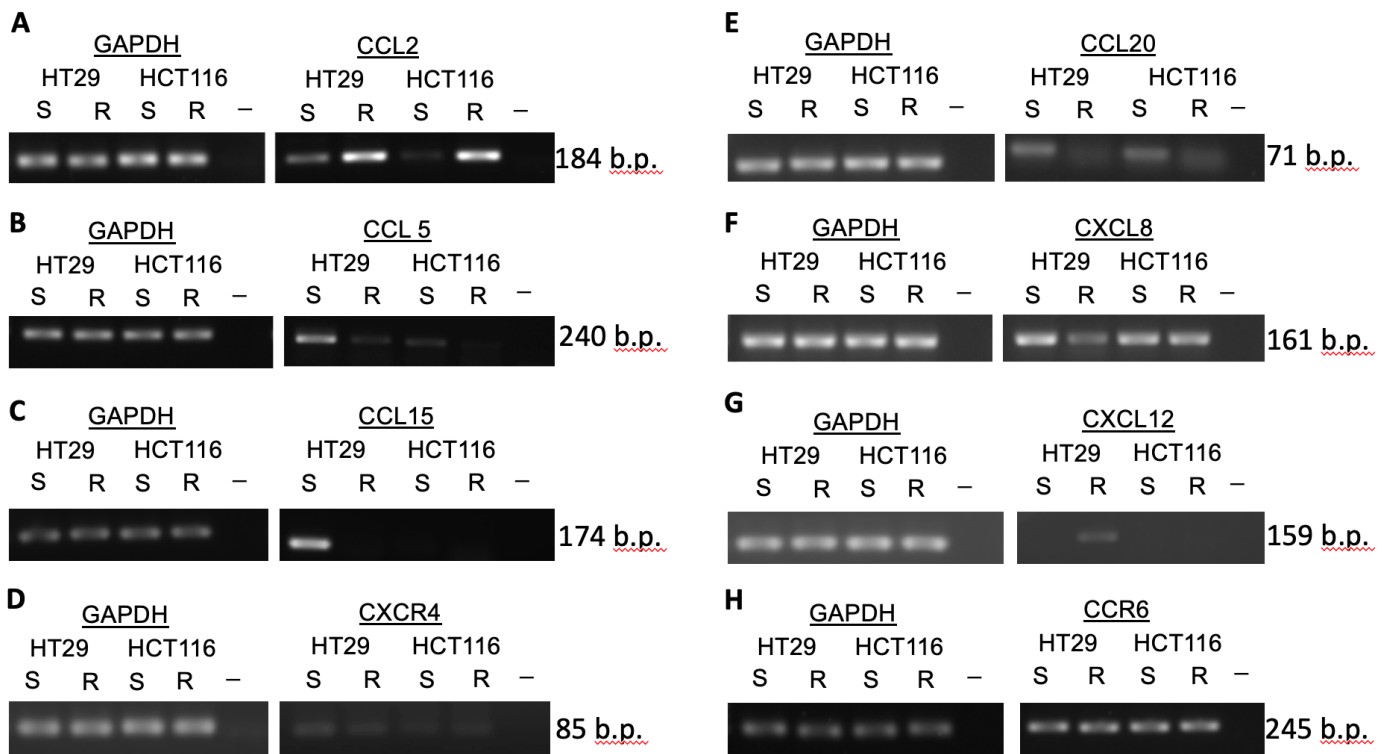


Figure 9 Comparison of changes in chemokine and chemokine receptor gene expression within two parental and resistant CRC lines.

(A-H) The expression of target genes from the chemokine panel in two CRC lines and their resistant counterparts over three independent experiments. L: 1 μ L 100 bp DNA ladder; - : Control (H₂O); S: SN38 drug-sensitive cell line; R: SN-38 drug-resistant cell line; b.p.: base pairs

Note: A full set of raw images are in the Appendix II: Raw images of the RT-PCR results.

Below (Table 5) is a summary of the overall changes that were observed from the three independent experiments carried out for each gene target.

Table 5 Summary of gene expression changes for chemokines and receptors between HT29 and HT29-R cells.

| Consistent changes | Variable changes | No change / No expression |
|---------------------------|-------------------------|----------------------------------|
| CCL2 (↑) | CCR1 | CCR4 |
| CCL5 (↓) | CXCL10 | CCR2 |
| CCL15 (↓) | CXCR3 | CCR9 |
| CXCL8 (↓) | CXCR1 | CCR7 |
| CXCL12 (↑) | CCR5 | CCL19 |
| CCL20 (↓) | | CCL21 |
| CCL25 (↑) | | CXCL13 |
| | | CXCR5 |
| | | CCR6 |
| | | CXCR4 |

Note: The arrows indicate the changes in HT29-R relative to HT29 cells. The candidates listed under ‘Variable changes’ were tested with more than one primer pair, however, resulted in inconsistent expression. These trends were confirmed following three independent replicates.

CCL2 and CXCL12 were upregulated in HT29-R cells, whereas CCL5, CCL15, CXCL8, CCL20, and CXCR4 were downregulated in HT29-R cells. Only CCR6 remained constant across all four cell-lines. The HCT116 pair showed similar changes for CCL2, CCL5, and CCL20 that matched the trends in the HT29 pair. Many of the gene targets in the HCT116 and HCT116-R had no expression and many were unchanged between the parental and resistant cells. CCL15, and CXCL12 had no expression in the HCT116 group whereas CXCL8 remained unchanged. Based

on these observations and their functional implications CCL2, CCL15, CXCL8, CXCL12, CCL20 were chosen to move for further analysis on qRT-PCR. Table 6 demonstrates the overall trends from the PCR results with the relative strengths of the changes observed.

Table 6 Trends observed for chemokine gene expression between HT29 and HT29-R cells.

| Potential candidates | | Relative change in HT29-R |
|----------------------|-------------------|---------------------------|
| Name | Conventional name | |
| Chemerin | TIG-2/RARRES2 | ↓ |
| IL-8 | CXCL8 | ↓↓↓ |
| MCP-1 | CCL2 | ↑↑ |
| MDC | CCL22 | ↑ |
| Midkine | - | ↓ |
| MIP-1δ | CCL15 | ↓↓ |
| RANTES | CCL5 | ↓↓ |
| SDF-1 | CXCL12 | ↑↑ |

Note: The direction of the arrows correlates with change in HT29-R cells relative to the HT29. Visual intensity of the bands was broken down into three categories: High (3 arrows), Medium (2 arrows), and Low (one arrow). The trends demonstrated here are not quantitative.

2.3.2 Potential chemokine markers confirmed through qRT-PCR method

To confirm the preliminary results from the RT-PCR, five potential target genes were chosen to be fully quantified using qRT-PCR. Targets quantified were CCL2 (MCP-1); CCL15; CXCL8 (IL-8); CXCL12 (SDF-1); and CCL20 (Figure 10). Primer pairs displayed in Table 4 were used for the qRT-PCR experiments. The results displayed in Figure 10 demonstrate the same pattern in changes as that observed in RT-PCR results (Figure 9).

CCL2 and CXCL12 were upregulated in HT29-R cells. The change in CCL2 was not statistically significant from Prism GraphPad[®] analysis, however, there is a strong trend indicating an upregulation in HT29-R. For the remaining three targets CCL15, CXCL8, and CCL20 there was a downregulation in the resistant cells and these changes were statistically significant.

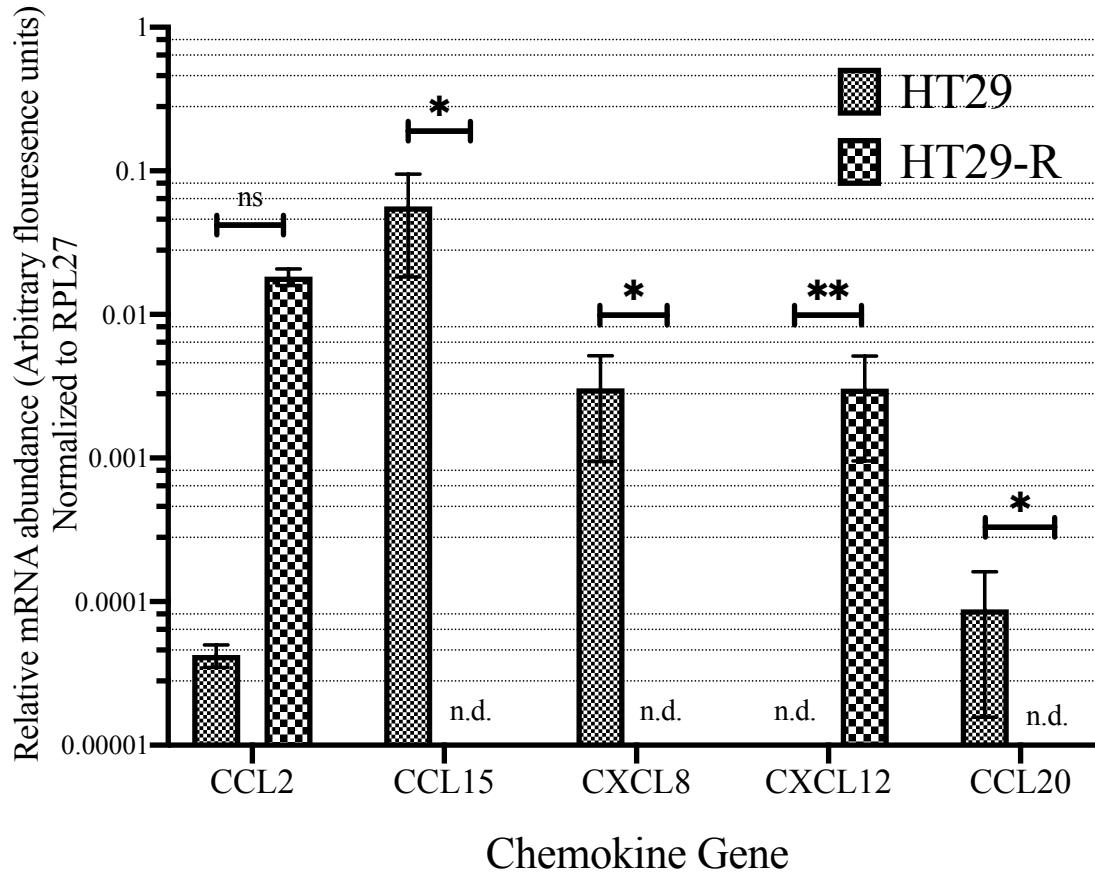


Figure 10 Changes in chemokine gene expression between HT29 and HT29-R cells. The results displayed are from three independent replicates using three independently collected cDNA samples. Statistical significance was calculated using two-way ANOVA and the post-test was done using the Bonferroni method. *: $p < 0.05$; **: $p < 0.01$; n.d.: none detected; ns: not significant

Based on the results observed, it was important to further analyze these targets at the protein level. One possibility was to conduct Western blot using the conditioned media from the cell lines. However, there are challenges with performing western blot on culture medium components. Depending on when the medium is collected, the cells are at different stages in their cell growth and it is difficult to predict when the most amount of chemokines are present. The half-life of secreted chemokines and what percentage of chemokines remain stored in the Golgi-apparatus are also factors that need to be considered. The smaller molecular weight (8-10 kDa) of the chemokines can be a challenge for the detection of protein band on gel electrophoresis. Quantifying the protein using ELISA (Enzyme-Linked Immunosorbent Assay) would help in absolute quantification of chemokines. ELISA is not an optimum technique for the screening approach as the kits available are generally for individual chemokines. However, we first wished to assess the cellular expression of chemokines through immunofluorescence technique followed by a semi-quantitative approach using chemokine arrays.

2.3.3 Expression of CXCL12 identified on HT29 and HCT116 cells via immunofluorescence

In order to examine the cellular localization of chemokines in the parental and drug-resistant CRC cell lines, the immunofluorescence technique was utilized. There have been reports of chemokine staining in the tissue samples of colorectal cancer patients, and also chemokines detected through intracellular staining in flow cytometry¹⁵⁵⁻¹⁵⁷. However, staining in immortal cell lines can be challenging and most often research groups utilize ELISA for absolute quantification¹⁵⁸. We wished to explore whether chemokines can be detected on a fixed monolayer of colorectal cancer cell lines. First, we started with epithelial markers EpCAM and pan-cytokeratin. Epithelial markers were chosen as a positive control and tested prior to the chemokine experiments. Figure 11 shows a typical EpCAM stain for HT29 cells and the same antibody was also tested with HCT116 cells (Figure 12). The cellular morphology is different between the two cell lines. Bright field and DAPI stain images help further to understand the staining patterns for different cancer cells. Using the same technique with CXCL12 antibody, HT29 cells were stained and found to express this chemokine (Figure 13). Similarly, HCT116 cells expressed CXCL12 in a diffuse pattern (Figure 14) which was different from HT29 cells. The resistant cells were not tested for the chemokine expression. The CCL2 antibody was tested using the same technique, however no expression was found for the HT29 and HCT116 cells.

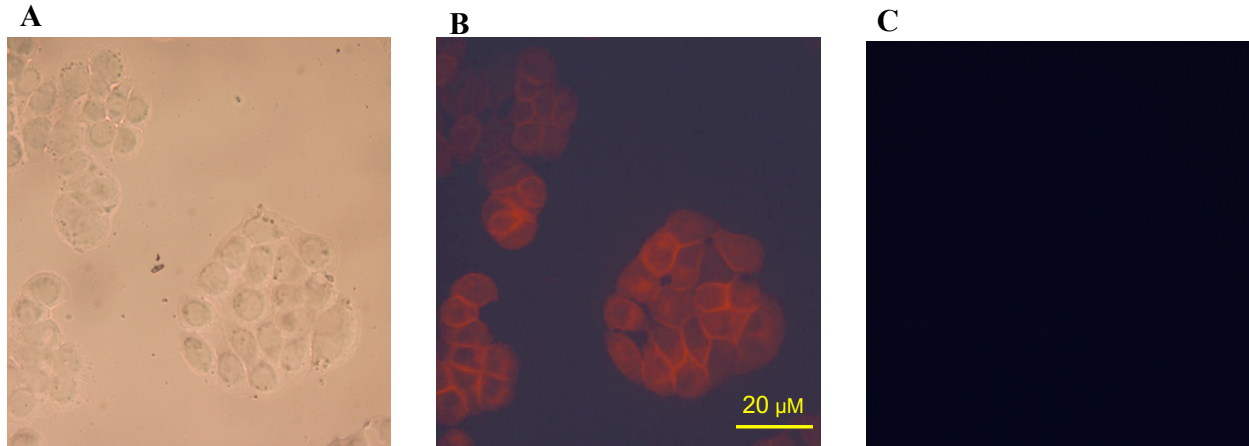


Figure 11 Expression of epithelial marker EpCAM on HT29 cells. Images were taken with 100X objective. Bright-field image showing a cluster of HT29 cells (B) EpCAM expression in red - as observed, the membranes show a brighter distinct pattern that is typical of an epithelial protein. (C) Negative control confirming a lack of expression due to the omission of primary antibody in the experiment. The figures are representative of three independent experiments.

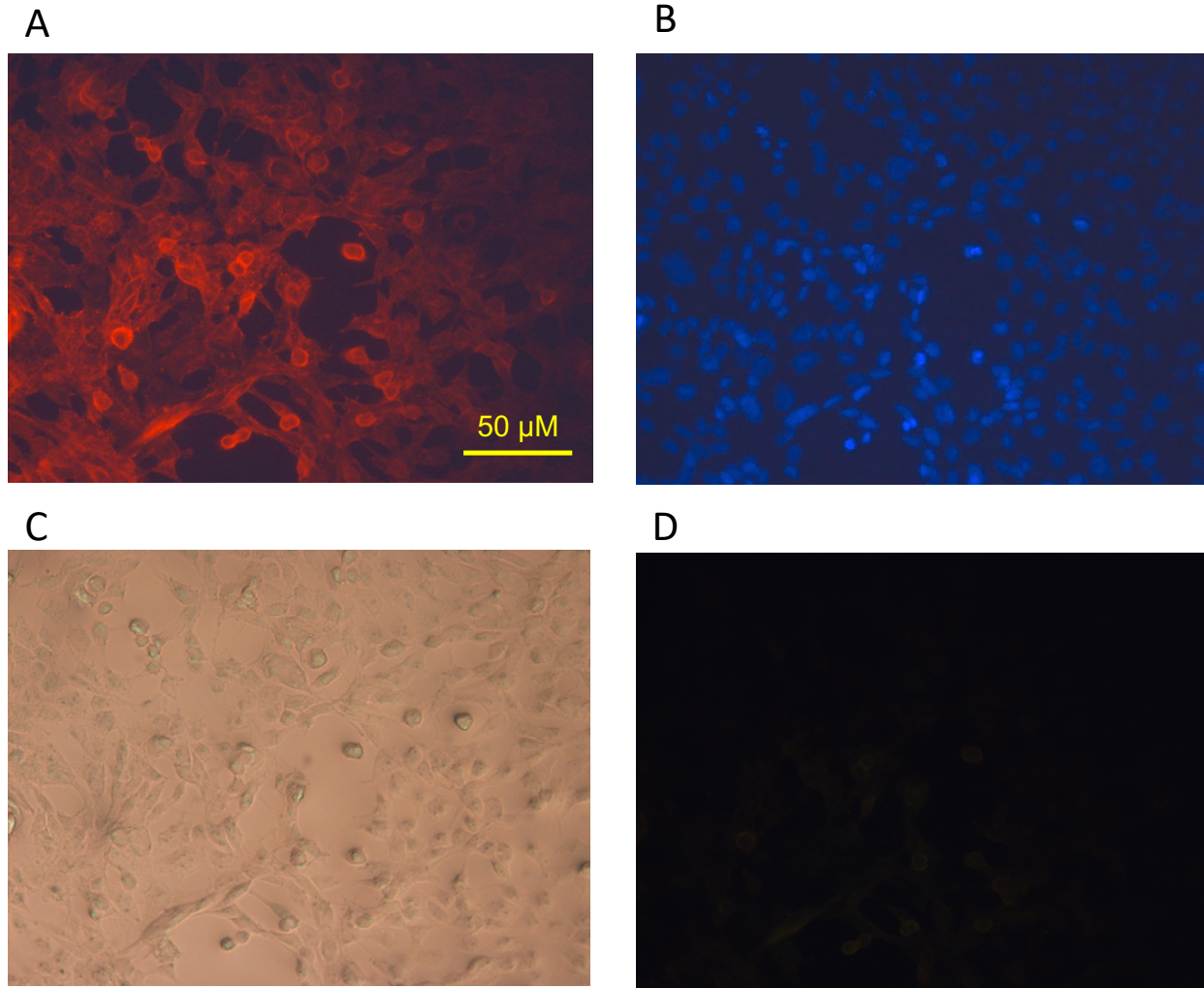


Figure 12 Representative images showing the expression of epithelial marker EpCAM on HCT116 cells. Images were taken with 40X objective. (A) Red immunofluorescence for rabbit anti-EpCAM antibody used at 1μg/mL. (B) DAPI staining showing nuclei stain (C) bright field demonstrating the HCT116 cellular morphology (D) Negative control with lack of primary EpCAM antibody.

The same EpCAM antibody was utilized for both HT29 and HCT116 cells to ensure that epithelial marker expression is captured in different CRC cell lines (Figure 11 and Figure 12). The results confirmed the utility of the immunofluorescence technique and paved the way for assessing chemokine expression through immunofluorescence.

Previously, a study in the Blay laboratory has examined the effects of chemotherapeutic agents on CXCL12 directed migration in CRC¹⁰¹. Generally, it is believed that distant organs release CXCL12 which attracts the CRC cells expressing CXCR4 on the surface. We wished to examine whether the CRC cell lines HT29 and HCT116 had any protein-level expression for this chemokine CXCL12.

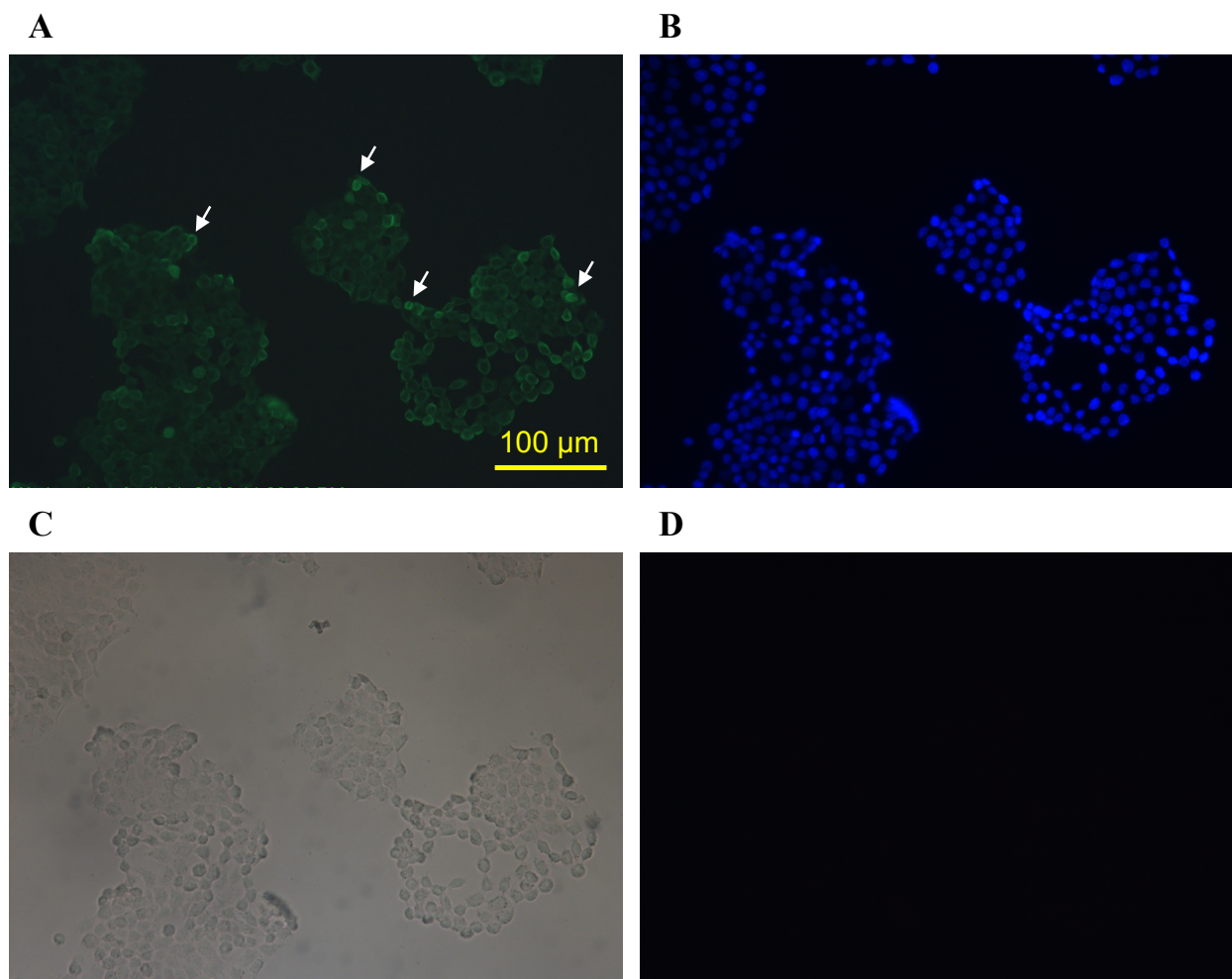


Figure 13 Immunofluorescence staining of HT29 cells for CXCL12 chemokine.

Images were taken with 20X objective. (A) Green immunofluorescence for mouse anti-CXCL12 (B) DAPI nuclei stain shown in blue (C) bright field demonstrating the cellular morphology (D) Negative control with lack of primary CXCL12 antibody. The pattern for chemokine expression is distinct in individual cells, with some cells showing increased expression of the protein (as marked by the irregular brighter spots in (A)).

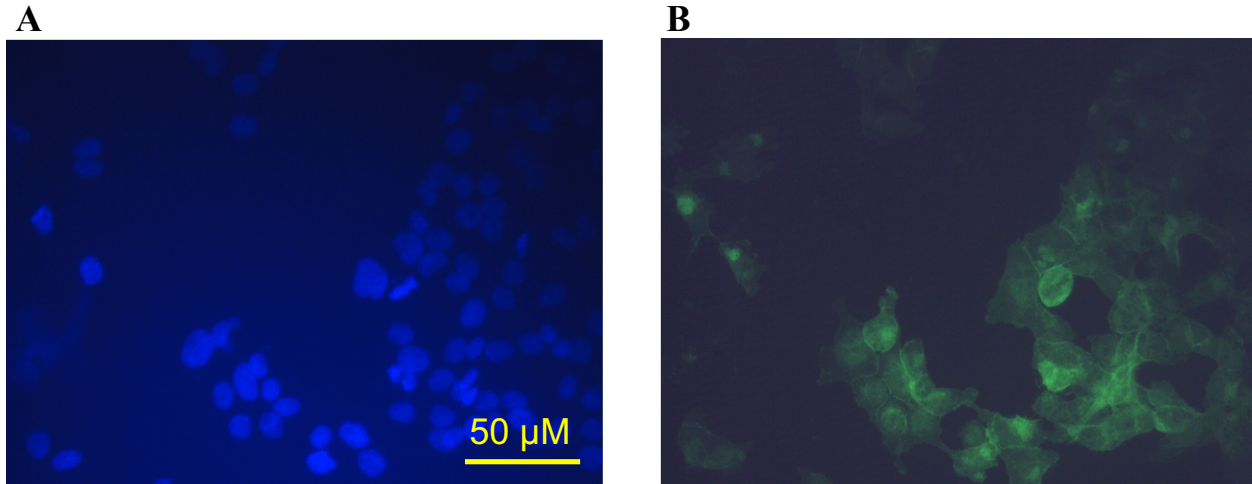


Figure 14 Immunofluorescence staining of HCT116 cells for CXCL12 chemokine Images were taken with 40X objective. (A) Blue DAPI stain showing nuclei (B) Green immunofluorescence for mouse anti-CXCL12 antibody. The staining pattern for chemokine is blurred through the monolayer and the distinct pattern in individual cells is difficult to observe.

Results from Figure 11 to Figure 14 demonstrate that epithelial marker and chemokine detection is possible through the immunofluorescence technique. This technique can help detect a loss of epithelial markers from aggressive cancer cells that are going through EMT (explained in Figure 1 and section 3.1). Successful staining of chemokines within the cells can become helpful in understanding the disease patterns in different types of cancer. There are research studies that assess how chemokines are stored and released into the environment^{159,160}. Released chemokines can be detected from the culture medium in cell lines. We employed a semi-quantitative approach to screen for chemokines present within the culture medium of the parental and resistant cell lines. Chemokine arrays built on nitrocellulose membranes provide a feasible platform to screen for multiple chemokines in one sample.

2.3.4 Secreted chemokines depict unique changes in drug-resistant HT29 cells.

Chemokine arrays are an efficient way of detecting multiple chemokines simultaneously in a quick and reliable method. Chemokine arrays can detect what is released into the extracellular environment, whereas the immunofluorescence technique lacks this feature. We obtained conditioned media from HT29 and HT29-R cells as experimental samples.

Human chemokine array kits utilized for these experiments detected 31 different chemokines in a semi-quantitative manner. Figure 15 shows that the overall trends are the same as those observed in RT-PCR and qRT-PCR (section 2.3.1 and section 2.3.2). The only exception was CCL20 as it was not detected in both HT29 and HT29-R cell line. CCL2 and CXCL12 had a relatively high expression in the resistant cell line HT29-R. In contrast, CCL15 and CXCL8 had relatively lower expression in the resistant cell line HT29-R. Figure 16 and Figure 17 demonstrates expression of chemokines from CC-group and CXC-group of chemokines respectively. The standard error is large for many markers. The negative control remained undetected in all samples and Fibrinogen was one of the sample control that was expressed in all samples. Method explained in section 2.2.4 was utilized for converting the obtained array images into the pixel density graphs.

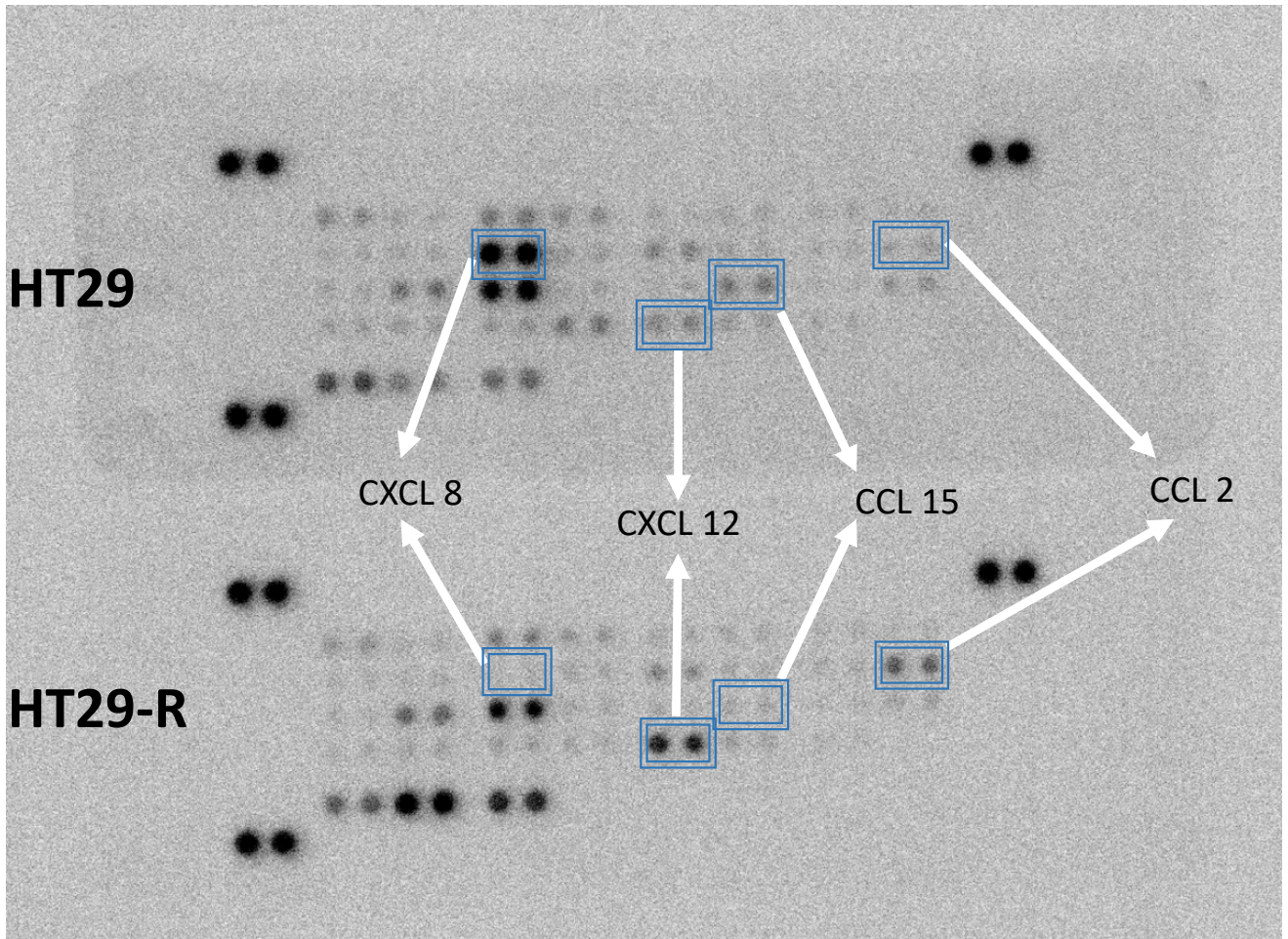


Figure 15 Representative image for chemokine array of conditioned media from HT29 and HT29-R cells. Relative changes in protein expression can be assessed by comparing the spot intensity. Each chemokine has duplicate spot on the array and the average pixel density is used in performing the comparison of changes between the parental and resistant cell lines.

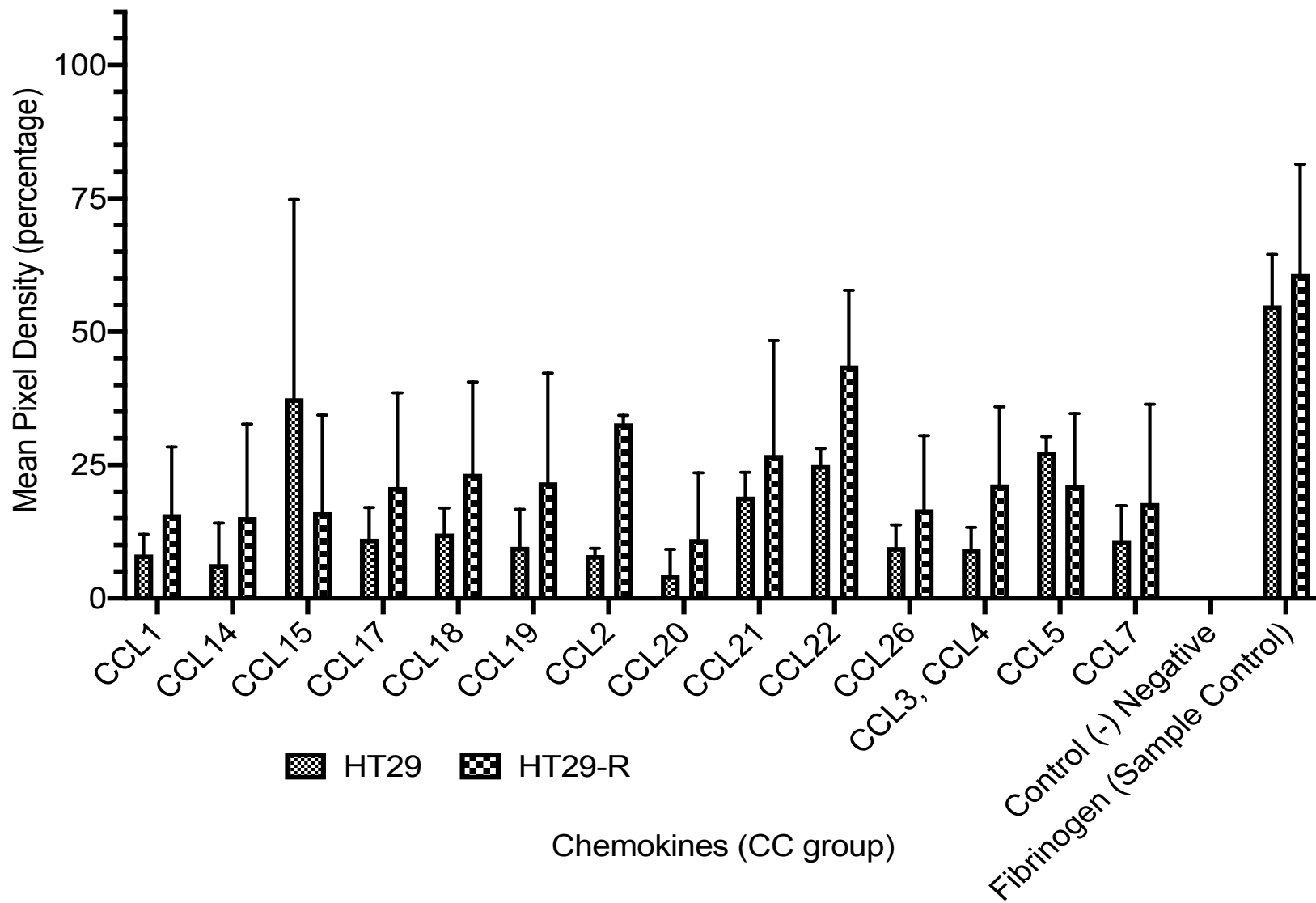


Figure 16 CC group of chemokines released in the conditioned media of CRC cell line HT29 and its drug-resistant counterpart HT29-R. The graph is prepared from three independent replicates with the standard error displayed on each bar.

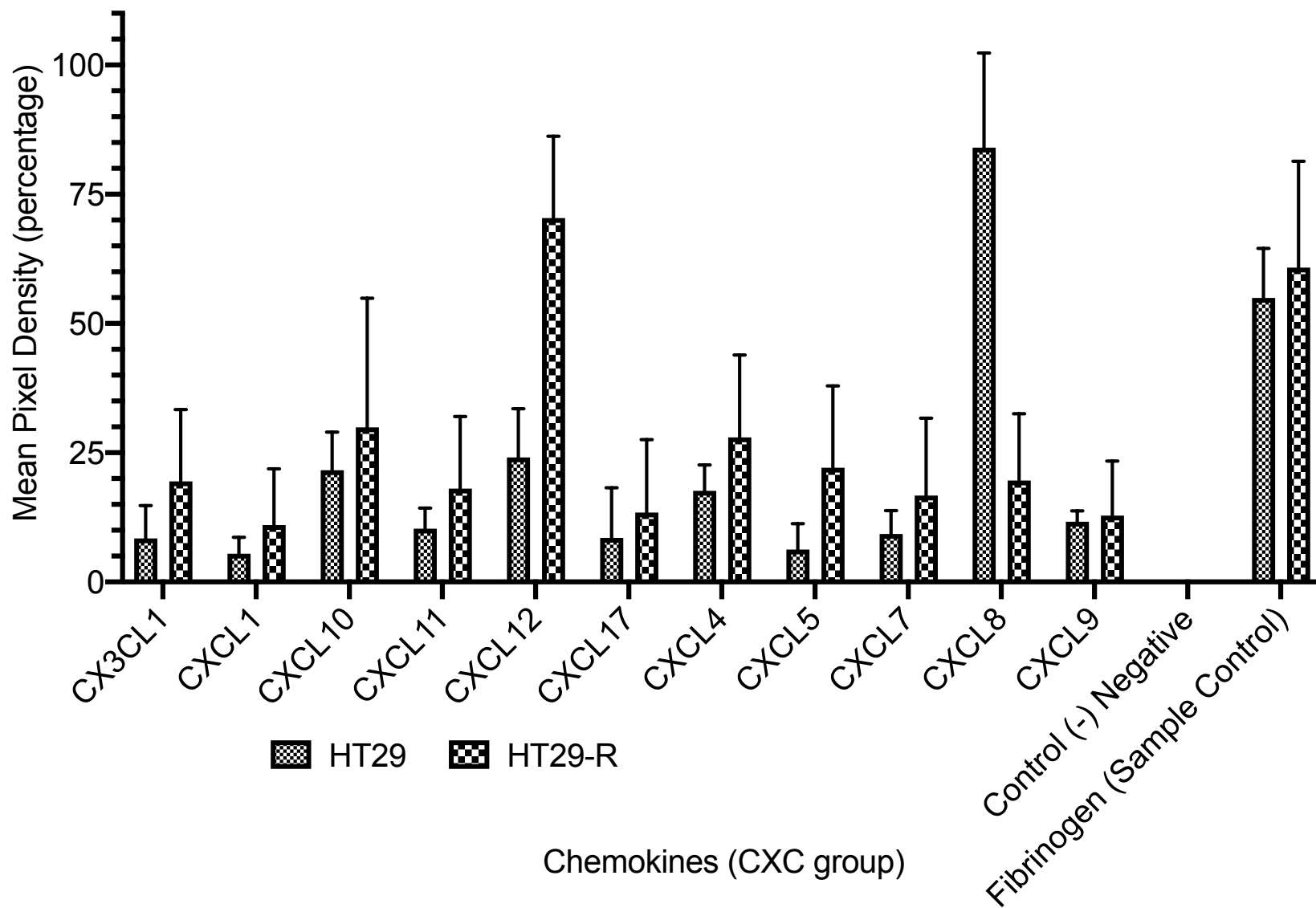


Figure 17 CXC group of chemokines released in the conditioned media of CRC cancer cell line HT29 and its drug-resistant counterpart HT29-R. The graph is prepared three from independent replicates with the standard error displayed on each bar.

2.3.5 Preliminary migration studies that assess microenvironmental effects of chemokines

It is evident from Figure 18 that a significantly high number of HCT116 cells are able to migrate through the extracellular matrix and be attracted towards the bottom chamber containing HepG2 cells. When the HepG2 cells are absent from the bottom chamber, HCT116 cells in the top chamber are not able to migrate through the ECM layer and pores and hardly any migration is observed. In the migration experiments, HCT116 cells migrated significantly more in comparison to HCT116-R, HT29, and HT29-R cells. Transwell results are different between the two groups – HT29 group and HCT116 group (Figure 18). Contrasting pattern was observed between the two groups as the HCT116 group had relatively higher migration for the parental line, and HT29 group had relatively higher migration in the resistant line. If we exclude the drug-resistant lines, it can be seen how HCT116 cells are more migratory compared to HT29. It is possible that HCT116 cells are more mesenchymal in nature, and HT29 cells are more adherent to the ECM proteins. Through *in vivo* studies, it is known that HCT116 cells are capable of forming tumours in mice and they are relatively more aggressive compared to HT29 cells¹⁶¹. However, it was contrary to our expectations that the HCT116-R cells migrated in very low numbers compared to the parental HCT116 cells. There could be different factors yielding this outcome. It is important to note that the parental cells were made resistant *in vitro* over a course of 12 weeks. It is possible that HCT116-R cells have switched into autophagy hindering any migration and functional activities in order to survive the stress from the chemotherapeutic agent SN38. It is also possible that HCT116-R cells lack the receptors for the chemokine that is driving the migration. Blocking the chemokines upregulated in HepG2 cells conditioned media could stop the migration of HCT116 cells and this can provide the link to mechanism for migration pathway towards hepatocytes. This can be an objective for a future study that extends this work.

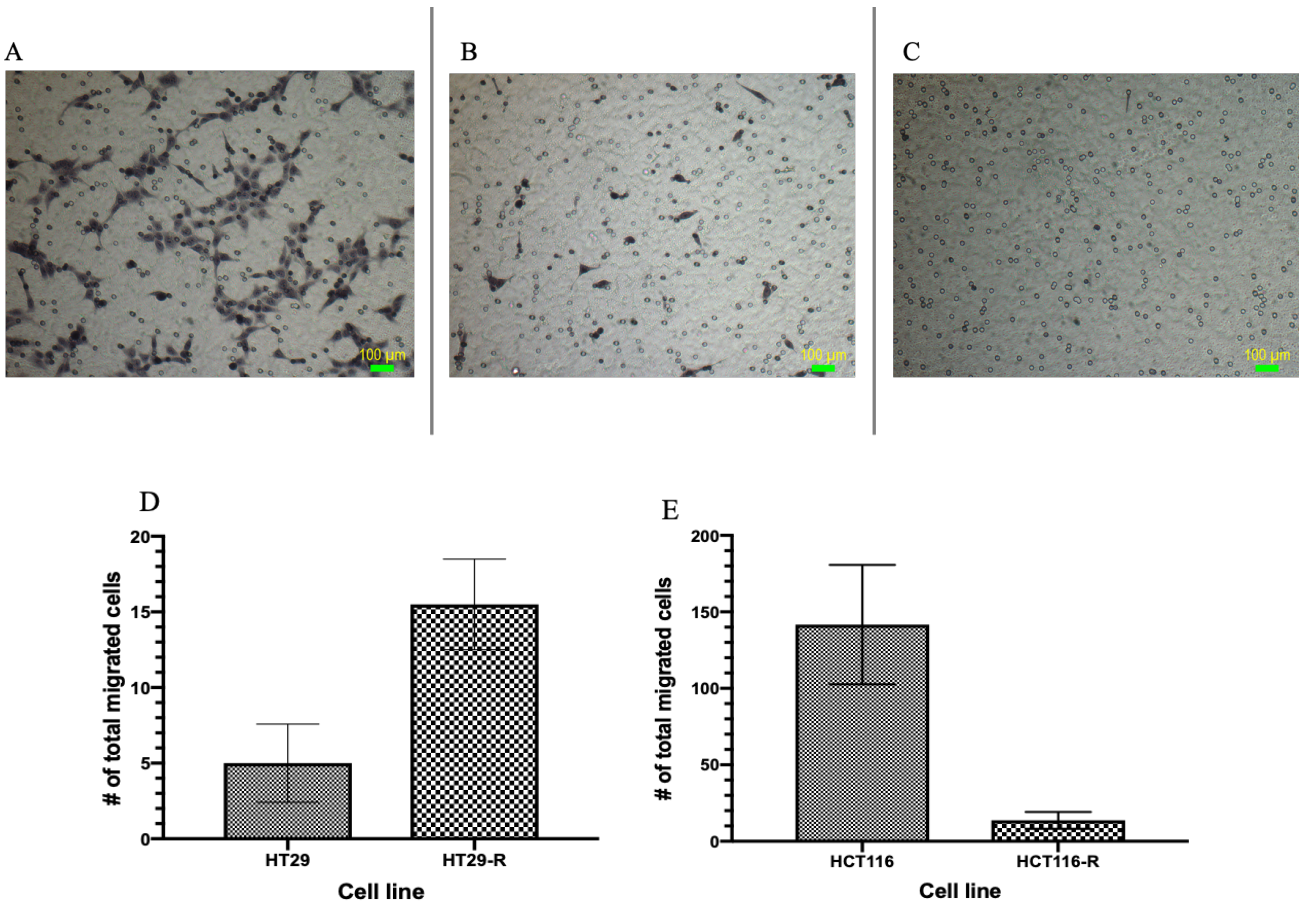
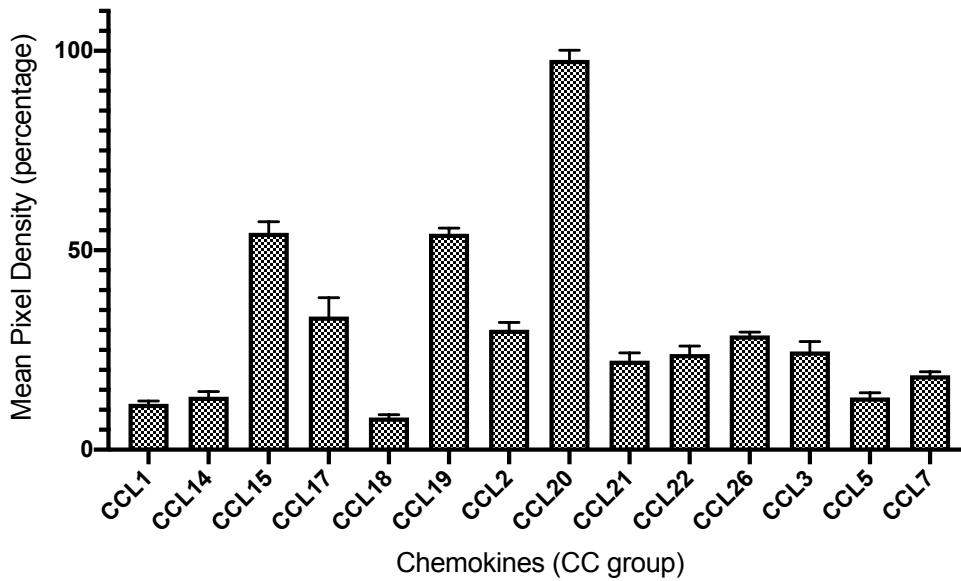


Figure 18 Representative figures from 3 independent experiments showing the ability of CRC cells to migrate. Images were taken with 40X objective. (A) HCT116 and (B) HCT116-R cells to migrate through the fibronectin and collagen type I matrix towards HepG2 cells in the bottom chamber. (C) control well with HCT116 cells in the top chamber and no HepG2 cells in the bottom chamber. (D & E) Quantified comparison of migratory potential of two parental CRC cell lines and their SN-38 resistant counterparts. Results are indicative of three independent replicates.

Opposite patterns are observed in the two groups (Figure 18). The HT29 group had a very low number of cells migrate through the membrane pores. Out of the four cell lines, the HCT116 cells were found to be the most migratory. The HepG2 cells confluency was also kept consistent across the experiments and the number of CRC cells plated in the transwell chambers also stayed consistent. These experiments did not have a group where the membranes were not coated with the extracellular matrix proteins.

Based on the observations here, it can be postulated that HepG2 cells release a chemoattractant in the media that are propagating CRC cells to migrate through the ECM. Hence, we wished to look at the profile of chemokines released in the conditioned media from the HepG2 cells (Figure 19). It is understood that once the CRC cells cross the endothelial barrier, they begin interactions with the hepatocytes⁵⁸. In the Blay laboratory, we had HepG2 cells available which possess similarities with the liver parenchymal cells. Chemokine array from the media of HepG2 cells was utilized in understanding potential chemokines attracting the CRC cells. It was observed that CCL20 and midkine were highly expressed in HeG2 cells when compared with the rest of the panel (Figure 19).

A



B

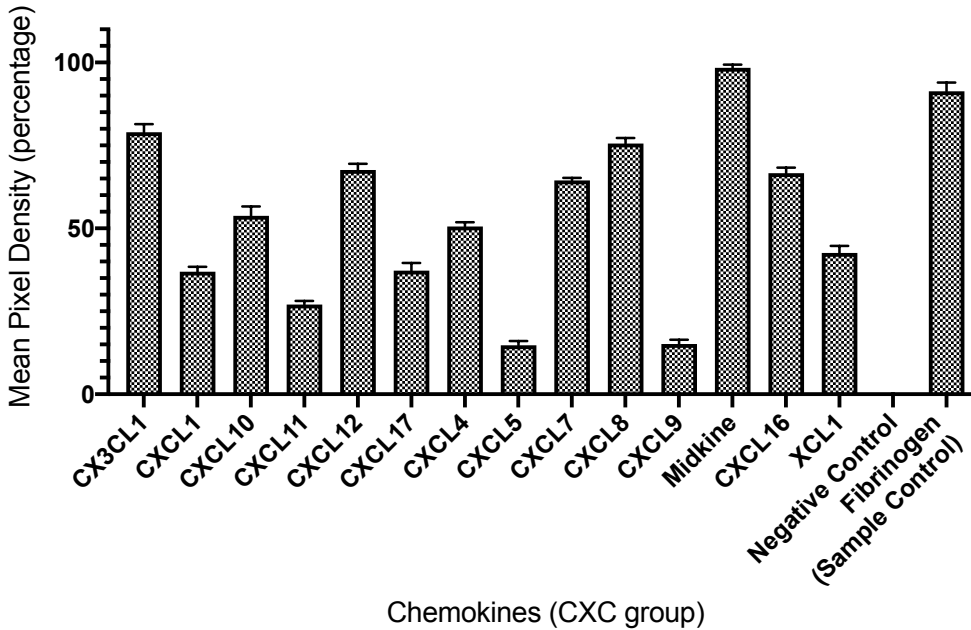


Figure 19 A & B Chemokine array of HepG2 cells' conditioned media from three independent experiments. The three reference spots in three experiments were equally positive and the sample control was fibrinogen.

The two chemokines with the highest intensities were Midkine and CCL20. Midkine and CCL20 could be the two chemokines that can be followed up further in functional experiments assessing interaction of HepG2 cells and colorectal cancer cells. Table 7 below provides a list of potential chemokines that can be studied further for their capabilities in attracting HCT116 cells.

Table 7 HepG2 conditioned media array: Trends observed based on the visual spot intensity.

| Light density spots (+) | Medium density spots (++) | High density spots (+++) |
|--------------------------------|----------------------------------|---------------------------------|
| CCL21 | CXCL7 | Midkine |
| CCL22 | CXCL16 | CCL20 |
| CCL17 | Chemerin | |
| Lymphotactin | IL-8 | |
| | CXCL10 | |
| | CXCL12 | |
| | CCL15 | |
| | CX3CL1 | |
| | CCL19 | |

2.4 Discussion

Understanding how the inflammatory microenvironment promotes tumour progression can lead to discovery of potential targets and pathways to intervene. There is evidence to show that many immune system cells are found to infiltrate the microenvironment at secondary sites³¹. For instance, there are studies demonstrating the role of tumour associated macrophages (TAMs) and how they can either possess an M1 phenotype that is tumour suppressing, or an M2 phenotype that is tumour promoting^{162,163}. Other myeloid derived cells can also infiltrate tumour microenvironment^{164,165}. Chemokines are driving factors that could decide the combination of cells that arrive in the tumour microenvironment and favour metastatic growth at secondary sites. In order to drive specific cells to the right location, chemokines act as messengers. Based on this rationale, I assessed the changes in chemokines that are derived as a result of the acquired drug-

resistance. The model we used was of CRC cell lines HT29 and HCT116 and their drug-resistant counterparts HT29-R and HCT116-R.

Chemokine receptors were included along with the chemokines in the original screening to explore any autocrine and paracrine signalling that might be evident for any of the targets. From the original screen, it was mostly the chemokines that depicted changes between parental and drug-resistant cell lines. Many receptors did not show changes at mRNA level, and many were not even detectable. There is a possibility that treatment with ligand(s) is required for receptor expression¹⁶⁶. For instance, NF-kappaB is a transcription factor that has been shown to induce CXCR4 expression in breast cancer cells¹⁶⁷. The other possibility is that not all chemokine receptors are present on CRC cell lines.

Out of the original screen, the targets that showed consistent and promising changes in endpoint PCR include CCL2, CCL5, CCL15, CCL20, CXCL8, and CXCL12. Same trends were observed when these targets were quantified for gene expression using qRT-PCR. Through literature, it is known that trends observed in gene expression and functional protein activity do not always correlate¹⁶⁸. It is important to assess whether the chemokines highly expressed at the gene level are in fact produced and released into the surrounding environment. Assessing this would provide further confirmation about the functional changes between parental and resistant CRC cells. Cell culture supernatant or conditioned media was analyzed for the presence of chemokines in HT29 and HT29-R cells using the chemokine array kits. The semi-quantitative and relative comparison of multiple targets revealed the same pattern for potential chemokines noted in Table 6. Some of these trends also aligned with changes that one might expect to see with disease progression in CRC. For instance, CCL2 is upregulated in the resistant cells and it is known through literature that it has a functional role in promoting the transendothelial migration in

liver¹⁶⁹. Migration studies with liver endothelial cells and CRC cells can be used to assess whether blocking CCL2 with neutralizing antibody impairs the migration of CRC cells. CCL2 and other chemokines of interest can be quantified using ELISA to obtain total protein concentration from the conditioned media. Time interval studies can show whether chemokine levels change as the cell culture ages and it can also be done at different passages. The in vitro data can then be followed up with animal studies and detecting chemokine levels in microenvironment or tissues.

We were also interested in trapping the chemokines within the Golgi apparatus and identify them with immunofluorescence. Hence, we performed an immunofluorescence experiment using Brefeldin-A, a reagent to induce a golgi-block for different incubation periods (data not shown). We were able to detect the expression of CXCL12, but not for CCL2. The CCL2 antibody was tested at different dilution including 1:250, 1:500, and 1:1000 and resulted in no signal. The CCL2 antibody utilized was a function-blocking antibody that was not validated for the immunofluorescence effect. In theory, it should still be able to bind to the target. It was observed that the cell morphology had changed at longer incubation periods (≥ 24 h) with Brefeldin-A as it is damaging to the cells. Lower concentrations and shorter duration studies can be carried out to explore this further. The results were, however, very preliminary to include here.

Another aspect to explore can be co-culture studies of chemokines with specific leukocyte population in Transwell[®] experiments. This can provide an insight into microenvironment infiltrates and signalling that supports metastatic growth. Chemokines are better understood from the inflammation perspective, and their role in malignancy has also been established. The process of diapedesis for white blood cells during an injury is a well-known example of how cancer cells are hypothesized to cross the endothelial barrier¹⁷⁰. The circulating chemokines in blood are instrumental in movement of specific cells to the location of interest. Studying the types and

concentrations of chemokines present in the blood can help deduce the state or severity of inflammatory processes such as cancer. Many groups have started exploring the relationship between plasma chemokines and prognosis in different types of solid cancers¹⁷¹⁻¹⁷³.The next chapter details our work on plasma chemokines from breast and colorectal cancer patient samples.

3. Chemokines and their analysis in plasma of colorectal and breast cancer patients

3.1 Background

There are various studies showing a correlation between the plasma chemokine levels and their implications in different types of cancer¹⁷¹⁻¹⁷³. It is interesting to note that the same chemokine can be favourable or unfavourable depending on the type of cancer¹⁷⁴. Upregulation of some and downregulation of other chemokines are associated with different types of solid tumours^{175,176}. CCL2, CCL5, and CCL20 have been identified as biomarkers in atherosclerosis, diabetes, and inflammatory diseases of the skin and gut¹⁷⁷. As explained by Dell'Angola, and Biragyn, chemokines are master controllers of migration and recruitment for various subsets of immune cells and malignant cells¹⁷⁸. Comparison of plasma chemokines with tissue expression has been widely investigated to understand specific patterns and pathways in cancer progression. It is important to identify which chemokines are responsible for driving a specific set of immune cells to the tumour tissue. Tumour cell migration can be driven through secondary tissue expression and released chemokines in the plasma that generates a directional gradient. This area is challenging as there are multiple chemokines and their plasma levels fluctuate in different individuals depending on their comorbidities. Pointing at one particular chemokine being responsible for promoting tumour progression requires a thorough study of patterns in a large set of individuals, comparison with tissue expression, and specific studies looking at functional consequences. One group (Thomas *et.al.*) has recently shown a trend between some of the CC group of chemokines and breast cancer progression¹⁷³. In the same study, there is a correlation between high mRNA levels of CCL 7,8,17,20, and 25 and decreased overall survival¹⁷³. Another study by Lubowicka *et.al.* demonstrated that ELISA measured plasma CCL2 levels were significantly higher in the

breast cancer group compared to the control group with benign breast tumours and healthy samples¹⁷⁹. A different study in breast cancer group found high levels of CCL2 and CCL5 in the estrogen-positive breast cancer patients¹⁷⁶ and this shows how certain chemokines can also be related to the sub-types within solid tumours. Some groups have attempted to compare the tissue and plasma expression of chemokines in different types of cancer^{180,181}. Niwa *et.al.* carried out a study that analyzed CCL5 levels in both tissue and plasma of breast and cervical patient samples along with healthy subjects¹⁸⁰. Looking at the elevation of plasma CCL5 in some healthy subjects – it was speculated that the unexplained increase in plasma chemokine could be from the platelets. Some studies have stressed the need to perform the analysis of platelet-poor plasma¹⁸²⁻¹⁸⁴. This is a technical issue when measuring chemokines from plasma. Certain chemokines measured from serum instead of plasma can also provide a significantly different result^{185,186}. The addition of anticoagulant like EDTA can result in a collection of plasma containing platelets following the centrifugation.

The presence of plasma chemokines is also being looked at in the context of microenvironmental consequences. For instance, a study by De La Fuente Lòpez *et.al.* correlated the plasma levels of CCL4 with the increase in pro-tumour macrophage CD163¹⁸¹. The studies discussed here demonstrate a need to carefully assess individual chemokines and also look at the pattern between the changing levels within a specific type of cancer and stratifying the results based on patient-specific factors.

Considering the challenges and limitation of these studies, we aimed to examine the relative plasma levels of different chemokines using the chemokine arrays. We were able to examine stage IV colorectal and breast cancer patients between each other as well as a comparison using the plasma from healthy volunteer samples. Some patients were able to provide further

samples at a 6-months and a 12-months interval. This comparison is also important as the individual plasma chemokines can change with the disease progression. Chemokine levels at different time-intervals, patients' response to therapies and whether or not they relapse can provide valuable information.

3.2 Materials and Methods

3.2.1 Coordination of blood sample procurement

The patient blood samples contained lithium heparin as the anticoagulant and they were picked up from the Grand River Regional Cancer Center within 30 min of collection and processed within 4 hours from the time of collection. The samples were kept between 2-8°C prior to processing. Special biohazard bags were used during transportation of the tubes and the information was de-identified for labelling the tubes. Procedures were followed as per the research ethics protocol approved through the University of Waterloo (ORE #21303) and Tri-Hospital Research Ethics Board (THREB #2016-0586). Approval copies are included in Appendix VI. In total, we have had 14 stage IV patient samples from the CRC group, and 7 stage IV patient samples from the breast cancer group. Healthy volunteer blood was collected as per the University of Waterloo Office of Research Ethics (ORE #31549) protocol. No compensation was provided for the patient or volunteer samples and the personal information of donors was kept deidentified. Details related to the disease progress of each patient were kept in an encrypted file and any printed material was kept in a locked cabinet within room PHR3021 at the School of Pharmacy, University of Waterloo.

3.2.2 Array Analysis

The method described in section 2.2.4 was followed for processing these samples. The array spots were measured from duplicate spots and the intensities were averaged. Each result was normalized using the reference spots.

3.2.3 Statistical analysis and patient characteristics

Statistical analysis of the results was carried out using the Prism GraphPad[®] software. Since only a single patient sample was received at each time point, there was no possibility for replicates within these results. A few months following the initial blood donations, two patients withdrew from this study as they were discouraged with their disease progression and their withdrawal was not in any-part due to the burden from any of the study procedures. Table 8 shows patient samples stratified by their metastatic location.

| A | | | B | | |
|--------------------|------|--------------|--------------------|-------|-------------|
| Colorectal Cancer | | | Breast Cancer | | |
| Site of metastasis | | | Site of metastasis | | |
| Liver | Lung | Lung + Liver | Lungs | Bones | Lymph nodes |
| 2 | 8 | 5 | 16 | 3 | 10 |
| 6 | 12 | 7 | | 9 | 13 |
| 17 | 21 | | | | 14 |
| 19 | | | | | 15 |
| 21 | | | | | |

Table 8 Distribution of patients based on tumour type and metastatic location.

Note: we did not have details for patient 1, 4, 11, 18, and 20.

3.3 Results

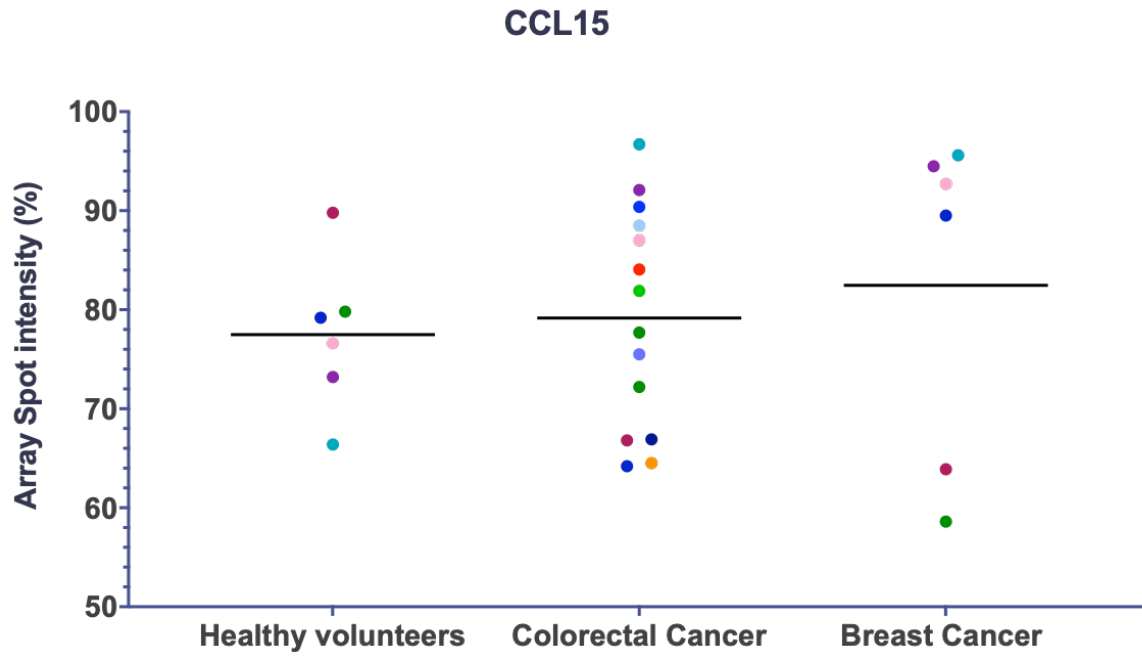
The semi-quantitative levels of plasma chemokines were investigated in both colorectal and breast cancer groups in comparison with the healthy volunteers. *Appendix V: Raw analysis plots of individual patients at 0 and 12 months* shows the semi-quantitative and relative expression of 31 different chemokines across 4 patients at different time points. Figure 20 shows six out of

the thirty-one chemokines plotted for all of the volunteer and patient samples received. Five of the six chemokines shown in Figure 20 were of our primary interest due to the results observed in section 2.3.2 and 2.3.4 that looked at the expression in CRC cell lines. A wide distribution of plasma CCL15 levels was observed in the CRC group (Figure 20A). The trend in breast cancer group is difficult to compare due to the lack of enough samples. Overall, the differences remained insignificant with the number of samples analyzed. The plasma CXCL8 levels remained low (below 10% array spot intensity) in most of the samples across all three groups and no significant differences were observed between the means (Figure 20B). The plasma levels for CXCL12 were relatively high (mean array spot intensity above 85%) in all three groups, however the means were very close and no significant differences were observed (Figure 20C). Similar pattern was observed for CCL5 in all three groups, and no significant difference between the means were observed (Figure 20D). Next, we analyzed CCL2 plasma levels and the array spots mostly had no expression. As evident from Figure 20E, the levels for most of the samples remained undetected. The values are negative for some of the samples as the array intensity spot was lighter than the overall background value. Lastly, looking over the overall data and comparison it was observed that the midkine had higher expression in CRC and breast cancer group when compared with the healthy volunteers. Midkine was not originally a chemokine of interest, but the results observed in Figure 20F depicted an upward trend. Further samples in healthy volunteers and breast cancer group can confirm this finding.

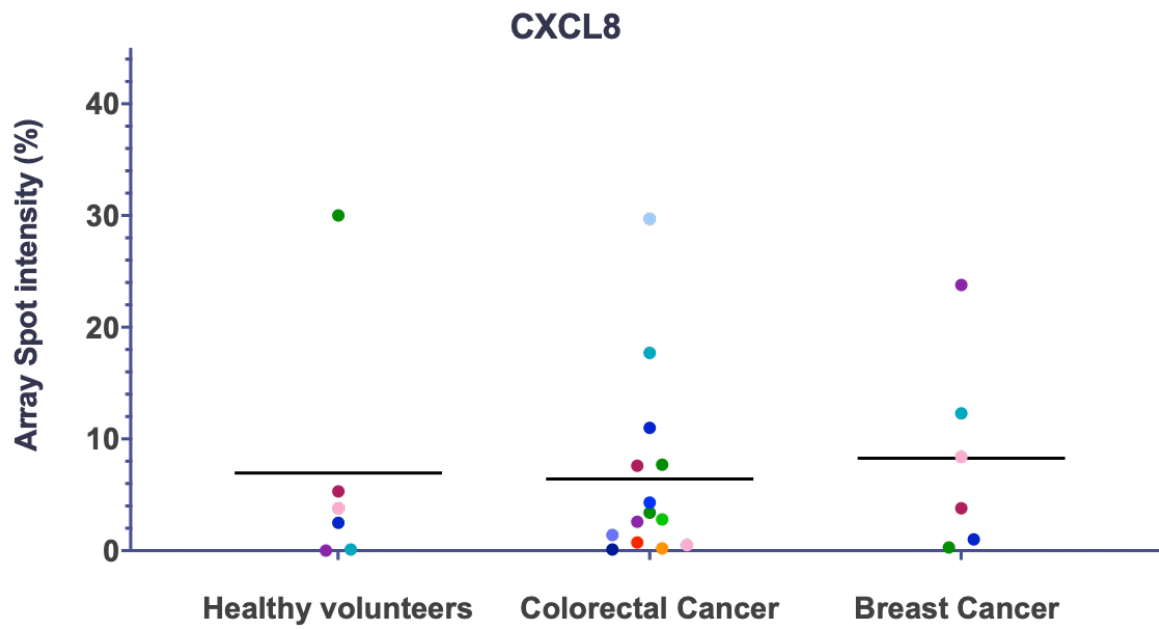
The relative expression of CCL15 mostly ranged between 55-95% in all three groups. The percentage means (with standard deviation) of healthy volunteers, colorectal cancer, and breast cancer group were 77.5 (± 7.8), 79.1 (± 11.1), and 82.5 (± 16.6) respectively. The relative expression of CXCL8 ranged between 0-30% in all three groups. The percentage means (with standard

deviation) were very close to each other and they were marked at 7.0 (± 1.5), 6.4 (± 8.3), and 8.3 (± 8.9) for healthy volunteers, colorectal cancer, and breast cancer group respectively. The relative expression of CXCL12 ranged between 70-100% with two exceptions in the breast cancer group. The percentage means (with standard deviation) were within a close range: healthy volunteers at 85.9 (± 6.4), colorectal cancer group at 88.3 (± 11.7), and breast cancer group at 89.9 (± 16.4). The relative expression of CCL5 had a wide range from 60-100%. The mean levels of CCL5 remained similar between the healthy volunteers and the colorectal cancer group – 84.6 \pm 12.9 versus 85.3 \pm 11.1 respectively. There was an upward trend in the breast cancer group with a mean of 91.3 \pm 13.5. The relative expression of CCL2 remained mostly undetected across all three groups. There are some negative values due to the software calculation assessing the background intensity as being higher than the spot intensity. Midkine showed a wide distribution for the expression level amongst colorectal and breast cancer patients. The levels in the healthy volunteer group remained mostly below 21%. However, the colorectal cancer and breast cancer group had a sample reaching over 100%* and 93% respectively. The three individual percentage means of the healthy volunteer group, colorectal cancer group, and breast cancer group were found to be 11.2 (± 8.5), 26.8 (± 29.8), and 51.7 (± 32.4) respectively. It is important to note that these are relative values and these numbers are in comparison to the average spot intensities of the reference spots.

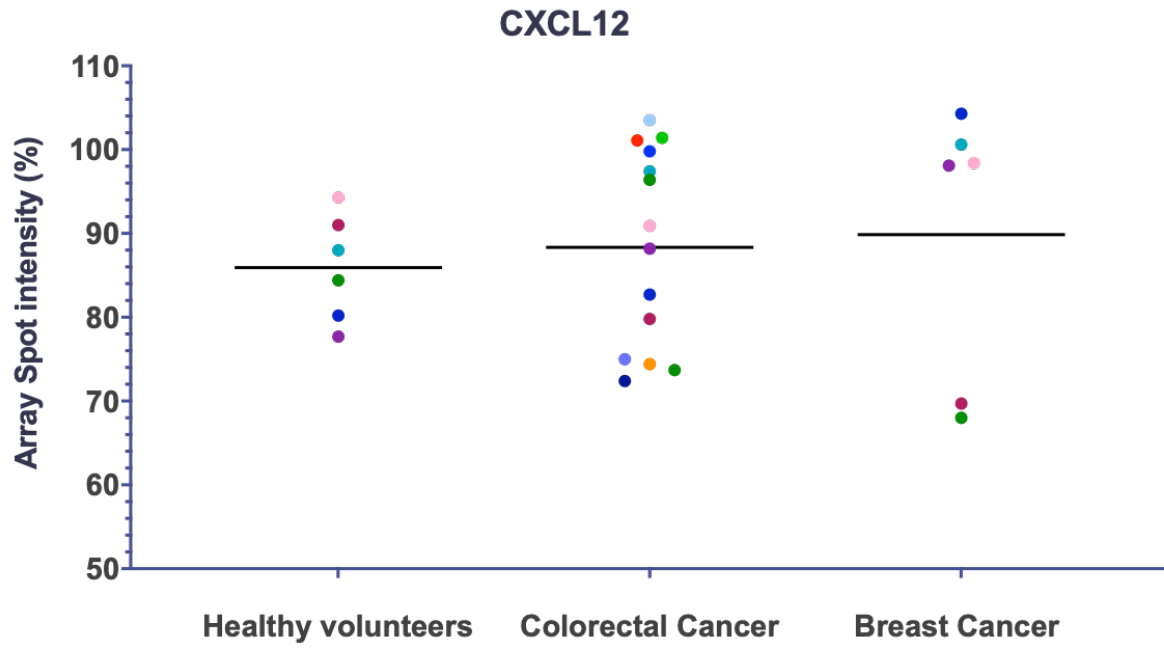
A



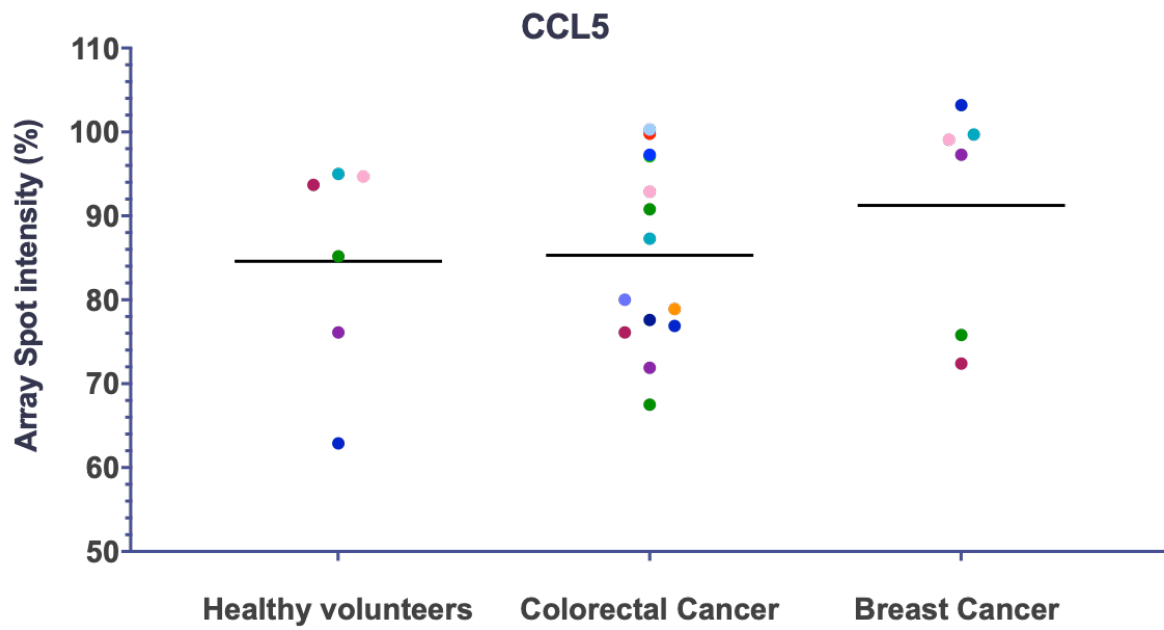
B



C



D



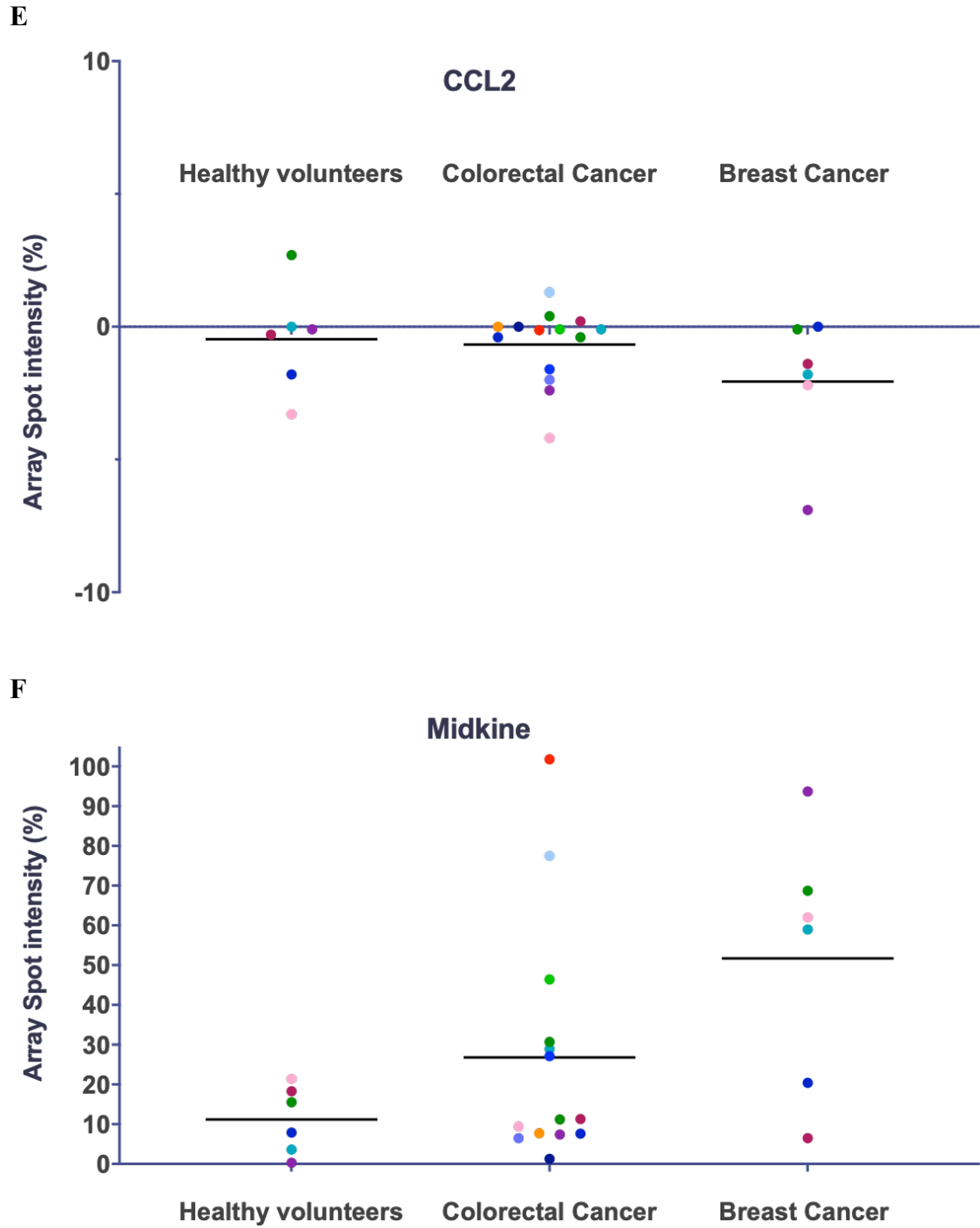


Figure 20 Relative comparison of plasma chemokines amongst healthy volunteers, CRC and breast cancer patients. The number of samples were not equal in the three groups and varied at n=6 for healthy volunteers, n=14 for colorectal cancer group, and n=6 for breast cancer group.

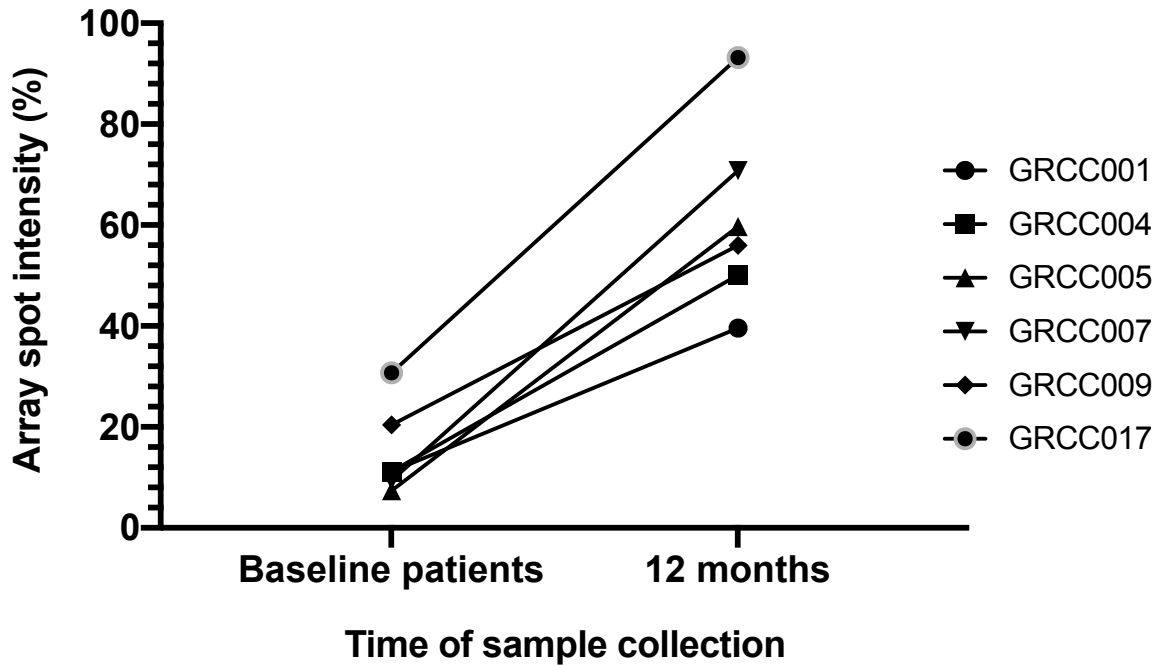


Figure 21 Changes in plasma midkine level among six patients with disease progression at 12 months. A clear upward trend is observed in the 12 months samples for all six patients.

The midkine data observed in Figure 20 prompted further investigation. We sought to compare the plasma levels in healthy volunteers with that of the baseline samples received and 12 months samples received from the same patients. Baseline samples were the first samples that we received from each patient. The term ‘baseline’ did not have any correlation with where in patient’s disease progress their first sample was collected. Figure 21 shows that the plasma levels in healthy volunteers and baseline samples were very similar and stayed below 20% in most cases. The 12-months samples from the same patients had more than double the array spot intensities when compared respectively.

3.4 Discussion

A comparison of various plasma chemokines across different patients and healthy volunteers helped in understanding patterns relating to the disease progression. It was observed that certain plasma chemokines were already present in a high amount in healthy volunteer samples. The reproducibility of plasma chemokines in the healthy volunteers is usually consistent. A study by Agalliu *et.al.* demonstrated a three-year within-subject reproducibility for multiple plasma chemokines in healthy human volunteers¹⁸⁷. Drawing parallels between the *in vitro* and *ex vivo* data can further our understanding of the disease models that we employ in the laboratory. For instance, CXCL12 was one of the chemokines of our interest from the qPCR data of HT29 and HT29-R cell lines. The conditioned media from HT29-R consistently revealed a high level of CXCL12 compared to the parental line and we attributed this increase to the development of *in vitro* drug-resistance. In plasma samples, the spot intensity for CXCL12 (SDF-1) was mostly between 80-100% across both cancer groups and the same was noted for healthy volunteer pool as well. Since the values from healthy volunteer pool were incipiently high, it was difficult to attribute the increase in plasma CXCL12 was due to the disease progression. For future analysis, a stability study of chemokines following the blood collection can reveal if any expression changes are attributable to the degradation of chemokines *ex vivo* after collection.

Looking at other chemokines of interest, such variability was noticed between the data from cell-lines and plasma samples. Patient characteristics such as tumour type and stage, chemotherapy, relapse, and location of the CRC can all be used to stratify the patients and identify patterns that correlate with disease progression. Looking at the scatter plots for the chemokines of interest, we can depict patterns, however, it is difficult to draw any firm conclusions. Since we have only looked at 6 samples from the healthy volunteer pool, it is required that further volunteer

samples are analyzed. The healthy volunteers pool mostly consisted of the younger individuals around the age of 30. On the contrary, the patient samples being compared are from the older age groups (above 50 years) and such factors might bring in variation in plasma chemokines. Other comorbidities including any acute or chronic inflammatory conditions can also skew the results and hinder a clear comparison. Age and sex-matched volunteer samples would be valuable for comparison of plasma chemokines in this project.

The level of plasma CCL2 remained undetected in both healthy volunteers and CRC patient samples. This is consistent with a study of 66 Japanese CRC patients that had undetected levels of CCL2 in plasma samples¹⁷¹. From Figure 20B, it can be observed that CXCL8 plasma levels mostly remained the same as that found in the healthy volunteers. There were some patient samples where a slight elevation was marked. However, more samples and further stratification can provide insight into why certain patients have an elevated level. Through literature, CXCL8 is found to be elevated in serum and tissue of various late-stage cancers^{188,189}. A study by Kantola *et.al.* assessed TNM stage-dependent changes in CXCL8 and CCL2 plasma levels in colorectal cancer¹⁹⁰. It was found that CXCL8 plasma level gradually elevated from stage I to stage IV and the finding was significant. CCL2 had an increasing trend from stage I to IV, however, the finding was not significant.

Midkine was not one of the chemokines that were originally of interest. However, it was noted through the analyzed data that between baseline and 12 months patient samples, it was consistently increased in the plasma. Midkine plasma levels in the healthy volunteer samples were also relatively lower when compared to the 12-months samples. The importance of midkine has been reported in the literature across different malignant disease states^{191,192}. A study conducted by Krzystek-Korpaczka *et.al.* demonstrated that gene expression of midkine was significantly

upregulated in stage III CRC and it was associated with lymph node metastasis¹⁹³. In the same study, the serum concentration of midkine in the early postoperative period was measured and compared with the pre-operative levels. A significant drop was noticed within 24h of surgery, however, the levels rose again at 48 and 72h¹⁹³. A study conducted by Ibusuki *et.al.* compared the plasma midkine levels of patients with breast cancer at different stages and healthy volunteers¹⁹⁴. The proportion of individuals with elevated plasma midkine levels increased gradually starting from the healthy volunteers to the groups with ductal carcinoma in-situ, primary invasive breast cancer without distant metastasis, and distant metastatic breast cancer¹⁹⁴. The tissue expression of midkine mRNA in breast and colorectal cancer also follows a similar pattern^{195,196}. Jones DR has assessed the utility of midkine as a biomarker and compiled a list of studies that assessed midkine expression in different types of solid cancers¹⁹⁷.

It is important to distinguish that chemokines circulating in plasma may be a result of different biological processes co-existing during cancer progression. One cannot simply assume the source of increased plasma chemokine to be the tumour tissue. There are examples of secondary distant organs releasing the chemokines in order to attract cells with specific receptor types¹⁰¹. Whether or not the chemokines released from cancer cells dictate their survival and metastatic journey remains a research question. Therefore, it is essential to understand the chemokines expressed by and released by tumour cells while they are in their metastatic journey. Isolating circulating tumour cells and characterizing them enables this investigation further. The next chapter of this thesis elaborates on the technical development of isolating CTCs and showcases possibilities for characterization of isolated cells.

4. Capturing circulating tumour cells from colorectal and breast cancer patients

4.1 Background

The term ‘precision medicine’ is often discussed these days and the central idea here is to identify and provide patient-centered therapies. One of the tools under precision medicine is liquid biopsy, and the National Cancer Institute, United States defines liquid biopsy as “a test done on a sample of blood to look for cancer cells from a tumour that are circulating in the blood or for pieces of DNA from tumour cells that are in the blood”^{198,199}. In 1869, Ashworth had first reported cells found from a person’s blood that resembled cells from that individual’s tumours²⁰⁰. Beginning in 1955, successive *in vivo* studies have shown that circulating tumour cells (CTCs) can be detected in the general circulation during the natural progression of solid tumour growth – even prior to detecting established metastases^{200,201}. Tumour cells are capable of travelling as clusters and this may also serve to protect them from the stresses faced in circulation¹⁹. In seeking possible clinical implications for defining prognosis and overall survival, detecting CTCs in the general circulation of cancer patients has become an area of interest. Many studies have used the number of CTCs found as a predictive biomarker for guiding treatment selection, therapeutic efficacy, and survival expectancy¹⁹. It has also been recognized that there is a greater need to characterize the CTCs periodically to understand the tumour behaviour and deal with unexplained results of disease progression that are based on CTC enumeration alone²⁰². Flow cytometry has been suggested as a platform that can efficiently isolate different sub-types of cells based on marker expression. Fluorescence-activated cell sorting is a step beyond normal flow cytometry as the cell-sorting would allow downstream analysis of isolated cells.

There are numerous technological advances aimed at isolation of circulating tumour cells. Ferreira *et.al.* have thoroughly reviewed CTC enrichment strategies based on immunoaffinity, biophysical properties, and functional assays²⁰³. Many of the studies undertaken based on immunoaffinity utilize epithelial markers such as cytokeratin (CK) 8,18,19, and epithelial cell adhesion molecule (EpCAM)¹⁹. The techniques that rely on immunoaffinity can be divided into two broad categories – positive selection and negative selection. EPIC, FASTCell™, and CytoTrack™ are examples of positive selection methods as they rely on CK, CD45, and DAPI for identification of CTCs. EasySep™ is an example of the negative selection technology as it removes all of the hematopoietic cells from the whole blood sample without requiring lysis or density-separation of red blood cells. However, the remaining product is a large volume of plasma with possible CTCs that requires further isolation. Some groups have utilized a multi-pronged approach and combined positive selection techniques with a microfluidic device²⁰⁴. Meunier *et.al.* showcased a combination of filtration and functional antibodies to capture CTCs from spiked blood samples with a high capture efficiency²⁰⁵. Studies that are only conducted on spiked blood cells require an extension to real patient samples and a comparison with an existing commercial technique.

There are other types of techniques that solely rely on biophysical properties of tumour cells. These include size, deformability, and density amongst others. Such key features can be utilized in a separation of intended cell population from a blood sample. The challenge with size based methods is a wide variability of tumour cell size. Studies have demonstrated that size difference between tumour cells from cell-lines and tumour cells from patient samples can vary significantly. A study by Allard *et.al.* noted that cells isolated from same patient varied between 4 and 30 μM . This type of variation hinders a pure isolation of CTC population. Some studies have

utilized an electrical charge difference between native cells and tumour cells in order to isolate the enriched CTC population under an electric field. DEPArray™ system (Menarini© Silicon Biosystems) partially utilizes the microelectrics combined with microfluidics to enrich CTC population²⁰⁶.

It has been pointed out that relying on a CTC specific marker could be problematic due to the heterogeneity of isolated cells and genetic instability of tumours^{207,208}. However, there have been studies that rely on enumeration alone to predict prognostic outcomes in solid cancers. For instance, Hayes *et.al.* categorized breast cancer samples based on the number of CTCs and assessed the probability of survival²⁰⁹. It was found that the group that had more than 5 CTCs at all time points had the lowest probability of survival compared to the group that had less than 5 CTCs at all time points during the study²⁰⁹. The cut-off for colorectal cancer is different and there have also been studies that looked at the progression free and overall survival in colorectal cancer patients. A study by Tol *et.al.* divided advanced stage CRC patients by the CTC count of more than or less than 3 in 7.5mL of whole blood. It was found that CTC count prior to and during treatment independently predicted progression-free-survival and overall survival in late-stage CRC patients²¹⁰. Some groups have investigated further to assess whether the CTC counts can inform treatment plans. As an example, the study by Krebs *et.al.* speculated and gathered data that hints towards use of four-drug regimen in advanced colorectal cancer based on the CTC cut-off groups of above and below 3 per sample²¹¹.

Techniques that solely employ epithelial markers such as CK and EpCAM would not detect CTCs that have gone through epithelial-mesenchymal transition (EMT) program and therefore predominantly express mesenchymal markers or other markers of stemness²¹². As defined by Kalluri and Weinberg, EMT is a biologic process that allows a polarized epithelial cell, which

normally interacts with basement membrane via its basal surface, to undergo multiple biochemical changes that enable it to assume a mesenchymal cell phenotype, which includes enhanced migratory capacity, invasiveness, elevated resistance to apoptosis, and greatly increased production of ECM components²¹³. While going through this transition, tumour cells with invasive potential lose expression of epithelial markers E-cadherin, epithelial cell adhesion molecule (EpCAM), and cyokeratin¹⁹. At the same instance, there is an acquisition of mesenchymal characteristics and expression of cytoskeletal and adhesion proteins such as vimentin, N-cadherin and fibronectin. It is the detection of these proteins that confirms the transition of epithelial to mesenchymal form and the phenotypic change in the CTC that makes detection by conventional methods difficult.

Hence, further methodology is required to identify specific tumour traits including but not limited to stemness, dormancy, tendency towards cluster formation, and abilities to escape normal immune surveillance. In order to understand and make best use of these characteristics, the emphasis should be on understanding how the disseminated cells will behave when they reach individual organs. Diversity in microenvironment at major secondary sites and tumour cell interactions could reveal the basis of specific phenotypic features that enable cells to successfully extravasate and establish detectable metastasis.

Cancers undergo progressive phenotypic changes as the primary tumour grows. The tumour cells activate endogenous gene programs such as EMT that reflect changes in normal tissue development and homeostasis²¹⁴. The process of distant metastasis begins with the detached tumour cells finding their way into the circulating blood system, in many ways comparable to normal homing mechanisms of immune cells. In the situation of cancer, breaking free from the extracellular matrix and basement membrane is essential for intravasation into the blood

circulation. It is the resulting circulating tumour cells in the blood that are of primary interest in understanding the contribution of cells within the heterogeneous disseminating cancer cell population in tumour invasion and metastases. Due to their success in having traversed the extracellular matrix, they have usually already gone through the process of epithelial to mesenchymal transition. It is also believed that a small proportion of these CTCs exhibit markers that reflect their ‘stemness’ or stem cell-like features and both contribute to initiation of secondary growth at distant sites and treatment resistance¹⁹.

In order to identify and detect the down or up-regulation of these markers, the CTCs have to be isolated or identified amongst the pool of erythrocytes, lymphocytes and platelets from a blood sample. There are different commercial CTC detecting platforms that target different markers – most of which though employ EpCAM and CD45 as mentioned earlier¹⁹. Stemcell Technologies, Menarini Silicon Biosystems, Vitatex, and Fluxion Biosystems currently have available techniques for CTC isolation from patient peripheral blood. Using any one of their platforms, it is now possible to define the number of circulating tumour cells by the operational definition within that platform.

However, it is significantly challenging to isolate, characterize and quantify CTCs as they are relatively very low in number versus millions of nucleated resident blood cells²¹⁴. In terms of numerical comparison with leukocytes, it is estimated that one will typically find 1 CTC per million leukocytes. The EpCAM-based platforms work by isolating nucleated non-hematopoietic cells expressing EpCAM and cytokeratin. Based on the subtype of cancer, the probability of detecting CTCs in the blood samples varies substantially. For example, the frequency of detecting CTCs in prostate cancer is more than 50% compared to pancreas cancer that has a possibility of less than 25%¹⁹.

There is a need for disseminated cancer cells to self-renew in order to form macroscopic metastases²¹⁵. It is hypothesized that the process of EMT provides cells with this additional advantage of self-renewal capacity and expanded stem-cell like features. In order to spawn macrometastases at a secondary site that correspond to the primary cancer histotype, the mesenchymal, stem-like cells surviving passage through the blood circulation need to revert back to the epithelial phenotype. Hence, the reverse process of mesenchymal to epithelial transition (MET) takes place at the secondary site and the disseminated cells sequentially proliferate and differentiate to grow into a new tumour tissue that reflects to some degree the character of the primary tumour²¹⁵. Work carried out by M. Yu *et. al.* demonstrated that a dynamic flux between EMT and MET in breast cancer CTCs is detectable and also corresponds with the response to therapy²¹⁶. Using quantification of the percentages of mesenchymal and epithelial CTCs, these investigators showed that the fraction of mesenchymal CTCs increased with resistance to the targeted therapy²¹⁶.

Although it may superficially appear that there is a smooth transfer from the primary to the secondary site, it is probably no more than one cell out of billions that possesses or acquires true metastatic potential, developed and sustained through natural selection after genetic changes during tumour formation, persisting in the hostile environment of blood and eventually enabling self-renewal at a favorable secondary location. Tumour cells may travel through the circulation in conjunction with platelets, and can become capable of escaping immune surveillance by forming tumour cell – platelet aggregates¹⁹. In one animal study, it was found that mice that are deficient in the platelet-specific receptor glycoprotein IB-alpha (GPIB- α) exhibit a 15-fold decrease in the formation of lung-metastatic foci formation²¹⁷. Additionally, it is believed that α -granule contents released by platelets provide many growth-promoting factors for tumour development, including

endothelial growth factor (EGF), vascular endothelial growth factor (VEGF), and transforming growth factor (TGF)- β ²¹⁴.

Another factor that may contribute to successful tumour metastasis is “collective cell migration”. This reflects the ability of tumour cells to disseminate as multicellular aggregates or clusters. CTC clusters have been observed in some studies and there is interest as to whether or not they are relevant to stemness, EMT and tumour progression¹⁹. Further investigation is required because there is a possibility that these CTC clusters are simply due to the partial shedding of cell clusters from primary tumour emboli or random formation of multicellular aggregates with these clusters being captured at distant sites to proliferate and grow as a consequence purely of their physical size. The idea that aggregation influences cell phenotype challenges other observations for which metastasis is has been fully attributed to EMT or stem cells being responsible for the initiation of secondary tumour growth at new sites. In a study by Ye *et. al.*, 2012 it was however noted that E-cadherin expression is elevated in tumour emboli found in lymphovascular regions, and cleavage of E-cadherin may directly initiate the formation of the clusters. The association of E-cadherin may hint towards the involvement of epithelial markers playing a role in the formation of clusters as well as changes due to EMT.

Tumour cells moving through the circulation as clusters are certainly more stable and possess survival advantage compared to CTCs moving independently¹⁷. In clinical settings, it was also observed that CTC clusters are present more when tumour cells display a mesenchymal phenotype¹⁷. Such observation opens the gateway to exploring whether originally detached epithelial clusters undergo EMT, or the transformed mesenchymal cells initiate the formation of clusters, perhaps utilizing their association with platelets.

Following the successful isolation of CTCs, they can be analyzed to answer specific questions regarding CTC clusters, stem-like character, EMT process and so forth. However, it is first necessary to be sure that the entire CTC population has been captured for assessment. As indicated earlier, using capture methods that rely on cell markers that may be lost in EMT may not retrieve the full population. This Chapter of the Thesis focuses on the methods used for the CTC isolation technique, building particularly on cancer cell - ECM protein interactions that the cell uses in order to traverse its metastatic journey (Section 1.4).

4.2 Materials and Methods

4.2.1 Separating different components of the blood

4.2.1.1 Procurement of blood samples

Blood samples from normal humans were obtained from Research Blood Components, LLC in Waterdown, Massachusetts. Under the University of Waterloo ethics approval ORE #22816 (Appendix VI), we also obtained further samples of healthy human volunteers. The samples contained lithium heparin as an anticoagulant. The samples from Research Blood Components were shipped in temperature-controlled conditions (2-8°C) and arrived within 2 days of collection. The blood was processed immediately to ensure the optimum quality of experiments.

4.2.1.2 Blood separation

The blood sample tubes and necessary material were wiped with 70% ethanol and set-up in the biosafety cabinet. Using a sterile pipette, 5mL of blood was transferred into the centrifuge tube. An equal amount of filtered RPMI 1640 medium was added and mixed with the whole blood creating a 1:1 dilution. Using a 21-gauge needle and a syringe, 4mL of well-mixed Ficoll-Paque PLUS® density gradient was transferred into a separate round-bottom centrifuge tube. The 10mL of diluted blood was carefully layered onto the Ficoll layer while avoiding disturbance of the

interface. The tubes were capped and taken to the centrifuge. Tubes were centrifuged at 400 x g for 30 min at 18-20°C. Figure 22 below depicts the separation of different components of the blood.

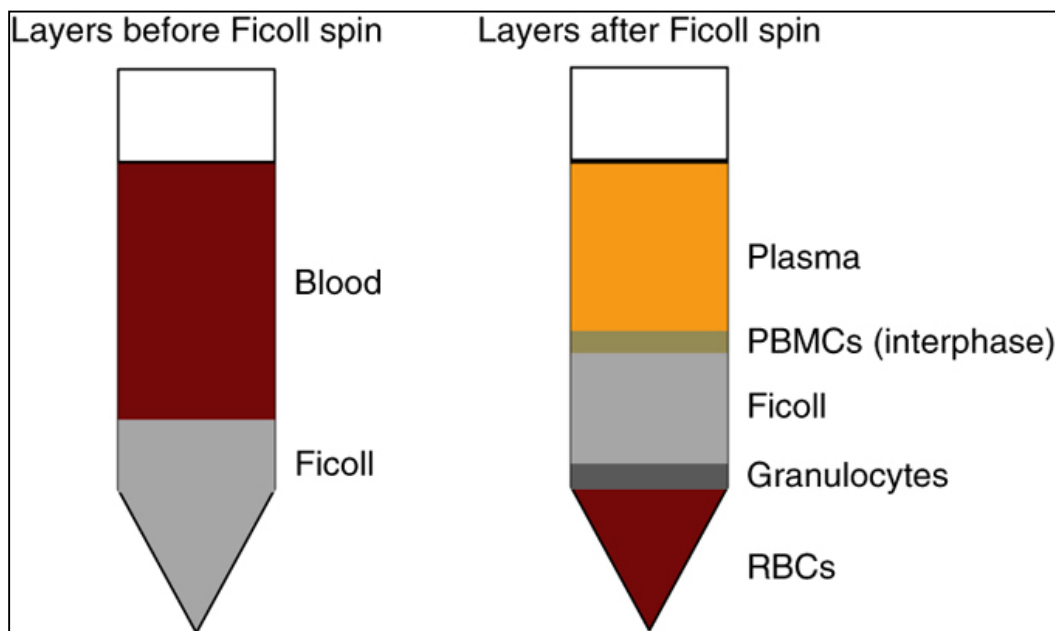


Figure 22 Separation of blood components using the polysaccharide medium Ficoll[®].

Following the centrifugation, components of the blood are separated into a red blood cell (RBC) layer at the bottom, peripheral blood mononuclear cells (PBMCs) in the middle where cancer cells are expected, and the yellowish layer on the top with plasma and platelets. Adapted from ²¹⁸

Following the centrifugation, the buffy layer or the interface (~1mL) with peripheral blood mononuclear cells (PMBCs) was taken up using a pipette tip and transferred into a new tube filled with 10mL of cold PBS with Ca²⁺/Mg²⁺ (Figure 23). These tubes were then centrifuged at 400 x g at 4°C. This step helps remove the contamination from Ficoll[®] and plasma layer and leaves the cell pellet at the bottom of the tube. The upper layer was aspirated, and the cell pellet was resuspended in a DMEM 10% FBS containing media. This was the enriched cell population that was used for further isolation and characterization.

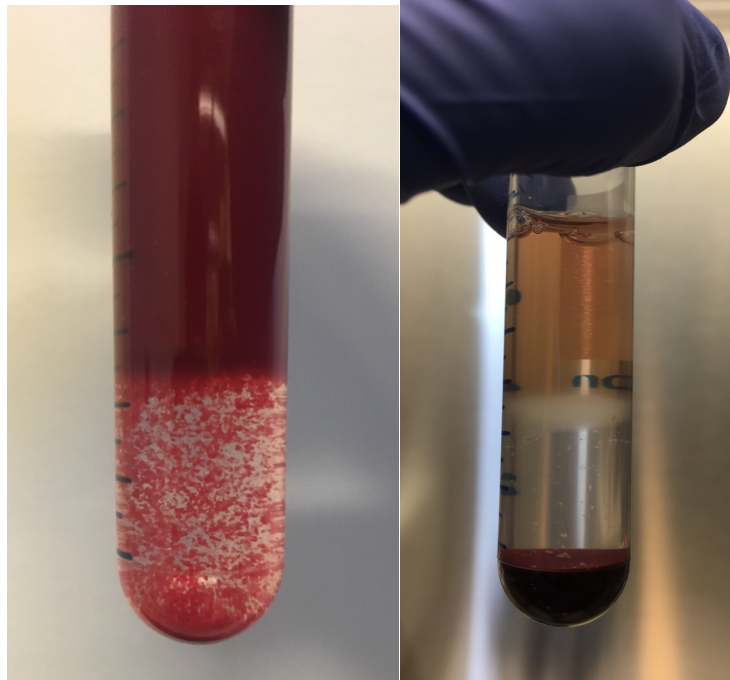


Figure 23 A representative set of pictures from a patient blood sample (GRCC014) processed through Ficoll[®]. Diagram on the left shows the diluted blood layered onto the Ficoll[®] and the red blood cells beginning to fall through the density gradient. The resulting product on the right is showing a white buffy PBMC layer in the center for collection and downstream processing.

4.2.2 Adhesion Assays

The adhesion assays were carried out to identify the ECM proteins that best capture an optimum number of CRC cells. Briefly, the cells growing in culture flasks were detached using Trypsin-EDTA and brought into suspension with DMEM 10% FBS. The cell suspensions were centrifuged at 4°C for 3 min at 400 x g. Following centrifugation, the supernatant was discarded and the pellet was re-suspended in 10 mL of serum-free DMEM. CellTracker[™] green CMFDA (5-chloromethylfluorescein diacetate) dye was added at a final concentration of 1 μ M to each tube and mixed well. The chloromethyl or bromomethyl groups from the dye reacts with thiol groups in the cell and this is facilitated through glutathione-S-transferase enzyme. The dye is designed to easily permeate through the cell membrane and convert into membrane-impermeable products.

This can help with the tracking of the cells under different experimental conditions. The cell suspension tubes with dye were then incubated at 37°C for 30 min. Following the incubation, tubes were centrifuged again for 3 min at 400 x g at room temperature. The supernatant was aspirated off and the cells were re-suspended into a new media with 1mg/mL BSA in DMEM. Cells were counted using the Beckman Multisizer™ 4 and new suspensions of desired concentrations were prepared. 1000 cells/well were plated in Nunc 6-well plates coated with different extracellular matrix proteins as shown below in Figure 24.

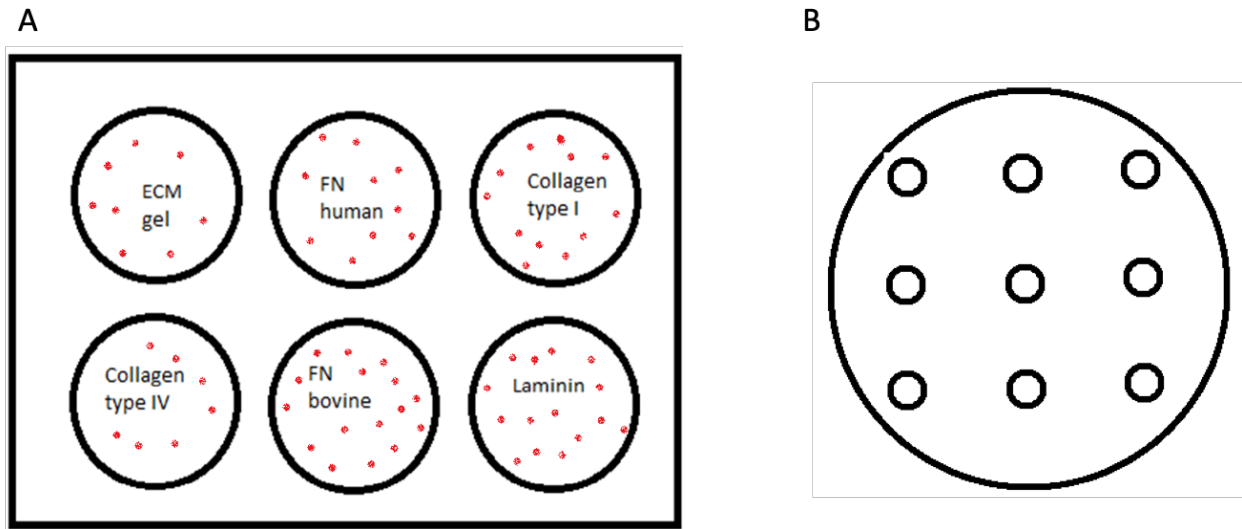


Figure 24 Schematic of the adhesion assay set-up, various ECM proteins and concentrations. (A) ECM gel (Matrigel®) used at 1/10th of the commercial stock; human fibronectin used at 5µg/mL; collagen type I at 10 µg/mL; collagen type IV at 10 µg/mL; bovine fibronectin at 5 µg/mL; laminin at 1-2 µg/mL. 700µL of each protein's working solution was layered onto the well and the plate was incubated for 2 h at 37°C. (B) Counting post-adhesion was carried out in a standard fashion with 9 pre-decided regions in the well.

After the initial coating, ECM solution was aspirated off and one wash with cold PBS Ca²⁺/Mg²⁺ was carried out. The cells were added to each well and incubated at 37°C in the 5% CO₂ incubator for 18 h. Next day, the media was taken up very gently using a 1mL pipette. One

gentle wash with PBS $\text{Ca}^{2+}/\text{Mg}^{2+}$ is carried out and the cells are then fixed with freshly prepared 3.7% PFA at room temperature for 10 min. The adherent cells with green CMFDA are viewed under the Leica DM2000 microscope. For all of these results, CMFDA stained cells were manually counted twice under the fluorescent microscope, and the average count was recorded.

4.2.3 Optimizing the ECM composition for circulating tumour cell capture

Following the initial adhesion assays, it was observed that human fibronectin and collagen type I was able to capture a high number of resistant CRC cells. Composition with two of these proteins was deemed suitable for further experiments. Next, the adhesion assays were carried out with increasing the concentrations of each protein in a combination. The original concentration used in the initial adhesion assays was labelled as 1x and the further increases included two times (2x), five times (5x), and ten times (10x) concentration of both proteins. In order to test the effect of increasing concentrations, two groups with 5000 cells and 500 cells were included. The conditions for incubation, washing and fixing remained the same as the adhesion assays explained in section 2.2.5.

4.2.4 Spiking Experiments

The procedure explained in section 4.2.1.2 was followed for preparing the blood for separation. Following the 1:1 dilution of blood with RPMI 1640 media, the intended number of cancer cells (HT29 or HCT116) were spiked and mixed. In these experiments, the cells were pre-labelled with CMFDA green dye. Two density separation media, Ficoll® and Optiprep® were compared for their separation efficiency. A series of cells (5000, 500 and 50) were spiked to gauge whether separation efficiency is affected by the number of cells present. The lower number was chosen due to the similarity in the number of CTCs that are reported with approved Cellsearch® (©Menarini Silicon Biosystems) technique. As a comparative control, the same number of cells

were plated directly onto the ECM coated plates without any exposure to blood or density barrier. This was done to identify where the loss of cells might be occurring in the separation process after spiking or following the fixation.

4.2.5 Immunostaining of CTCs

Following the separation of blood components as described in section 4.2.1.2, the enriched cell population was obtained from the PBMC layer. This cell suspension contains white blood cells, circulating tumour cells, and possible contaminating red blood cells and platelets. The volume was split into four wells of the Nunc Lab Tek II chamber slides (Thermo Scientific) and incubated at 37°C in the 5% CO₂ incubator for 18 h. Following the incubation period, the existing solution was carefully aspirated from each well without disturbing the bottom layer. A gentle wash with cold PBS Ca²⁺/Mg²⁺ was applied following a fixation step with freshly prepared 3.7% paraformaldehyde (PFA). If an intracellular target such as cytokeratin was to be tagged with the antibody, permeation step with 0.1% Triton X-100 in PBS Ca²⁺/Mg²⁺ was carried out. For the membrane-bound target such as EpCAM, no permeation was required. Details of the antibody used are provided in the following section 3.2.5.1. After the fixation and wash, blocking step was carried out with 5% FBS in PBS Ca²⁺/Mg²⁺ for 30 min at room temperature. In the meanwhile, the primary antibodies were prepared at the desired concentration in 1mg/mL BSA in PBS Ca²⁺/Mg²⁺. Three out of the four chamber slide wells were treated with the primary antibody, whereas the fourth well was used as a negative control where 1mg/mL BSA in PBS Ca²⁺/Mg²⁺ was applied instead of the primary antibody. The slide was kept on a gentle rocker in a humid chamber for 60 min at room temperature. Two washes (5 min each) with 1mg/mL BSA in PBS Ca²⁺/Mg²⁺ were carried out and secondary antibodies were prepared in the meanwhile. Following the washes, the secondary antibody was applied to each well under a dark environment. Aluminum foil was used

to cover the slide and it was incubated for 60 min at room temperature on a gentle rocker. At the end of the secondary antibody incubation, two washes with 1mg/mL BSA in PBS $\text{Ca}^{2+}/\text{Mg}^{2+}$ were carried out. The wash solution was aspirated and the slide chamber was removed using the slider provided. Two drops of Fluoroshield® aqueous gel mounting medium containing DAPI was added on top of each well surface. A rectangular 50mm coverslip (Fisher) was carefully placed onto the slide and allowed to dry for 60 min in dark. The fluorescence was observed using the Leica DM2000 microscope and the images were captured with Micropublisher 5.0 RTV camera and QCapture Pro 5 software. Cells were manually counted going across the slide in a standardized pattern shown below (Figure 25).

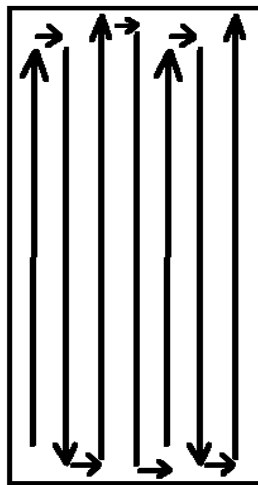


Figure 25 Schematic of the cell-counting pattern for spiking studies and patient CTCs.

A duplicate count was conducted and the final number recorded was an average of two counts. Using the cells at an edge of a particular field of view as a reference point, the slide was moved over a field ensuring no overlap and no missed fields during counting.

4.2.5.1 Antibodies used in immunofluorescence

Primary antibodies

Cytokeratin - Abcam ab9377 anti-wide spectrum cytokeatin
Rabbit polyclonal IgG

EpCAM - Abcam ab71916 anti-EpCAM
Rabbit polyclonal IgG

CCL2 - GeneTex GTX10390 anti-human CCL2
Mouse monoclonal (clone 24822.11) IgG1

SDF-1 - Millipore ab1868p anti-human SDF-1 α
Rabbit polyclonal IgG

Secondary antibodies (Cell Signalling Technology®)

Antimouse secondaries

| | | | | | |
|--------------------------|------|-----------|-----------|-----|---------|
| Green - Molecular Probes | goat | mouse IgG | Alexa 488 | IgG | 2 mg/mL |
| Red - Molecular Probes | goat | mouse IgG | Alexa 568 | IgG | 2 mg/mL |

Antirabbit secondaries

| | | | | | |
|--------------------------|------|------------|-----------|-----|---------|
| Green - Molecular Probes | goat | rabbit IgG | Alexa 488 | IgG | 2 mg/mL |
| Red - Molecular Probes | goat | rabbit IgG | Alexa 568 | IgG | 2 mg/mL |

4.3 Results

4.3.1 Technique development to capture circulating tumour cells

Based on the past work in Blay laboratory (MSc Thesis, Spencer Berg), we were interested in capitalizing on the cancer cells' ability to interact with ECM proteins in order to capture CTCs. The reliability of many commercial techniques on marker-based capturing platform lacks such a functional aspect in their approach. We began by exploiting different ECM proteins and their combinations at different concentrations for optimization of the technique. First, we performed adhesion assays for CRC cell lines HT29 and HT29-R on different ECM proteins. The rationale here was that cancer cells possess surface receptors like integrins and CD44 that can bind with ECM proteins, whereas the majority of the native cells from blood will lack this ability. This functional approach based on adhesion should provide a wider capture of CTCs in the situation of loss of expression of the epithelial markers they usually possess.

4.3.1.1 Adhesion assays to identify matrix protein(s) suitable for CTC capture

We compared 5 different types of matrix proteins available from human and murine sources (human and bovine fibronectin, collagen type I and IV, and laminin). Fibronectin, laminin, and collagen are amongst the most common extracellular matrix proteins found throughout the body⁵⁹. Commercially, there is a product called Matrigel® which consists of different ECM proteins and is normally utilized as an extracellular matrix in various laboratory experiments. We used the Matrigel® at 1/10th of its original dilution and tested the adhesion between parental and drug-resistant HT29 cells. After the technique was established, six independent experiments were carried out as described in section 4.2.2.

The difference in the adhesion capacity of parental and resistant HT29 cells on Matrigel® (ECM gel) was not significantly different (Figure 26). The difference between the cell-lines when

tested on both types of collagen (type I and type IV), was also not significantly different (Figure 27). When the different types of fibronectin were compared however, it was found that HT29-R cells adhered significantly better to the human fibronectin when compared to HT29 cells (Figure 28A). In terms of the adhesion on bovine fibronectin, similar trend was observed as the human fibronectin, but the difference between HT29 and HT29-R was not statistically significant (Figure 28B). Recent work in the Blay laboratory has shown that HT29-R cells express a higher amount of integrin alpha 5-beta 1 (receptor for fibronectin) compared to HT29 cells (MSc thesis, Spencer Berg), which likely underlies this distinction.

Lastly, for laminin, it was found that HT29-R cells adhered better and the difference was statistically significant (Figure 29). When the absolute number of cells adhered were compared between different proteins, it was found that collagen type I had captured the highest number of cells.

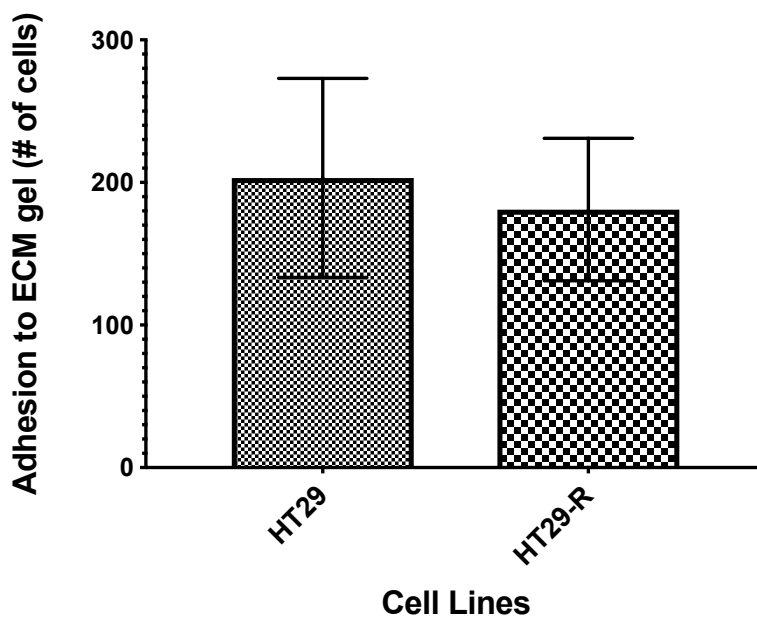


Figure 26 Adhesion of HT29 and HT29-R cells on commercial ECM gel.

Sigma at 1/10th of stock dilution. The figure is representing mean of 6 independent experiments.

Due to a negligible difference in the adhesion between the two cell lines (HT29 and HT29-R) on the ECM gel, these numbers were used to normalize the values obtained from other extracellular matrix proteins to account for the effect of variation between individual experiments.

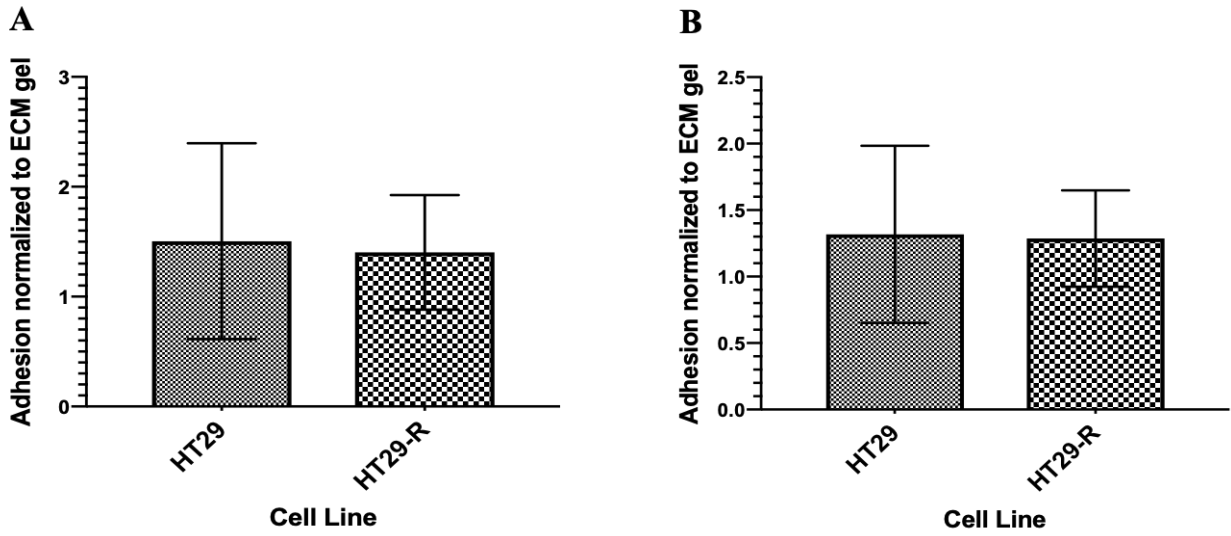


Figure 27 Adhesion of HT29 and HT29-R cells on two types of collagen.

(A) Collagen I (10 µg/mL) and (B) Collagen IV (10 µg/mL). The figure combines 6 independent experiments and each experiment had 2 replicates.

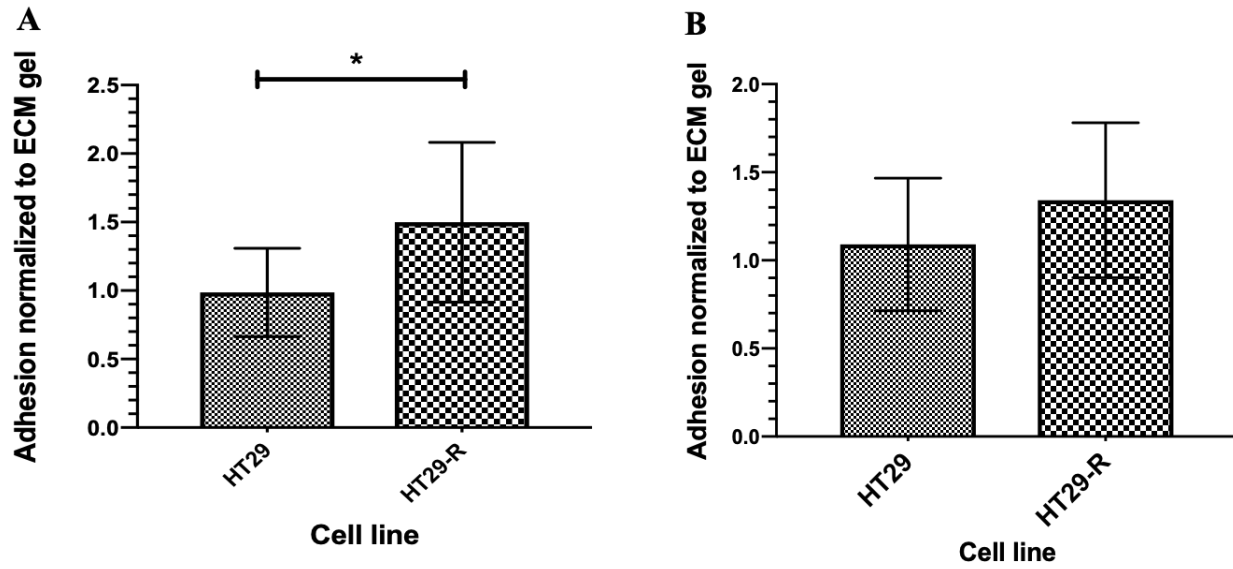


Figure 28 Adhesion of HT29 and HT29-R cells on two types of fibronectin.

(A) human fibronectin (5 µg/mL) and (B) bovine fibronectin (5 µg/mL). The figure combines 6 independent experiments and each experiment had 2 replicates. *: $p < 0.05$

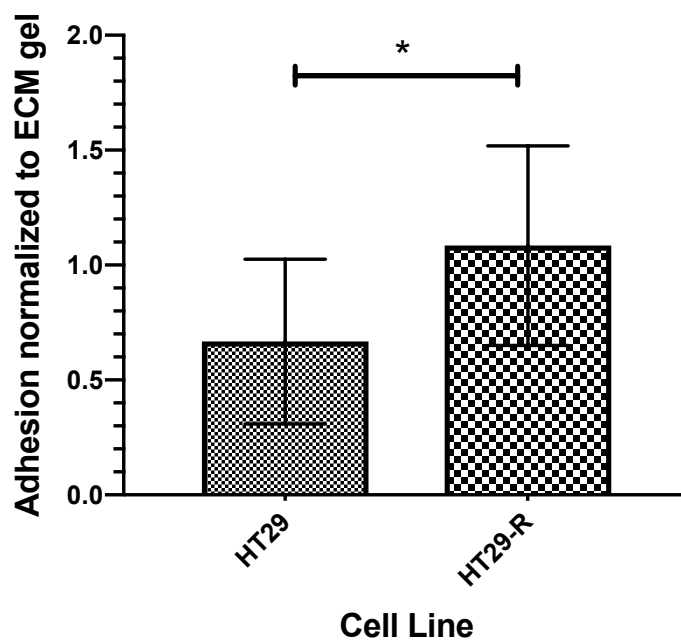


Figure 29 Adhesion of HT29 and HT29-R cells on the murine laminin (1-2 $\mu\text{g/mL}$) matrix. The figure is representative of 6 independent experiments and each experiment had two replicates. *: $p < 0.05$

The results from this set of experiments (Figure 26 to Figure 29) provided valuable information to narrow down the choice for the extracellular matrix combination that was used for CTC isolation in patient samples. The difference between the two cell lines' adhesion was not significant for either type of collagen. However, there is a slight trend of decreased HT29-R cell adhering in both collagen groups. In contrast, the resistant cells were more adherent to both types of fibronectin matrices. The difference between two cell lines was statistically significant for human fibronectin matrix. Human fibronectin, and laminin emerged as two candidates that yielded statistically significant result between the two cell lines. Collagen type I captured the highest number of cells overall.

It is known that laminin forms a major part of the commercial Matrigel[®]. We sought for a novel combination that was not tested previously, and decided to exclude laminin for this project. It can be utilized in future studies based on its biological role and functional interactions. It is known that collagen type I is the most abundant protein in human body²¹⁹. This is essential as cells around the human body have routine interactions with this protein. The thesis of Spencer Berg (Blay laboratory) provided important basis for the interactions of fibronectin. Through these considerations, human fibronectin and collagen type I were chosen as the two proteins going forward as a combination matrix in CTC studies.

4.3.1.2 Optimization of CTC capture platform

To assess the impact of increasing concentrations of extracellular matrix proteins, collagen type I and human fibronectin were combined at the concentrations used in the initial adhesion assays. This combination is referred to as the 1x ECM in the following experiments. The concentration of both proteins was increased by two times, five times, and ten times the initial concentration (referred as 2x, 5x, and 10x).

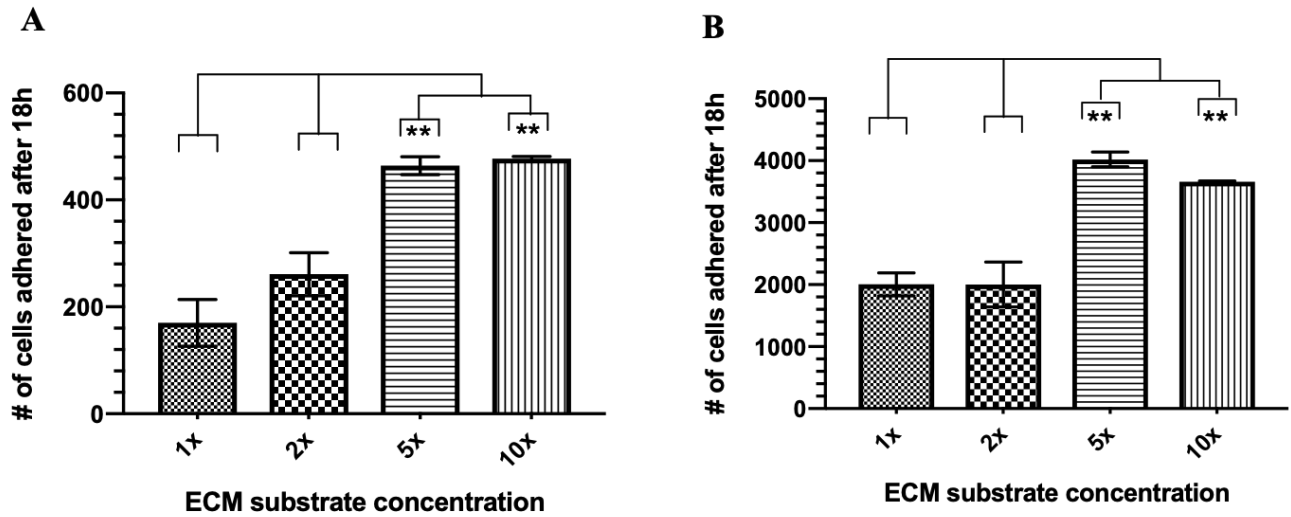


Figure 30 Increased ECM protein concentrations leads to an improved capture efficiency.

(A) 500 cells were plated onto the ECM and (B) 5000 cells were plated onto the ECM. Results displayed are averaged from three independent experiments. The cells were counted twice under the microscope using a cell-counter. Increasing concentration of extracellular matrix proteins to 5x and 10x demonstrated a significant difference in the number of cells captured on the extracellular matrix.

Based on the results observed (Figure 30), the 5x and 10x concentrations captured significantly higher number of cells when compared to the 1x and 2x group. However, the difference between the 5x and 10x group was not significant. Increasing the concentration beyond 5x could not yield a greater number of the captured cells. Hence, 5x was sought to be an appropriate concentration to use for patient samples in the latter stage.

4.3.1.3 Successful recovery of CTCs from spiked blood samples

After the identification of an optimal extracellular matrix combination, we looked for the most efficient method for the initial separation of the blood components. We compared the recovery of cancer cells with two commercially available density media – Ficoll® and Optiprep®. Both of these density media have been used successfully in many research studies²²⁰⁻²²². Ficoll® is a solution that comes ready to use at the appropriate density of 1.077 g/mL, whereas Optiprep® (iodixanol at 1.32g/mL density) is a solution that requires an appropriate dilution with buffer such as PBS or cell culture medium such as serum-free DMEM. We sought to identify which medium is more effective in rescuing the mononuclear cells from the blood sample. HCT116 cells were spiked into the diluted blood samples and these samples were layered onto either of the two media followed by centrifugation at 400 x g at 18°C for 30 min. The results below (Figure 31) demonstrated no significant difference between two media when cells were recovered and counted from the PBMC layer.

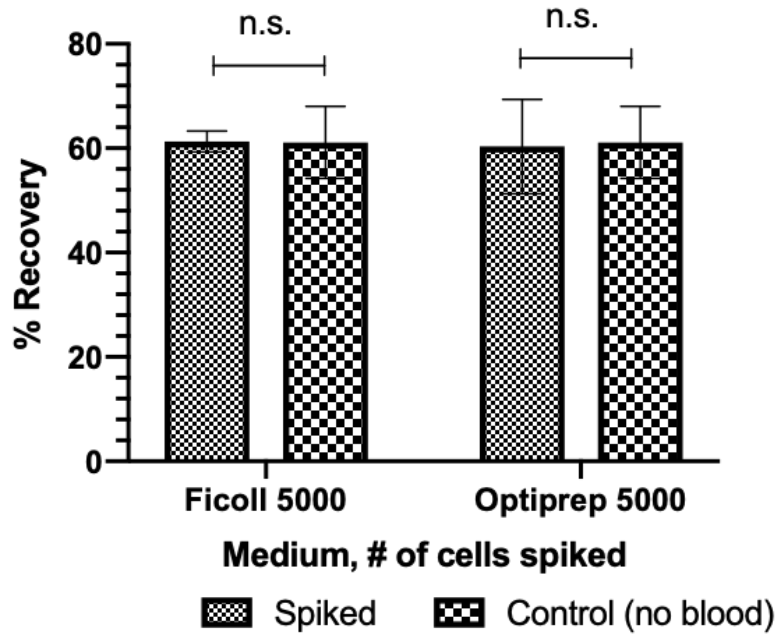


Figure 31 Recovery of spiked cancer cells from whole blood using density gradient medium Ficoll[®] and Optiprep[®]. No difference is observed statistically when the two are compared after spiking and recovering the cancer cells from the PBMC interphase. Cells were counted manually using the fluorescence microscope (Leica DM2000). n.s.: not significant

One of the major advantages of Ficoll[®] is that it is pre-mixed and ready to use. Based on simple pilot experiments (results not shown), its ease of usability, and similar recovery compared to Optiprep[®], Ficoll[®] was chosen as the separation medium for successive experiments. Next, we wished to determine the variation in recovery numbers when as low as 50 cells are spiked into 5mL of diluted blood (1:1 with RPMI1640 medium). The intent here was to assess whether the technique would be feasible for real-life patient samples that may possess low number of cancer cells. Experimental conditions in section 3.2.4 were followed and three successive increments of 50, 500, and 5000 cells were chosen for spiking.

Figure 31 shows that the recovery of cancer cells from the blood ranges between 55-75%. The cancer cells in the control group are directly placed onto the ECM matrix without any exposure to the blood. The difference in recovery between the spiked samples and control samples is insignificant. There is greater variation in the samples spiked with lower cell numbers, as evident by the errors bar in the group with 50 cells. This should be taken into account when dealing with patient samples, as the yield for patient CTCs could be even lower.

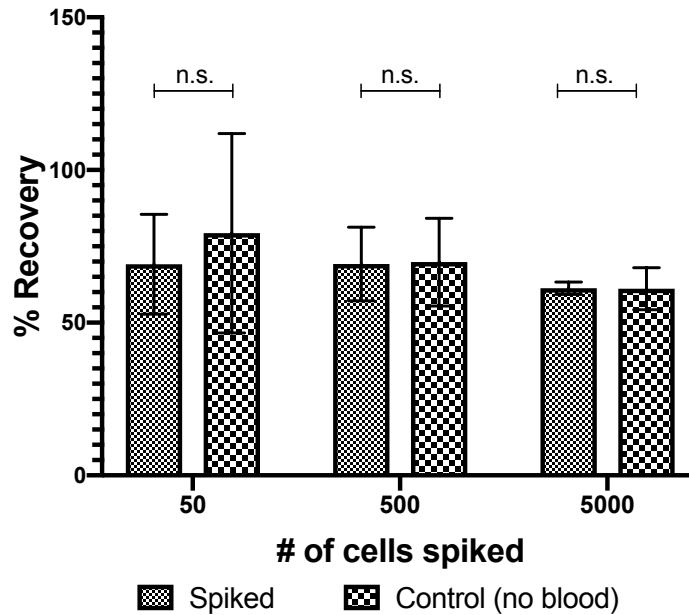


Figure 32 Recovery from spiked blood samples using Ficoll® medium. Control group had no exposure to blood and the cells were placed directly on the extracellular matrix. The figures represent three independent replicates and significance was calculated using multiple t-tests and Bonferroni-Dunn post-test where significance is established at $p \leq 0.05$ and non-significant results are denoted as n.s.

Results from Figure 31 and Figure 32 did not only allow assessment of the recovery from the spiked blood samples, but also demonstrated that CRC cells are able to survive in this *ex vivo* blood environment. The experiments up to this point provided us with a density gradient of choice, an expected recovery of between 55-75%, a best combination of ECM proteins and their optimum concentration for CTC capture. Next, we used immunofluorescence technique for CTC identification.

4.3.1.4 Characterization of isolated CTCs

EpCAM and pan-cytokeratins (8,18, and 19) are markers that are widely used for identification of CTCs in clinical studies^{19,223-225}. We wished to identify the captured CTCs using these commonly used markers first. We also employed CD45 antibody which identifies any cell that is of the hematopoietic origin. The PBMC layer (Figure 22) that is plated on the ECM matrix contains a heterogeneous cell population. It is therefore important to accurately identify the CTCs without any ambiguity. The presence of an epithelial marker and absence of CD45 provides a confirmation of a captured CTC.

To establish a working method, HCT116 and HT29 cells were utilized first to understand the staining patterns with two epithelial marker antibodies. Figure 33 shows HCT116 cells recovered and identified from a spiked blood sample using EpCAM antibody. The staining pattern of HCT116 cells varies with the cytokeratin stain as observed in Figure 34. For some of the work-up experiments, HCT116 cells were pre-stained with green CMFDA dye (Figure 35) and identified later without having to perform the immunostaining. Figure 36 is an example of how multiple markers can be screened on a single isolated CTC. A wider exploration with tumour-specific markers can be carried out in future studies.

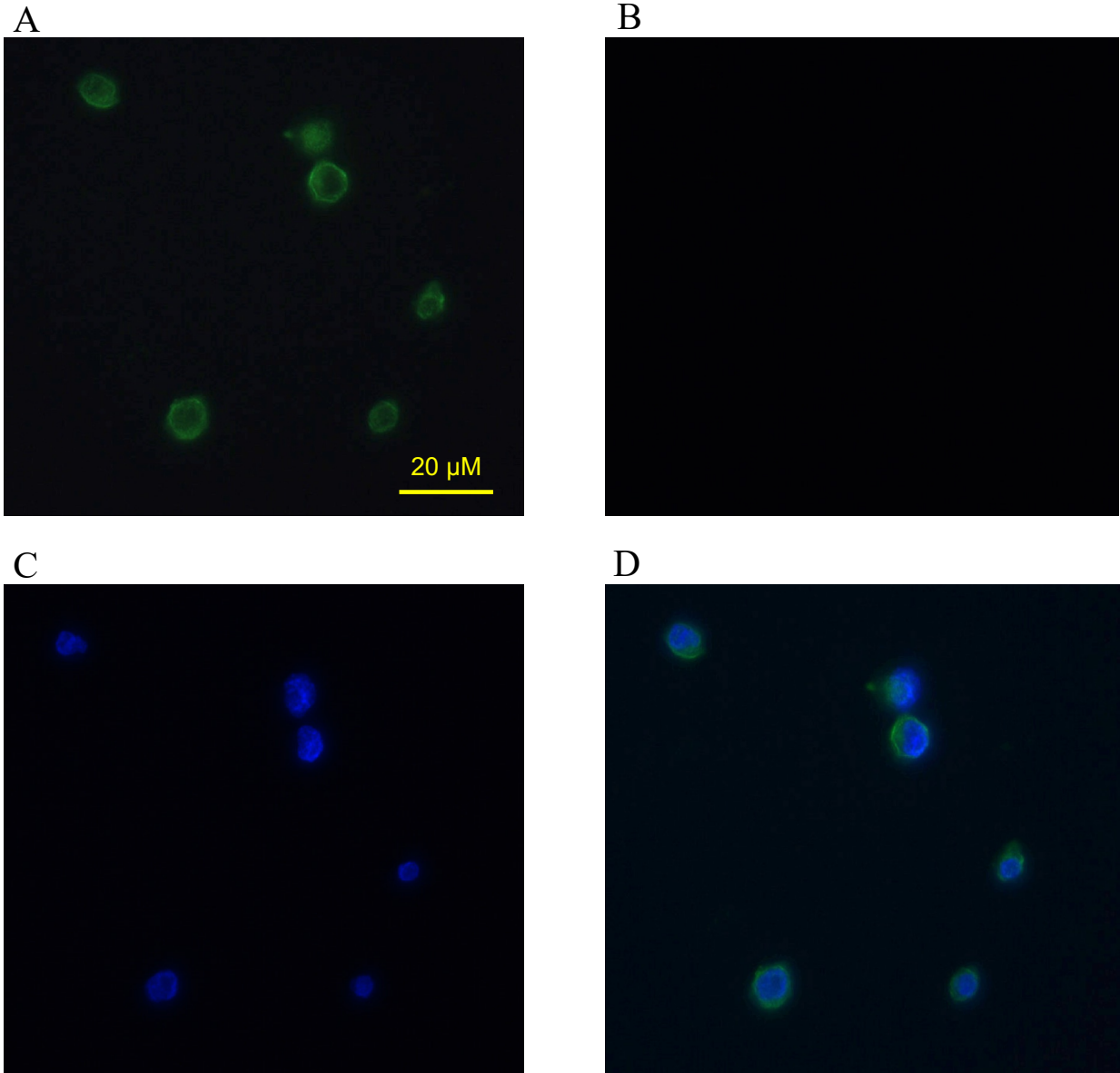


Figure 33 Spiked and recovered HCT116 cells from peripheral blood sample – stained with (A) EpCAM antibody (B) Negative control with no primary antibody (C) DAPI stain (D) merged EpCAM and DAPI. Images were taken with 100X objective.

Figure 34 (white arrows) demonstrates an artificial effect where an area with a green circular stain lacks nuclei and stretched cytokeratin pattern. Such artifacts were excluded from the counting. Both of the antibodies (EpCAM and cytokeratin) successfully detected the isolated CTCs from peripheral blood samples. Negative control well (lacking primary antibody) was found clear and this added to the confirmation in identification of the CTCs. The cytokeratin positive cells show a stretched appearance which is consistent with what is expected for keratin proteins. For some of the optimization experiments, we decided to use the green CMFDA stain and this helped during the spiking experiments where only the cell count was required.

As observed in Figure 35, the green CMFDA dye retained inside the CRC cells helps differentiate between the native cells from the blood and spiked cancer cells. Three cancer cells are visible in Figure 35 and they also have nuclei stained with DAPI. This is a representative image for CMFDA tagged cells detected from blood samples. Next, we tested the identification of spiked HT29 cells that were tagged with CMFDA and in addition we also used EpCAM antibody as an added marker.

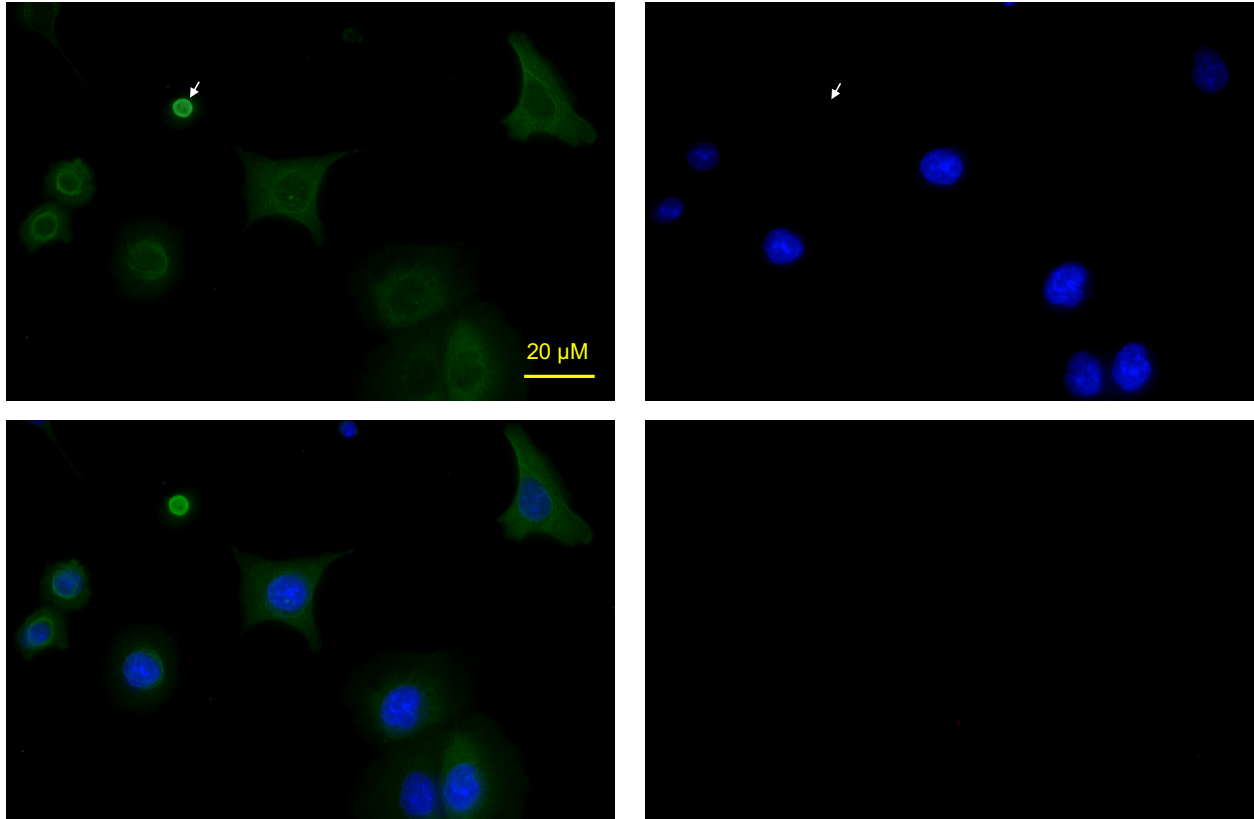


Figure 34 Spiked and recovered HCT116 cells from peripheral blood sample – stained with (A) wide-spectrum CK antibody (B) blue DAPI stain (C) merged EpCAM and DAPI (D) Negative control with no primary antibody. Images were taken with 100X objective.

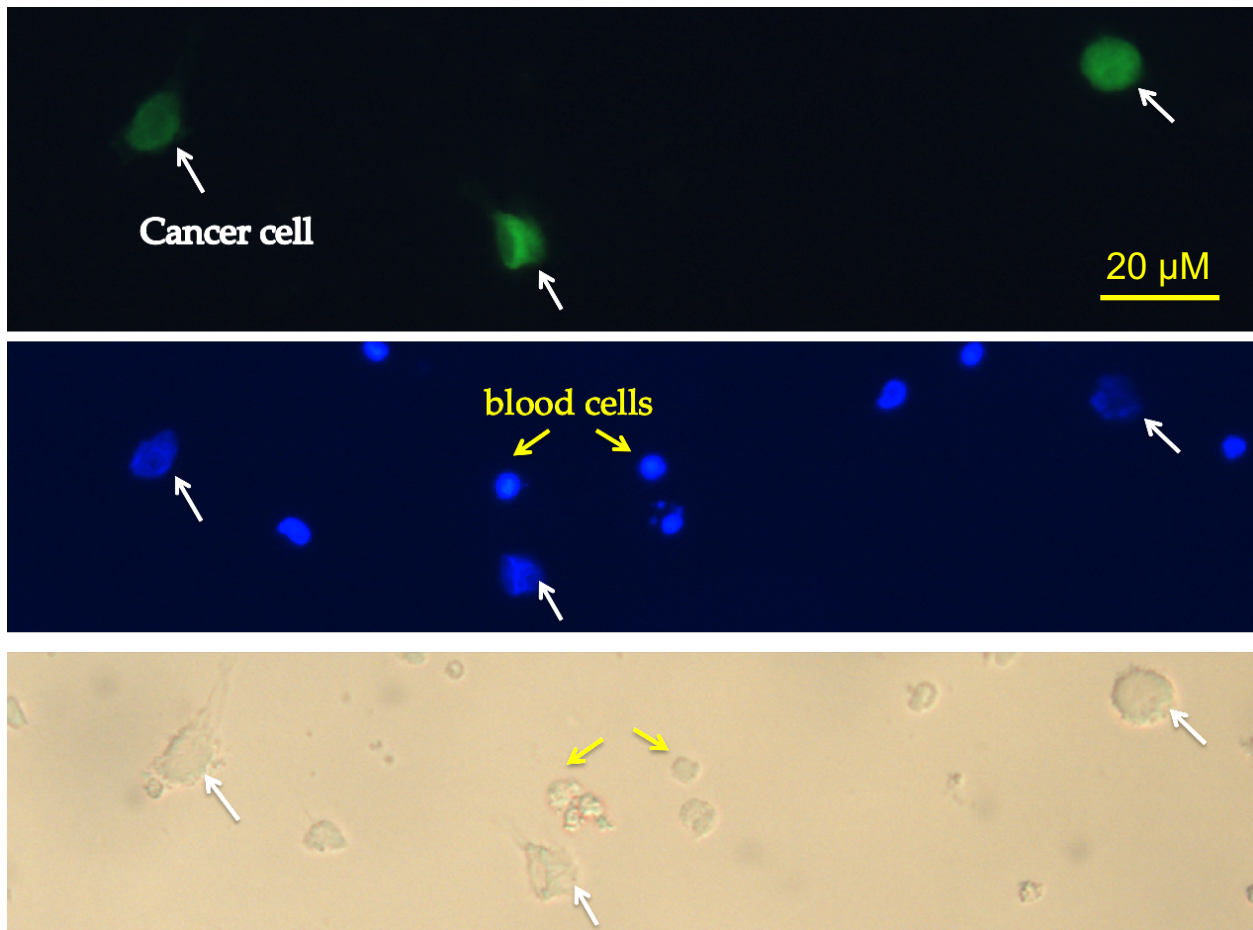


Figure 35 CMFDA stained HCT116 cells spiked in blood and recovered. The cells marked with yellow do not reflect the CMFDA stain, however they have the nuclei stain. This characteristic identifies with cells from the blood origin that remained on the surface along with CTCs. Images were taken with 100X objective.

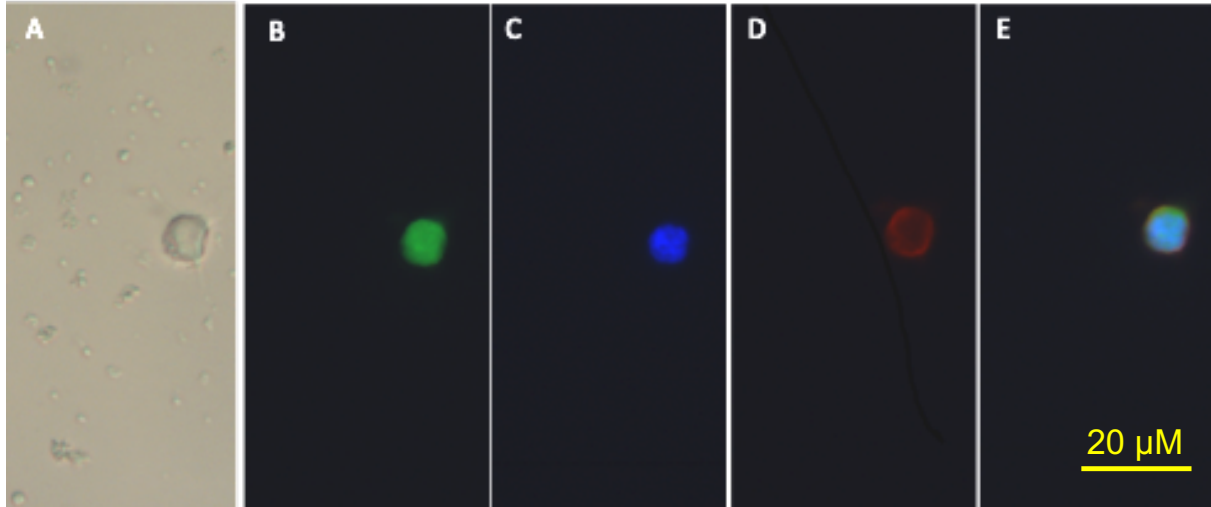


Figure 36 Example of a recovered HT29 cell showing possible screening of multiple markers on a single cell. Images were taken with 100X objective. The figure panels show (A) bright field image (B) green CMFDA dye (C) blue DAPI stain for nuclei (D) red EpCAM stain (E) Merged image for red, blue, and green markers.

Similar to what is demonstrated here (Figure 36), isolated cancer cells can be further analyzed with markers of interest in different types of solid cancer – for example EGFR, HER2, and CEA just to name a few. Building upon these experiments, we sought to refine the technique further and assessed different incubation periods, fixation methods, and ECM concentrations. The next section highlights that stepwise improvement in the CTC isolation technique.

4.3.1.3 Stepwise optimization of the CTC isolation protocol

Having optimised the model process of CTC isolation from human peripheral blood using human cancer cells obtained from cell culture, we applied our knowledge to the recovery of CTC from human patient samples. This was initiated concurrently with the later stages of the above optimisation process and modified successively as we obtained further informative data.

We first began the isolation for patient samples using a combination of collagen type I and human fibronectin at regular 1x concentration along with 1% PFA for fixation. PFA was originally chosen as a fixative to preserve the cellular morphology, and the original concentration was kept at 1% in order to incur the least stress possible on sensitive population of CTCs. However, we were not getting any cell counts for the beginning samples and gradually, we increased the PFA concentration to 2% and by sample 13, we had increased it to 3.7%. When the experiment with increasing ECM concentration (Figure 30) was completed, we utilized the 5x ECM concentration starting with patient sample 14. However, the recovery was not significantly higher and remained below 20 cells from 8-10mL of whole blood. We also included CD45 antibody as a negative control and this helped rule out any artifacts. The addition of CD45 contributed to less ambiguous counting as we made sure to exclude any cells that were clearly positive for CD45. Although the original approach was to follow a gentle approach with 1% PFA, starting from sample 23, we experimented by using methanol fixation with pan-cytokeratin antibody. The recovery increased consistently for the continued samples following that approach. The background was much cleaner in methanol fixed wells and the staining pattern was more convincing. Some cytokeratin positive membranes lacked nuclei stain and they were counted separately as cytokeratin positive entities. Table 7 demonstrates the changes in our technical approach and resulting recovery from this optimization.

Table 9 Increased recovery of CTCs from patient blood using a progressively refined technique based upon capture by adherence to ECM.

| Sample # | Date Received | Patient | Expt Condition | Epithelial Marker Positive Cells (EpCAM/CK) |
|-----------|---------------|---------|--------------------------|---|
| Sample 1 | 29-Aug-16 | GRCC001 | 1x ECM + PFA | 0 |
| Sample 2 | 15-Sep-16 | GRCC002 | 1x ECM + PFA | 0 |
| Sample 3 | 23-Sep-16 | GRCC003 | 1x ECM + PFA | 0 |
| Sample 4 | 21-Oct-16 | GRCC004 | 1x ECM + PFA | 0 |
| Sample 5 | 30-Nov-16 | GRCC005 | 1x ECM + PFA | 0 |
| Sample 6 | 30-Nov-16 | GRCC006 | 1x ECM + PFA | 0 |
| Sample 7 | 01-Dec-16 | GRCC007 | 1x ECM + PFA | 0 |
| Sample 8 | 21-Dec-16 | GRCC008 | 1x ECM + PFA | 0 |
| Sample 9 | 18-Jan-17 | GRCC009 | 1x ECM + PFA | 0 |
| Sample 10 | 19-Jan-17 | GRCC010 | 1x ECM + PFA | 0 |
| Sample 11 | 28-Mar-17 | GRCC001 | 1x ECM + PFA | 0 |
| Sample 12 | 25-Apr-17 | GRCC004 | 1x ECM + PFA | 0 |
| Sample 13 | 10-May-17 | GRCC011 | 1x ECM + PFA | 5 |
| Sample 14 | 15-Jun-17 | GRCC005 | 5X ECM + PFA | 19 |
| Sample 15 | 28-Jun-17 | GRCC007 | 5X ECM + PFA | 12 |
| Sample 16 | 13-Jul-17 | GRCC009 | 5X ECM + CD45 + PFA | 13 |
| Sample 17 | 04-Aug-17 | GRCC012 | 5X ECM + CD45 + PFA | 7 |
| Sample 18 | 15-Aug-17 | GRCC001 | 5X ECM + CD45 + PFA | 6 |
| Sample 19 | 06-Sep-17 | GRCC013 | 5X ECM + CD45 + PFA | 3 |
| Sample 20 | 15-Sep-17 | GRCC014 | 5X ECM + CD45 + PFA | 11 |
| Sample 21 | 19-Oct-17 | GRCC015 | 5X ECM + CD45 + PFA | 18 |
| Sample 22 | 06-Nov-17 | GRCC011 | 5X ECM + CD45 + PFA | 0 |
| Sample 23 | 24-Nov-17 | GRCC004 | 5X ECM + CD45 + Methanol | 296 |
| Sample 24 | 11-Jan-18 | GRCC016 | 5X ECM + CD45 + Methanol | 97 |
| Sample 25 | 23-Jan-18 | GRCC007 | 5X ECM + CD45 + Methanol | 30 |
| Sample 26 | 21-Feb-18 | GRCC009 | 5X ECM + CD45 + Methanol | 32 |
| Sample 27 | 18-Apr-18 | GRCC017 | 5X ECM + CD45 + Methanol | 28 |
| Sample 28 | 01-Jun-18 | GRCC018 | 5X ECM + CD45 + Methanol | 54 |
| Sample 29 | 05-Jul-18 | GRCC019 | 5X ECM + CD45 + Methanol | 36 |
| Sample 30 | 09-Jul-18 | GRCC020 | 5X ECM + CD45 + Methanol | 40 |
| Sample 31 | 09-Jul-18 | GRCC021 | 5X ECM + CD45 + Methanol | 22 |
| Sample 32 | 10-Aug-18 | GRCC016 | 5X ECM + CD45 + Methanol | - |
| Sample 33 | 31-Oct-18 | GRCC017 | 5X ECM + CD45 + Methanol | 63 |
| Sample 34 | 14-Nov-18 | GRCC023 | 5X ECM + CD45 + Methanol | 31 |
| Sample 35 | 28-Nov-18 | GRCC024 | 5X ECM + CD45 + Methanol | 42 |

4.3.2 Identification of the recovered circulating tumour cells from patient samples

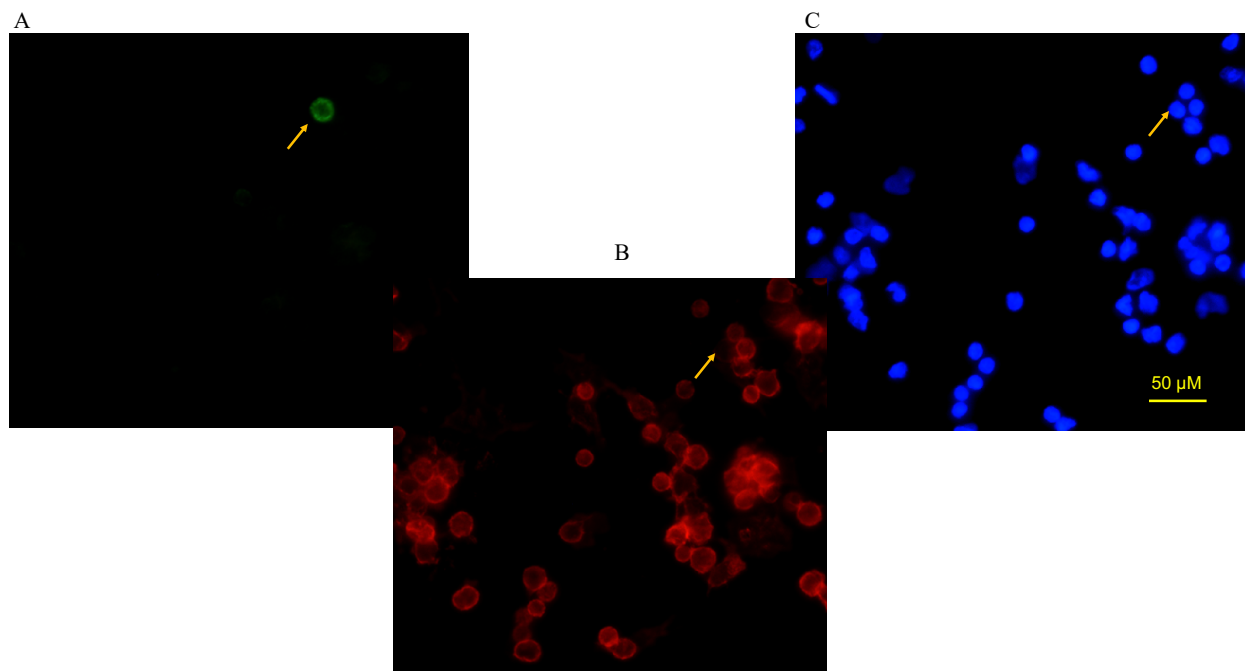


Figure 37 Recovered CTC example from patient sample GRCC019. Images were taken with 40X objective. (A) Green pan-cytokeratin; (B) Red CD45 (hematopoietic marker); (C) Blue DAPI (nuclei stain). The green cell that is cytokeratin positive does not express CD45 and possess a clear blue nuclei stain.

Many of the CTCs possessed a strong ring-like membrane structure that fluoresced green for pan-cytokeratin, and had no hint of the red stain for CD45 (Figure 37). In some cases, it was observed that the CD45 stain was present in a very dull background like stain (Figure 38 and Figure 39) for the cells that fluoresced green as CTCs. In rare cases, it was found that the structures that had a positive cytokeratin stain, and a clear negative stain for CD45 lacked the blue nuclei stain – these were not counted as CTCs.

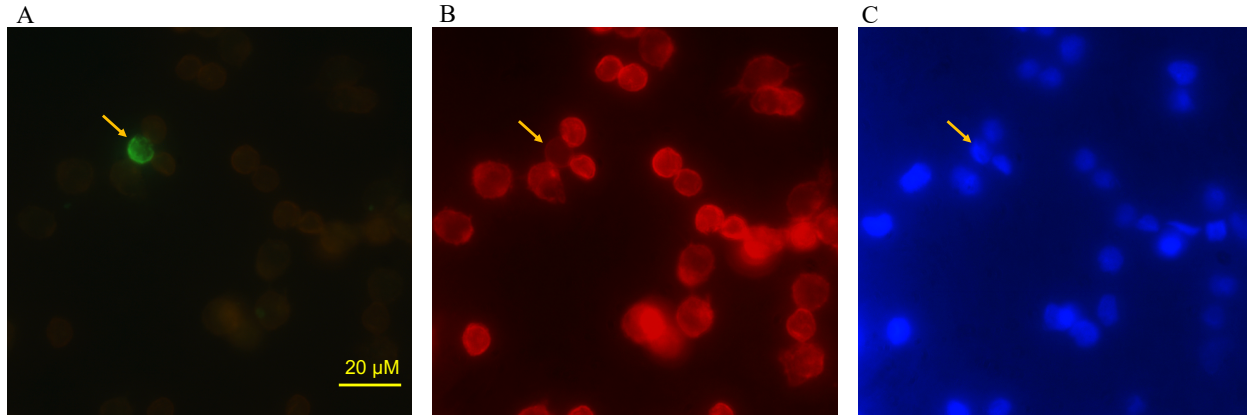


Figure 38 Recovered CTC example from patient GRCC017 Images were taken with 100X objective. (A) Green pan-cytokeratin; (B) Red CD45 (hematopoietic marker); (C) Blue DAPI (nuclei stain).

The green cytokeratin positive cell has a very dull hint of CD45 as marked in (B). In order to assess the localization and staining pattern better, some images were captured under the oil immersion with 100X objective. This is one of the examples of a dull CD45 stain, however the strong cytokeratin pattern and a presence of the nuclei led us to believe that the identified cell was indeed a CTC. Cells with this appearance in Figure 38 were counted positive as CTCs.

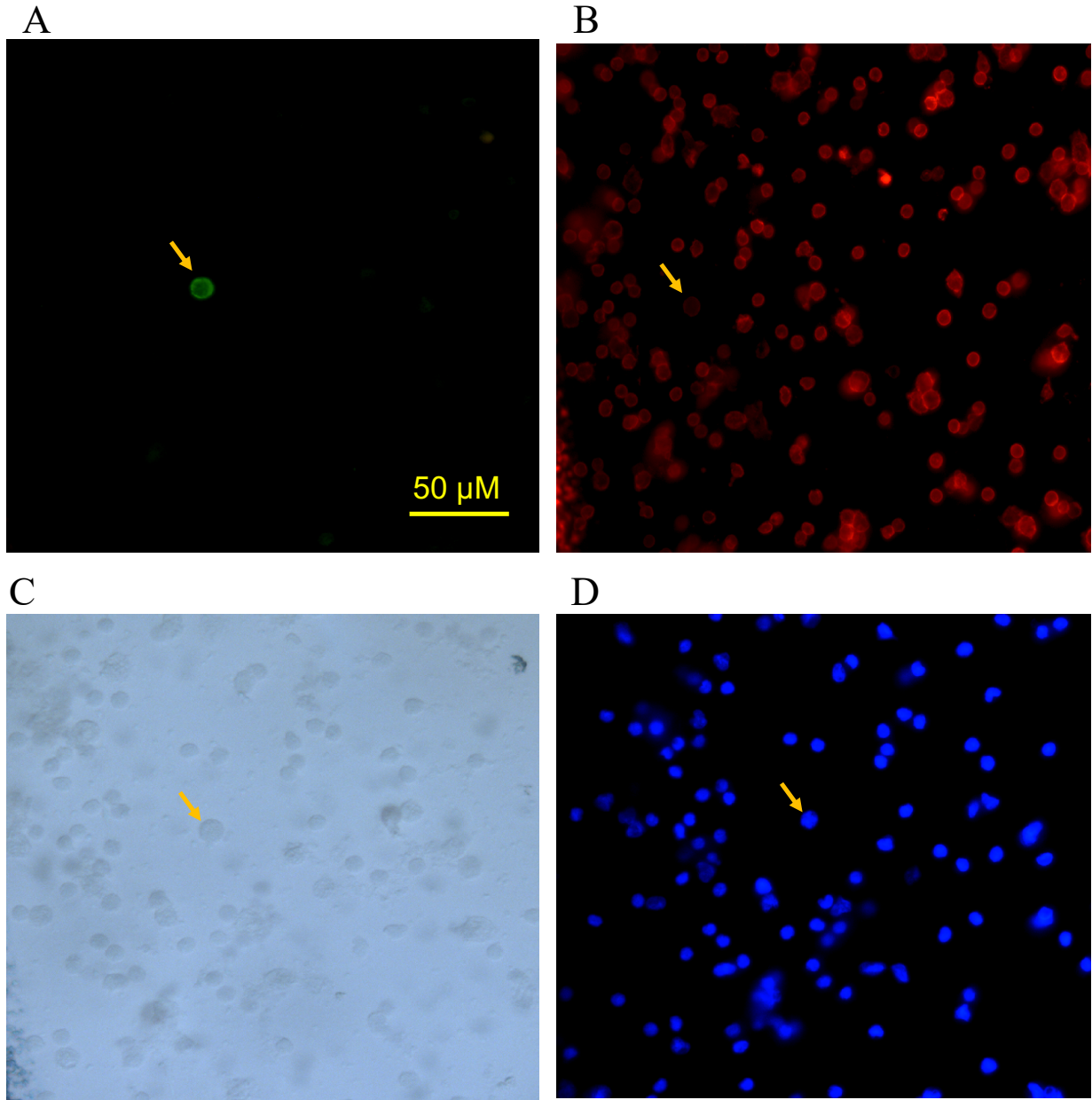


Figure 39 Recovered CTC from patient GRCC016. Images were taken with 40X objective (A) Green pan-cytokeratin stain (B) Red CD45 (hematopoietic marker) (C) Bright field image (D) Blue DAPI (nuclei stain).

It can be observed through the images (Figure 39) that a lot of white blood cells are adhering to the ECM. The technique does not get rid of all of the white blood cells and it is not specific to capture only the CTCs. Hence, a marker-based approach is required to identify the cancer cell after the initial separation, washes, and fixation.

4.4 Discussion

There are various groups exploring the optimum method to isolate circulating tumour cells from patients with solid cancer²²⁵⁻²²⁸. Some techniques are based on the physical characteristics (size, electric potential, density) of cancer cells, whereas some are based on the biological characteristics (protein expression, functional behavior) and few also use a combination of both (microfluidic chips with capture proteins, filters with antibody tags)²²⁹. Due to the previous work in the Blay laboratory – exploring interactions of extracellular matrix proteins (e.g. fibronectin) with cancer cell receptors such as integrins, we were interested in using the functional approach that utilizes such interactions in capturing tumour cells from peripheral blood^{54,230,231}.

We first began with adhesion assays of different CRC cell lines on various extracellular matrix proteins including collagen type I and IV, human and bovine fibronectin, laminin, and commercial Matrigel[®]. The intent here was to assess whether the drug-resistant cells are better able to adhere to particular matrix proteins in comparison with the parental cells. This is presumed to reflect how the more aggressive or metastasizing cells behave when they interact with ECM proteins in their external environment or at secondary sites of metastases.

Resistant HT29 cells adhered to human fibronectin significantly better in comparison to the parental HT29 cells – possibly due to the interaction of integrin alpha5beta1 on the surface of cancer cells. A study by Pelillo *et.al.* demonstrated that alpha5 beta1 integrin can play a role in CRC metastases into liver tissue²³¹. There is evidence to show that alpha2beta1 receptors on cancer

cells can form interactions with collagen type I²³². In fact, collagen type I was found to have captured the highest number of both HT29 and HT29-R cells compared to any other protein matrix. Laminin did show a significant result for the difference between parental and resistant HT29 cells, but the absolute number of captured cells in laminin group was the lowest. A study by Cioce *et.al.* assessed 23 CRC patient tissues and found an elevated mRNA level of laminin receptor²³³. This could mean that laminin as well can form a crucial role in capturing CTCs and future experiments can include that as a part of the ECM combination. Another 72 paraffin sections of colon tissues from the same study showed a positive correlation of laminin receptor expression and the Dukes' classification which is – an older staging system used for CRC²³³.

In my work, collagen type I and human fibronectin were chosen as the combination to capture human CTCs. Using this combination of proteins, we carried out a further adhesion experiment to assess whether increasing the protein concentration provided a better capture of cancer cells. A study by Hsiao *et.al.* tested increasing concentration of fibronectin and its effect on adhesion of osteosarcoma cells (U2OS). They demonstrated over three-fold increase in the number of adherent cells with 10µg/mL of human and porcine fibronectin in comparison to no fibronectin on the surface²³⁴. In our work, when the increasing ECM concentrations were tested, it was found that the combination of human fibronectin and collagen type I at five times the original concentration captured significantly increased number of cells (>75% recovery in comparison to 40% with 1x ECM). The absolute concentration at 5x for human fibronectin was 25 µg/mL and for collagen type I was 50 µg/mL.

With the 5x ECM combination matrix, we performed spiking experiments using the normal human volunteer peripheral blood samples. Recovery from the spiking experiments varied between 55 and 75%. There have been studies that reported over 80% recovery following spiking

experiments using different methods combining mechanical and molecular techniques²⁰⁵. It is important to note a few points with regards to the lower than expected recovery. The cells from immortalized cell lines are not the same as primary cells from cancer patients. The lower recovery could be a result of cell death upon spiking in the hostile environment amongst blood cells. It is known that not all the cells leaving the primary site are able to survive the hostile environment of blood and secondary tissue microenvironment. The heterogeneity of the cells in primary tumour is also a contributing factor to the cell survival. There have been studies to demonstrate that tissue samples from patient biopsies that were classified as being negative for certain mutations had contrary results when their CTCs were characterized^{235,236}. The study by Marchetti *et.al.* demonstrated that EGFR mutation in lung cancer can be different between the primary lesion and the metastatic sites²³⁵. Due to this heterogeneity, certain cells may have gained ability to survive through varying mechanisms including but not limited to travelling in clusters, being covered with platelets, or autophagy activation.

Some of the later optimization experiments were conducted while patient samples were being received. Table 9 demonstrates the gradual refinements in the technique that improved the recovery in patient samples. The major changes included increase in the ECM concentration to 5x and the fixation method with methanol. The cytokeratin stain was better with methanol fixation in comparison with the PFA fixation. For the initial few samples, the background fluorescence was making it difficult to identify the CTCs from a cluster of many other cells. The change from PFA to methanol fixation alleviated the background issue.

A group from Stony Brook, New York has previously looked at utilizing functional approach by using the extracellular matrix protein in order to capture the invasive circulating tumour cells (iCTCs)^{237,238}. Instead of the initial separation through density medium like Ficoll®, they used the

red cell lysis buffer and placed the remaining cells on the substrata composed of collagen type I²³⁷. However, the approach with only one of the ECM proteins may not be ideal for capturing CTCs of different origins. A multi-pronged approach such as the one used by Schneck *et.al.* can create an organ specific platform that utilizes a combination of both ECM proteins and organ-specific markers to capture the cell population of interest²³⁹. The issue with density medium like Percoll, Ficoll-paque (GE healthcare), and OncoQuick® (Grenier Bio-One) is that large CTCs and CTC-clusters could fall to the bottom layer of the tube given their density²⁴⁰. Performing red cell lysis can become chemically stressful for sensitive CTCs that have barely survived in the circulation. A study by Kallergi *et.al.* demonstrated a better recovery of breast cancer CTCs with red cell lysis in comparison with Ficoll® density gradient²⁴¹. However, the EpCAM staining was more intense and clear with Ficoll® separated cells.

Following the isolation of CTCs, they could be further characterized for different markers depending on the primary cancer site^{242,243}. For instance, presence of absence of markers such as EGFR or KRAS can be interesting to see for solid tumour samples such from CRC patients. A study by Fusi *et.al.* isolated melanoma CTCs and analyzed them for expression of chemokine receptors on the surface²⁴⁴. There is a commercial test called AdnaTest BreastCancerSelect (Qiagen®) which helps detect CTCs from breast cancer patients' blood samples and characterize them for specific markers including MUCIN-1-EpCAM, ALDH-1, HER2, Twist1, ER, Akt2, and PI3K²⁴⁵. The prognostic implications of enumerated and characterized CTCs have been looked at in several studies. A study by Connor *et.al.* demonstrated usability of specific subset of CTCs isolated from peripheral versus hepatic vein in liver metastasis of colorectal cancer²⁴⁶. Another study by Tol *et.al.* demonstrated that a CTC count before and after treatment in advanced colorectal

cancer could predict progression free survival and overall survival²¹⁰. Besides CRC, the value of CTC is well-established in other types of solid cancers²⁴⁷.

There are many different technologies for detecting CTCs from peripheral blood, however they all come with one challenge and that is the feasibility of the downstream application. Whether or not the identified cells are possible to be separated and put through a functional assay is a critical question. Many single-cell functional assays and models are described in the literature²⁴⁸⁻²⁵¹. Single cell sequencing, and fluorescence-activated cell sorting (FACS) are examples of techniques that allow for analysis of single cells. In addition, there are also techniques such as single-cell western blot and CyTOF, a mass cytometry where antibodies are labelled with heavy metal ions²⁵². Budnik *et.al.* demonstrated a technique called Single Cell Proteomics by Mass Spectrometry and this enables multiple proteins to be analyzed from a single cell²⁵³.

Any technique that fully or partially relies on a marker for CTC identification might have cells being affixed or punctured for the application of immunofluorescence. This generally makes it difficult for the cells to be utilized post-identification. However, if such analysis is successful it can provide valuable information. For instance, Babayan *et.al.* assessed isolated CTCs for estrogen receptor positivity and found that only some cells expressed the protein – which relates to why 20% of the estrogen targeted therapies can fail²⁵². There are some groups that have explored carrying out single-cell genomic analysis from the isolated CTCs²⁵⁴. Leukocytes possess many properties that are similar to cancer cells and this makes it challenging for a rich population of CTCs to be isolated in a discrete manner. Some studies have used a combination of CellSearch™ followed by DEPArray™ (©Menarini Silicone Biosystems) in order to isolate single cells^{255,256}. DEPArray™ uses dielectrophoretic force to separate individual cells. A study by Dhar *et.al.* carried out a functional study on single CTCs by encapsulating them into microdroplets and

introducing matrix metalloproteinase (MMP) substrate²⁵¹. These were CTCs isolated from prostate cancer and their MMP activity was higher than simultaneously separated leukocytes²⁵¹.

It is clear through these studies that enumeration of CTCs alone may not fully explain why certain mutations occur part-way through the disease and why certain patients relapse. Optimal isolation techniques and functional studies including single-cell studies can provide mechanistic insight into the complexity of disease progression. Expanding the isolated CTC population, injection in animal models and assessing metastatic capability of these cells hold value for future studies.

5. Overall discussion: challenges in studying chemokines and their relevance to the behaviour of circulating tumour cells

5.1 The key findings of this research

5.1.1 Drug resistance, chemokines, and migration studies

The results from RT-PCR and qPCR experiments confirm that the development of drug resistance influences the regulation of chemokines and chemokine receptors. The initial screening helped establish targets that demonstrated consistent and marked changes at the gene level between parental and resistant HT29 cells. These targets of interest (CCL2, CXCL8, CXCL12, CCL15, CCL20) were analyzed for protein expression using the conditioned media released from the cells. A semi-quantitative measurement of released chemokines coincided with changes observed at the gene level. To understand the functional effects of released chemokines in a microenvironment, HepG2 cells were employed and migration assays were carried out with HT29 and HCT116 cells. In comparison with HT29 cells, HCT116 cells were highly migratory in the presence of HepG2 cells. Colon cancer cell migration remained nil in the absence of HepG2 cells, which further highlights the importance of studying microenvironmental interactions.

5.1.2 Linking chemokines in patient plasma with disease progression

Through the plasma chemokine analysis, differences were noted between healthy volunteers and cancer patients. Many chemokines remained unchanged with the exception of a few that demonstrated an upward trend. Midkine was a chemokine that was relatively high in breast patients' plasma when compared to colon cancer patients and healthy volunteers. Another significant change was an increase in plasma midkine from 6 to 12 months samples within individual patients.

5.1.3 Capture platform for Circulating Tumour cells

The adhesion assays carried out with different ECM proteins led to a combination substratum with fibronectin and collagen (2:1) to capture CTCs. Further optimization was carried out by assessing different density gradient solutions, fixation methods, and antibodies to effectively capture and identify CTCs from blood samples. CD45, a marker of hematopoietic cells that was used to further confirm the identity of CTCs from epithelial origin. A successful working method was developed that captures CTCs using a functional attachment to the ECM proteins. These CTCs were identified through immunofluorescence using epithelial markers like EpCAM and CK. This opens up a possibility to further characterize isolated CTCs for other markers such as EGFR, HER2, CD44, chemokines etc.

5.2 Considerations in interpretation and future directions

The initial experiments for chemokines' gene and protein-level expression provided a strong foundation to understand changes that come along with drug-resistance. It is important to note that these changes are from one of the CRC cell lines and resistance against one of the chemotherapeutic agents. Consistent patterns in different CRC cells and different chemotherapeutic agents could provide stronger data to identify targets for animal studies. The migration studies with a model cell line of liver parenchyma added further insight into the importance of chemokines. HCT116 cells aggressively migrating towards HepG2 cells opened up opportunities for further studies looking at the specific mechanism behind this migration. The array data for chemokines released from the HepG2 cells can be useful in identifying which chemokine(s) are responsible for this functional behaviour. The overall results from the migration experiments demonstrated that chemokines released in the microenvironment can have

implications for processes such as transendothelial migration and growth at secondary sites. Function-blocking antibodies could be used to assess the effect of an attenuated chemokine release. Quantifying chemokines with ELISA kits can provide a direct comparison and subsequent expression changes upon drug treatment. To assess the localization and release patterns of chemokines, it would be helpful to identify a suitable method for golgi-block with Brefeldin-A. This can help retain the chemokines within the cells and detect them through immunofluorescence. Some success was achieved with immunofluorescence of CXCL12; however, we could not detect CCL2 expression. It is known that the effect of chemokines is on the recruitment of different immune system cells. Further studies including other cells from the hematopoietic lineage could help understand the microenvironmental communication between different cells. For instance, the type of macrophages and other myeloid or lymphoid cells recruited by cancer cells can generate further understanding of how specific chemokines exert their effects in the complex environment at secondary sites of metastasis.

In terms of the technique for capturing circulating tumour cells, a reasonable working method was developed. The initial adhesion assays laid the foundation to understand interactions between CRC cells and different proteins forming the extracellular matrix. Similar to previous work on fibronectin and integrin alpha5 beta1 interaction, specific ligand-receptor interactions can be further looked at for each protein to understand their adhesion pathways. It is possible that cancer cells binding to specific extracellular matrix proteins induce further signalling in the metastatic process. The binding of integrin alpha5 and fibronectin was shown to initiate a pro-survival PI3K/Akt pathway (Spencer Berg's thesis). Similar pathways relating to cancer cells binding with ECM proteins and increasing MMP production leads to cancer cells carving their way out of the ECM network^{257,258}. These areas can be explored further in future studies.

In terms of the chemokine arrays with plasma, a higher number of patient samples and healthy volunteer samples might be required for a proper comparison. A total of 30 samples in each group might provide a proper comparison to comment on whether or not differences observed are significant. For the plasma chemokine comparisons, age and sex-specific control samples would ideally provide an accurate comparison. It is difficult to control for all of the patient factors as there is bound to variation based on comorbidities and genetics. Lastly, comparing the working technique for CTC isolation with a commercially available positive control can provide more details in terms of how the technique compares to other available options. The FDA approved Cellsearch[®] would have been a good comparison as it is marker dependent technique compared to the functional approach adopted in my work.

5.3 Limitations of this research

It is important to acknowledge that certain parts of this work were carried out *in vitro*. The drug-resistance model with cell lines demonstrated changes in chemokines at mRNA and protein level, however, there was no animal model to establish whether these changes were transferrable. A CRC mouse model that includes sequential treatment with chemotherapeutic agent (e.g. Irinotecan) up to the point of developed resistance can reveal whether the chemokine expression is altered following multiple sequential therapies. Measurement of released chemokines in a cancer tissue microenvironment can link the results of the chemokine array of the conditioned cell line media.

Patients' plasma chemokines were analyzed using a semi-quantitative method through array analysis. ELISA, a direct quantitative measure of plasma chemokines could have provided a better understanding of the differences between patient samples and healthy volunteers. The healthy volunteer samples were not matched by age and sex and these factors bring unaccounted

heterogeneity making this comparison difficult. Having a positive control sample with a known amount of chemokine could provide valuable information to support the validity of obtained results.

For the adhesion assays, a known number of cells were plated and incubated overnight. The experiment did not control for cell-growth and quantified the results based on adherent cells. Since the growth rate between cell lines differ, adding a cell proliferation inhibitor could improve the accuracy of results obtained.

Prior to CTC isolation from patient samples, a series of experiments were carried out by spiking the CRC cells from cell lines into normal human volunteer blood. The recovery ranged between 55-75% and it was uncertain whether the low recovery was due to CRC cells not being able to survive in a hostile blood environment of another individual. For patient samples, the optimized technique was used for CTC isolation and identification. However, there was no commercial technique employed in parallel to understand whether the in-house recovery was comparable or not. For example, if 30 CTCs were isolated from 7.5mL of patient blood, it was difficult to indicate whether a commercially available technique would provide more or less number of cells.

6. References

1. Arnold M, Sierra MS, Laversanne M, Soerjomataram I, Jemal A, Bray F. Global patterns and trends in colorectal cancer incidence and mortality. *Gut*. 2017;66(4):683-691.
2. Canadian Cancer Society. Colorectal Cancer Statistics. <http://www.cancer.ca/en/cancer-information/cancer-type/colorectal/statistics/?region=on>. Published 2019. Accessed 2019-03-07.
3. Ontario Government. Colorectal cancer screening and prevention. <https://www.ontario.ca/page/colorectal-cancer-screening-and-prevention>. Published 2014. Updated December 11, 2018. Accessed 2019-03-07, 2019.
4. Ontario CC. Colorectal Cancer Risk. MyCancerIQ. Published 2014. Updated June 08, 2018. Accessed 2019.
5. Giovannucci E. Modifiable risk factors for colon cancer. *Gastroenterol Clin North Am*. 2002;31(4):925-943.
6. Qiu M, Hu J, Yang D, Cosgrove DP, Xu R. Pattern of distant metastases in colorectal cancer: a SEER based study. *Oncotarget*. 2015;6(36):38658-38666.
7. Riihimaki M, Hemminki A, Sundquist J, Hemminki K. Patterns of metastasis in colon and rectal cancer. *Sci Rep*. 2016;6:29765.
8. Mehlen P, Puisieux A. Metastasis: a question of life or death. *Nat Rev Cancer*. 2006;6(6):449-458.
9. Guan X. Cancer metastases: challenges and opportunities. *Acta Pharm Sin B*. 2015;5(5):402-418.
10. Senthebane DA, Rowe A, Thomford NE, et al. The Role of Tumor Microenvironment in Chemoresistance: To Survive, Keep Your Enemies Closer. *Int J Mol Sci*. 2017;18(7).
11. Samulitis BK, Pond KW, Pond E, et al. Gemcitabine resistant pancreatic cancer cell lines acquire an invasive phenotype with collateral hypersensitivity to histone deacetylase inhibitors. *Cancer Biol Ther*. 2015;16(1):43-51.
12. Vincan E, Barker N. The upstream components of the Wnt signalling pathway in the dynamic EMT and MET associated with colorectal cancer progression. *Clin Exp Metastasis*. 2008;25(6):657-663.
13. Guo P, Cai B, Lei M, Liu Y, Fu BM. Differential arrest and adhesion of tumor cells and microbeads in the microvasculature. *Biomech Model Mechanobiol*. 2014;13(3):537-550.
14. Weinberg RA. *The Biology of Cancer* 2ed. New York, USA: Garland Science; 2014.
15. Van den Eynden GG, Majeed AW, Illemann M, et al. The multifaceted role of the microenvironment in liver metastasis: biology and clinical implications. *Cancer Res*. 2013;73(7):2031-2043.
16. Langley RR, Fidler IJ. Tumor cell-organ microenvironment interactions in the pathogenesis of cancer metastasis. *Endocr Rev*. 2007;28(3):297-321.
17. Giuliano M, Shaikh A, Lo HC, et al. Perspective on Circulating Tumor Cell Clusters: Why It Takes a Village to Metastasize. *Cancer Res*. 2018;78(4):845-852.
18. Aceto N, Bardia A, Miyamoto DT, et al. Circulating tumor cell clusters are oligoclonal precursors of breast cancer metastasis. *Cell*. 2014;158(5):1110-1122.
19. Friedlander TW, Premasekharan G, Paris PL. Looking back, to the future of circulating tumor cells. *Pharmacol Ther*. 2014;142(3):271-280.

20. Lambert AW, Pattabiraman DR, Weinberg RA. Emerging Biological Principles of Metastasis. *Cell*. 2017;168(4):670-691.
21. Chaffer CL, Weinberg RA. A perspective on cancer cell metastasis. *Science*. 2011;331(6024):1559-1564.
22. Zhang L, Shay JW. Multiple Roles of APC and its Therapeutic Implications in Colorectal Cancer. *J Natl Cancer Inst*. 2017;109(8).
23. Porru M, Pompili L, Caruso C, Biroccio A, Leonetti C. Targeting KRAS in metastatic colorectal cancer: current strategies and emerging opportunities. *J Exp Clin Cancer Res*. 2018;37(1):57.
24. Wang Q, Hu WG, Song QB, Wei J. BRAF V600E mutation as a predictive factor of anti-EGFR monoclonal antibodies therapeutic effects in metastatic colorectal cancer: a meta-analysis. *Chin Med Sci J*. 2014;29(4):197-203.
25. Loes IM, Immervoll H, Sorbye H, et al. Impact of KRAS, BRAF, PIK3CA, TP53 status and intraindividual mutation heterogeneity on outcome after liver resection for colorectal cancer metastases. *Int J Cancer*. 2016;139(3):647-656.
26. Ahn BK, Jang SH, Paik SS, Lee KH. Smad4 may help to identify a subset of colorectal cancer patients with early recurrence after curative therapy. *Hepatogastroenterology*. 2011;58(112):1933-1936.
27. Huang D, Sun W, Zhou Y, et al. Mutations of key driver genes in colorectal cancer progression and metastasis. *Cancer Metastasis Rev*. 2018;37(1):173-187.
28. Nguyen HT, Duong HQ. The molecular characteristics of colorectal cancer: Implications for diagnosis and therapy. *Oncol Lett*. 2018;16(1):9-18.
29. National Cancer Institute. Cancer Staging. <https://www.cancer.gov/about-cancer/diagnosis-staging/staging>. Published 2015, March 09. Accessed 2015.
30. Hanahan D, Weinberg RA. The hallmarks of cancer. *Cell*. 2000;100(1):57-70.
31. Hanahan D, Weinberg RA. Hallmarks of cancer: the next generation. *Cell*. 2011;144(5):646-674.
32. Bathe OF, Farshidfar F. From genotype to functional phenotype: unraveling the metabolomic features of colorectal cancer. *Genes (Basel)*. 2014;5(3):536-560.
33. National-Cancer-Institute. NCI Dictionary of Cancer Terms. National Institute of Health. <https://www.cancer.gov/publications/dictionaries/cancer-terms/def/carcinoma-in-situ>. Accessed May 29, 2019, 2019.
34. Tontono M. *Coley to Cure: The story of the Cancer Research Institute*. New York: Cancer Research Institute; 2014 2014.
35. Wolpin BM, Mayer RJ. Systemic treatment of colorectal cancer. *Gastroenterology*. 2008;134(5):1296-1310.
36. Van der Jeught K, Xu HC, Li YJ, Lu XB, Ji G. Drug resistance and new therapies in colorectal cancer. *World J Gastroenterol*. 2018;24(34):3834-3848.
37. Sharma S, Saltz LB. Oral chemotherapeutic agents for colorectal cancer. *Oncologist*. 2000;5(2):99-107.
38. André T, Boni C, Navarro M, et al. Improved Overall Survival With Oxaliplatin, Fluorouracil, Resistance to chemotherapy: new treatments and novel insights into an old problem and Leucovorin As Adjuvant Treatment in Stage II or III Colon Cancer in the MOSAIC Trial. *Journal of Clinical Oncology*. 2009;27(19):3109-3116.
39. Hagan S, Orr MC, Doyle B. Targeted therapies in colorectal cancer-an integrative view by PPPM. *EPMA J*. 2013;4(1):3.

40. Wilson TR, Longley DB, Johnston PG. Chemoresistance in solid tumours. *Ann Oncol*. 2006;17 Suppl 10:x315-324.
41. Raguz S, Yague E. Resistance to chemotherapy: new treatments and novel insights into an old problem. *Br J Cancer*. 2008;99(3):387-391.
42. Hammond WA, Swaika A, Mody K. Pharmacologic resistance in colorectal cancer: a review. *Ther Adv Med Oncol*. 2016;8(1):57-84.
43. Peters GJ, Backus HH, Freemantle S, et al. Induction of thymidylate synthase as a 5-fluorouracil resistance mechanism. *Biochim Biophys Acta*. 2002;1587(2-3):194-205.
44. Rouquette I, Mazieres J. [A brief overview of a lung cancer biomarker: thymidylate synthase]. *Rev Mal Respir*. 2011;28(6):773-777.
45. Xu Y, Villalona-Calero MA. Irinotecan: mechanisms of tumor resistance and novel strategies for modulating its activity. *Ann Oncol*. 2002;13(12):1841-1851.
46. Tagen M, Zhuang Y, Zhang F, et al. P-glycoprotein, but not multidrug resistance protein 4, plays a role in the systemic clearance of irinotecan and SN-38 in mice. *Drug Metab Lett*. 2010;4(4):195-201.
47. Westover D, Li F. New trends for overcoming ABCG2/BCRP-mediated resistance to cancer therapies. *J Exp Clin Cancer Res*. 2015;34:159.
48. Nikolaou M, Pavlopoulou A, Georgakilas AG, Kyrodimos E. The challenge of drug resistance in cancer treatment: a current overview. *Clin Exp Metastasis*. 2018;35(4):309-318.
49. Lee HH, Bellat V, Law B. Chemotherapy induces adaptive drug resistance and metastatic potentials via phenotypic CXCR4-expressing cell state transition in ovarian cancer. *PLoS One*. 2017;12(2):e0171044.
50. Yardley DA. Drug resistance and the role of combination chemotherapy in improving patient outcomes. *Int J Breast Cancer*. 2013;2013:137414.
51. Loupakis F, Ruzzo A, Cremolini C, et al. KRAS codon 61, 146 and BRAF mutations predict resistance to cetuximab plus irinotecan in KRAS codon 12 and 13 wild-type metastatic colorectal cancer. *Br J Cancer*. 2009;101(4):715-721.
52. Dornier E, Norman JC. Cancer cells with trapped nuclei cut their way through the extracellular matrix. *Nat Commun*. 2018;9(1):3954.
53. Gouirand V, Vasseur S. Fountain of youth of pancreatic cancer cells: the extracellular matrix. *Cell Death Discov*. 2018;4:1.
54. Lu P, Weaver VM, Werb Z. The extracellular matrix: a dynamic niche in cancer progression. *J Cell Biol*. 2012;196(4):395-406.
55. Hojilla CV, Wood GA, Khokha R. Inflammation and breast cancer: metalloproteinases as common effectors of inflammation and extracellular matrix breakdown in breast cancer. *Breast Cancer Res*. 2008;10(2):205.
56. Crotti S, Piccoli M, Rizzolio F, Giordano A, Nitti D, Agostini M. Extracellular Matrix and Colorectal Cancer: How Surrounding Microenvironment Affects Cancer Cell Behavior? *J Cell Physiol*. 2017;232(5):967-975.
57. Zervantonakis IK, Hughes-Alford SK, Charest JL, Condeelis JS, Gertler FB, Kamm RD. Three-dimensional microfluidic model for tumor cell intravasation and endothelial barrier function. *Proc Natl Acad Sci U S A*. 2012;109(34):13515-13520.
58. Mook OR, van Marle J, Jonges R, Vreeling-Sindelarova H, Frederiks WM, Van Noorden CJ. Interactions between colon cancer cells and hepatocytes in rats in relation to metastasis. *J Cell Mol Med*. 2008;12(5B):2052-2061.

59. Frantz C, Stewart KM, Weaver VM. The extracellular matrix at a glance. *J Cell Sci.* 2010;123(Pt 24):4195-4200.
60. Barbazan J, Alonso-Alconada L, Elkhatib N, et al. Liver Metastasis Is Facilitated by the Adherence of Circulating Tumor Cells to Vascular Fibronectin Deposits. *Cancer Res.* 2017;77(13):3431-3441.
61. Nishida-Aoki N, Gujral TS. Emerging approaches to study cell-cell interactions in tumor microenvironment. *Oncotarget.* 2019;10(7):785-797.
62. Nguyen DX, Bos PD, Massague J. Metastasis: from dissemination to organ-specific colonization. *Nat Rev Cancer.* 2009;9(4):274-284.
63. Fidler IJ. The organ microenvironment and cancer metastasis. *Differentiation.* 2002;70(9-10):498-505.
64. Graves DT, Jiang Y. Chemokines, a family of chemotactic cytokines. *Crit Rev Oral Biol Med.* 1995;6(2):109-118.
65. Mantovani A. The chemokine system: redundancy for robust outputs. *Immunol Today.* 1999;20(6):254-257.
66. Cameron MJ, Kelvin DJ. Cytokines and chemokines--their receptors and their genes: an overview. *Adv Exp Med Biol.* 2003;520:8-32.
67. Deshmane SL, Kremlev S, Amini S, Sawaya BE. Monocyte chemoattractant protein-1 (MCP-1): an overview. *J Interferon Cytokine Res.* 2009;29(6):313-326.
68. Chow MT, Luster AD. Chemokines in cancer. *Cancer Immunol Res.* 2014;2(12):1125-1131.
69. Lazennec G, Richmond A. Chemokines and chemokine receptors: new insights into cancer-related inflammation. *Trends Mol Med.* 2010;16(3):133-144.
70. Fernandez EJ, Lolis E. Structure, function, and inhibition of chemokines. *Annu Rev Pharmacol Toxicol.* 2002;42:469-499.
71. Turner MD, Nedjai B, Hurst T, Pennington DJ. Cytokines and chemokines: At the crossroads of cell signalling and inflammatory disease. *Biochim Biophys Acta.* 2014;1843(11):2563-2582.
72. Frick VO, Rubie C, Kolsch K, et al. CCR6/CCL20 chemokine expression profile in distinct colorectal malignancies. *Scand J Immunol.* 2013;78(3):298-305.
73. Frick VO, Rubie C, Keilholz U, Ghadjari P. Chemokine/chemokine receptor pair CCL20/CCR6 in human colorectal malignancy: An overview. *World J Gastroenterol.* 2016;22(2):833-841.
74. Galluzzi L, Buque A, Kepp O, Zitvogel L, Kroemer G. Immunological Effects of Conventional Chemotherapy and Targeted Anticancer Agents. *Cancer Cell.* 2015;28(6):690-714.
75. Huang H, Langenkamp E, Georganaki M, et al. VEGF suppresses T-lymphocyte infiltration in the tumor microenvironment through inhibition of NF-kappaB-induced endothelial activation. *FASEB J.* 2015;29(1):227-238.
76. Aldinucci D, Pinto A, Gloghini A, Carbone A. Chemokine receptors as therapeutic tools in Hodgkin lymphoma: CCR4 and beyond. *Blood.* 2010;115(3):746-747; author reply 748.
77. Erreni M, Mantovani A, Allavena P. Tumor-associated Macrophages (TAM) and Inflammation in Colorectal Cancer. *Cancer Microenviron.* 2011;4(2):141-154.

78. Wolf MJ, Hoos A, Bauer J, et al. Endothelial CCR2 signaling induced by colon carcinoma cells enables extravasation via the JAK2-Stat5 and p38MAPK pathway. *Cancer Cell*. 2012;22(1):91-105.
79. Eferl R. CCL2 at the crossroad of cancer metastasis. *JAKSTAT*. 2013;2(2):e23816.
80. Chun E, Lavoie S, Michaud M, et al. CCL2 Promotes Colorectal Carcinogenesis by Enhancing Polymorphonuclear Myeloid-Derived Suppressor Cell Population and Function. *Cell Rep*. 2015;12(2):244-257.
81. Natsagdorj A, Izumi K, Hiratsuka K, et al. CCL2 induces resistance to the antiproliferative effect of cabazitaxel in prostate cancer cells. *Cancer Sci*. 2019;110(1):279-288.
82. Han R, Gu S, Zhang Y, et al. Estrogen promotes progression of hormone-dependent breast cancer through CCL2-CCR2 axis by upregulation of Twist via PI3K/AKT/NF-kappaB signaling. *Sci Rep*. 2018;8(1):9575.
83. Aldinucci D, Casagrande N. Inhibition of the CCL5/CCR5 Axis against the Progression of Gastric Cancer. *Int J Mol Sci*. 2018;19(5).
84. Smeets A, Brouwers B, Hatse S, et al. Circulating CCL5 Levels in Patients with Breast Cancer: Is There a Correlation with Lymph Node Metastasis? *ISRN Immunology*. 2013;2013:1-5.
85. Cambien B, Richard-Fiardo P, Karimjee BF, et al. CCL5 neutralization restricts cancer growth and potentiates the targeting of PDGFRbeta in colorectal carcinoma. *PLoS One*. 2011;6(12):e28842.
86. Singh SK, Mishra MK, Eltoun IA, Bae S, Lillard JW, Jr., Singh R. CCR5/CCL5 axis interaction promotes migratory and invasiveness of pancreatic cancer cells. *Sci Rep*. 2018;8(1):1323.
87. Soria G, Ben-Baruch A. The inflammatory chemokines CCL2 and CCL5 in breast cancer. *Cancer Lett*. 2008;267(2):271-285.
88. Aldinucci D, Colombatti A. The inflammatory chemokine CCL5 and cancer progression. *Mediators Inflamm*. 2014;2014:292376.
89. Wang SW, Liu SC, Sun HL, et al. CCL5/CCR5 axis induces vascular endothelial growth factor-mediated tumor angiogenesis in human osteosarcoma microenvironment. *Carcinogenesis*. 2015;36(1):104-114.
90. Ivanoff J, Talme T, Sundqvist KG. The role of chemokines and extracellular matrix components in the migration of T lymphocytes into three-dimensional substrata. *Immunology*. 2005;114(1):53-62.
91. Wang SW, Wu HH, Liu SC, et al. CCL5 and CCR5 interaction promotes cell motility in human osteosarcoma. *PLoS One*. 2012;7(4):e35101.
92. Yi EH, Lee CS, Lee JK, et al. STAT3-RANTES autocrine signaling is essential for tamoxifen resistance in human breast cancer cells. *Mol Cancer Res*. 2013;11(1):31-42.
93. Zhou B, Sun C, Li N, et al. Cisplatin-induced CCL5 secretion from CAFs promotes cisplatin-resistance in ovarian cancer via regulation of the STAT3 and PI3K/Akt signaling pathways. *Int J Oncol*. 2016;48(5):2087-2097.
94. Tsukishiro S, Suzumori N, Nishikawa H, Arakawa A, Suzumori K. Elevated serum RANTES levels in patients with ovarian cancer correlate with the extent of the disorder. *Gynecol Oncol*. 2006;102(3):542-545.

95. Bronte V, Bria E. Interfering with CCL5/CCR5 at the Tumor-Stroma Interface. *Cancer Cell*. 2016;29(4):437-439.
96. Walentowicz-Sadlecka M, Sadlecki P, Bodnar M, et al. Stromal derived factor-1 (SDF-1) and its receptors CXCR4 and CXCR7 in endometrial cancer patients. *PLoS One*. 2014;9(1):e84629.
97. Kryczek I, Wei S, Keller E, Liu R, Zou W. Stroma-derived factor (SDF-1/CXCL12) and human tumor pathogenesis. *Am J Physiol Cell Physiol*. 2007;292(3):C987-995.
98. Richard CL, Tan EY, Blay J. Adenosine upregulates CXCR4 and enhances the proliferative and migratory responses of human carcinoma cells to CXCL12/SDF-1alpha. *Int J Cancer*. 2006;119(9):2044-2053.
99. Richard CL, Lowthers EL, Blay J. 15-Deoxy-delta(12,14)-prostaglandin J(2) down-regulates CXCR4 on carcinoma cells through PPARgamma- and NFkappaB-mediated pathways. *Exp Cell Res*. 2007;313(16):3446-3458.
100. Richard CL, Blay J. Thiazolidinedione drugs down-regulate CXCR4 expression on human colorectal cancer cells in a peroxisome proliferator activated receptor gamma-dependent manner. *Int J Oncol*. 2007;30(5):1215-1222.
101. Cutler MJ, Lowthers EL, Richard CL, Hajducek DM, Spagnuolo PA, Blay J. Chemotherapeutic agents attenuate CXCL12-mediated migration of colon cancer cells by selecting for CXCR4-negative cells and increasing peptidase CD26. *BMC Cancer*. 2015;15:882.
102. de Oliveira S, Reyes-Aldasoro CC, Candel S, Renshaw SA, Mulero V, Calado A. Cxcl8 (IL-8) mediates neutrophil recruitment and behavior in the zebrafish inflammatory response. *J Immunol*. 2013;190(8):4349-4359.
103. Moore BB, Kunkel SL. Attracting Attention: Discovery of IL-8/CXCL8 and the Birth of the Chemokine Field. *J Immunol*. 2019;202(1):3-4.
104. Mukaida N. Pathophysiological roles of interleukin-8/CXCL8 in pulmonary diseases. *Am J Physiol Lung Cell Mol Physiol*. 2003;284(4):L566-577.
105. Nagarsheth N, Wicha MS, Zou W. Chemokines in the cancer microenvironment and their relevance in cancer immunotherapy. *Nat Rev Immunol*. 2017;17(9):559-572.
106. Mizuno R, Kawada K, Itatani Y, Ogawa R, Kiyasu Y, Sakai Y. The Role of Tumor-Associated Neutrophils in Colorectal Cancer. *Int J Mol Sci*. 2019;20(3).
107. Xiao YC, Yang ZB, Cheng XS, et al. CXCL8, overexpressed in colorectal cancer, enhances the resistance of colorectal cancer cells to anoikis. *Cancer Lett*. 2015;361(1):22-32.
108. Liu Q, Li A, Tian Y, et al. The CXCL8-CXCR1/2 pathways in cancer. *Cytokine Growth Factor Rev*. 2016;31:61-71.
109. Todorovic-Rakovic N, Milovanovic J. Interleukin-8 in breast cancer progression. *J Interferon Cytokine Res*. 2013;33(10):563-570.
110. Celik B, Yalcin AD, Genc GE, Bulut T, Kuloglu Genc S, Gumuslu S. CXCL8, IL-1beta and sCD200 are pro-inflammatory cytokines and their levels increase in the circulation of breast carcinoma patients. *Biomed Rep*. 2016;5(2):259-263.
111. Rubie C, Frick VO, Pfeil S, et al. Correlation of IL-8 with induction, progression and metastatic potential of colorectal cancer. *World J Gastroenterol*. 2007;13(37):4996-5002.

112. Ueda T, Shimada E, Urakawa T. Serum levels of cytokines in patients with colorectal cancer: possible involvement of interleukin-6 and interleukin-8 in hematogenous metastasis. *J Gastroenterol.* 1994;29(4):423-429.
113. Bai Z, Tai Y, Li W, et al. Gankyrin activates IL-8 to promote hepatic metastasis of colorectal cancer. *Cancer Res.* 2013;73(14):4548-4558.
114. Khazali AS, Clark AM, Wells A. Inflammatory cytokine IL-8/CXCL8 promotes tumour escape from hepatocyte-induced dormancy. *Br J Cancer.* 2018;118(4):566-576.
115. Vegran F, Boidot R, Michiels C, Sonveaux P, Feron O. Lactate influx through the endothelial cell monocarboxylate transporter MCT1 supports an NF-kappaB/IL-8 pathway that drives tumor angiogenesis. *Cancer Res.* 2011;71(7):2550-2560.
116. Williams IR. CCR6 and CCL20: partners in intestinal immunity and lymphorganogenesis. *Ann N Y Acad Sci.* 2006;1072:52-61.
117. Hauser AE, Hopken, U.E. B Cell Localization and Migration in Health and Disease (chapter 12). In: *Molecular Biology of B-cells.* 2 ed. Berlin, Germany: Academic Press; 2014:187-214.
118. Ghadjar P, Rubie C, Aebbersold DM, Keilholz U. The chemokine CCL20 and its receptor CCR6 in human malignancy with focus on colorectal cancer. *Int J Cancer.* 2009;125(4):741-745.
119. Zeng W, Chang H, Ma M, Li Y. CCL20/CCR6 promotes the invasion and migration of thyroid cancer cells via NF-kappa B signaling-induced MMP-3 production. *Exp Mol Pathol.* 2014;97(1):184-190.
120. Liu B, Jia Y, Ma J, et al. Tumor-associated macrophage-derived CCL20 enhances the growth and metastasis of pancreatic cancer. *Acta Biochim Biophys Sin (Shanghai).* 2016;48(12):1067-1074.
121. Zhang S, Youn BS, Gao JL, Murphy PM, Kwon BS. Differential effects of leukotactin-1 and macrophage inflammatory protein-1 alpha on neutrophils mediated by CCR1. *J Immunol.* 1999;162(8):4938-4942.
122. Park KH, Lee TH, Kim CW, Kim J. Enhancement of CCL15 expression and monocyte adhesion to endothelial cells (ECs) after hypoxia/reoxygenation and induction of ICAM-1 expression by CCL15 via the JAK2/STAT3 pathway in ECs. *J Immunol.* 2013;190(12):6550-6558.
123. Shimizu Y, Dobashi K. CC-chemokine CCL15 expression and possible implications for the pathogenesis of IgE-related severe asthma. *Mediators Inflamm.* 2012;2012:475253.
124. Gao Y, Zhou Z, Lu S, et al. Chemokine CCL15 Mediates Migration of Human Bone Marrow-Derived Mesenchymal Stem Cells Toward Hepatocellular Carcinoma. *Stem Cells.* 2016;34(4):1112-1122.
125. Li Y, Wu J, Zhang P. CCL15/CCR1 axis is involved in hepatocellular carcinoma cells migration and invasion. *Tumour Biol.* 2016;37(4):4501-4507.
126. Itatani Y, Kawada K, Fujishita T, et al. Loss of SMAD4 from colorectal cancer cells promotes CCL15 expression to recruit CCR1+ myeloid cells and facilitate liver metastasis. *Gastroenterology.* 2013;145(5):1064-1075 e1011.
127. Mehrvarz Sarshekeh A, Advani S, Overman MJ, et al. Association of SMAD4 mutation with patient demographics, tumor characteristics, and clinical outcomes in colorectal cancer. *PLoS One.* 2017;12(3):e0173345.

128. Inamoto S, Itatani Y, Yamamoto T, et al. Loss of SMAD4 Promotes Colorectal Cancer Progression by Accumulation of Myeloid-Derived Suppressor Cells through the CCL15-CCR1 Chemokine Axis. *Clin Cancer Res.* 2016;22(2):492-501.
129. Li Y, Wu J, Zhang W, Zhang N, Guo H. Identification of serum CCL15 in hepatocellular carcinoma. *Br J Cancer.* 2013;108(1):99-106.
130. Milioli HH, Vimieiro R, Riveros C, Tishchenko I, Berretta R, Moscato P. The Discovery of Novel Biomarkers Improves Breast Cancer Intrinsic Subtype Prediction and Reconciles the Labels in the METABRIC Data Set. *PLoS One.* 2015;10(7):e0129711.
131. Yu Y, Blokhuis B, Derks Y, Kumari S, Garssen J, Redegeld F. Human mast cells promote colon cancer growth via bidirectional crosstalk: studies in 2D and 3D coculture models. *Oncoimmunology.* 2018;7(11):e1504729.
132. Chen HJ, Edwards R, Tucci S, et al. Chemokine 25-induced signaling suppresses colon cancer invasion and metastasis. *J Clin Invest.* 2012;122(9):3184-3196.
133. Kawada K, Hosogi H, Sonoshita M, et al. Chemokine receptor CXCR3 promotes colon cancer metastasis to lymph nodes. *Oncogene.* 2007;26(32):4679-4688.
134. Bedossa P, Paradis V. Liver extracellular matrix in health and disease. *J Pathol.* 2003;200(4):504-515.
135. Frevert U, Engelmann S, Zougbede S, et al. Intravital observation of Plasmodium berghei sporozoite infection of the liver. *PLoS Biol.* 2005;3(6):e192.
136. Vidal-Vanaclocha F. The prometastatic microenvironment of the liver. *Cancer Microenviron.* 2008;1(1):113-129.
137. Chambers AF, Groom AC, MacDonald IC. Dissemination and growth of cancer cells in metastatic sites. *Nat Rev Cancer.* 2002;2(8):563-572.
138. Matsusue R, Kubo H, Hisamori S, et al. Hepatic stellate cells promote liver metastasis of colon cancer cells by the action of SDF-1/CXCR4 axis. *Ann Surg Oncol.* 2009;16(9):2645-2653.
139. Malik P, Phipps C, Edginton A, Blay J. Pharmacokinetic Considerations for Antibody-Drug Conjugates against Cancer. *Pharm Res.* 2017;34(12):2579-2595.
140. Sarin H. Physiologic upper limits of pore size of different blood capillary types and another perspective on the dual pore theory of microvascular permeability. *J Angiogenes Res.* 2010;2:14.
141. Hirakata K, Nakata H, Nakagawa T. CT of pulmonary metastases with pathological correlation. *Semin Ultrasound CT MR.* 1995;16(5):379-394.
142. Chen Z, Fillmore CM, Hammerman PS, Kim CF, Wong KK. Non-small-cell lung cancers: a heterogeneous set of diseases. *Nat Rev Cancer.* 2014;14(8):535-546.
143. Rintoul RC, Sethi T. The role of extracellular matrix in small-cell lung cancer. *Lancet Oncol.* 2001;2(7):437-442.
144. Aoudjit F, Vuori K. Integrin signaling in cancer cell survival and chemoresistance. *Chemother Res Pract.* 2012;2012:283181.
145. Loyher PL, Hamon P, Laviron M, et al. Macrophages of distinct origins contribute to tumor development in the lung. *J Exp Med.* 2018;215(10):2536-2553.
146. Mariani Costantini R, Falcioni R, Battista P, et al. Integrin (alpha 6/beta 4) expression in human lung cancer as monitored by specific monoclonal antibodies. *Cancer Res.* 1990;50(18):6107-6112.

147. Zhang Y, Sime W, Juhas M, Sjolander A. Crosstalk between colon cancer cells and macrophages via inflammatory mediators and CD47 promotes tumour cell migration. *Eur J Cancer*. 2013;49(15):3320-3334.
148. Feng B, Dong TT, Wang LL, et al. Colorectal cancer migration and invasion initiated by microRNA-106a. *PLoS One*. 2012;7(8):e43452.
149. Donato MT, Tolosa L, Gomez-Lechon MJ. Culture and Functional Characterization of Human Hepatoma HepG2 Cells. *Methods Mol Biol*. 2015;1250:77-93.
150. Ramakers C, Ruijter JM, Deprez RH, Moorman AF. Assumption-free analysis of quantitative real-time polymerase chain reaction (PCR) data. *Neurosci Lett*. 2003;339(1):62-66.
151. Ruijter JM, Ramakers C, Hoogaars WM, et al. Amplification efficiency: linking baseline and bias in the analysis of quantitative PCR data. *Nucleic Acids Res*. 2009;37(6):e45.
152. de Jonge HJ, Fehrmann RS, de Bont ES, et al. Evidence based selection of housekeeping genes. *PLoS One*. 2007;2(9):e898.
153. Krasnov GS, Kudryavtseva AV, Snezhkina AV, et al. Pan-Cancer Analysis of TCGA Data Revealed Promising Reference Genes for qPCR Normalization. *Front Genet*. 2019;10:97.
154. Health NIO. Dot Blot Analysis. 2017. <https://imagej.nih.gov/ij/docs/examples/dot-blot/>. Accessed 22 September 2017.
155. Ohlsson L, Hammarstrom ML, Lindmark G, Hammarstrom S, Sitohy B. Ectopic expression of the chemokine CXCL17 in colon cancer cells. *Br J Cancer*. 2016;114(6):697-703.
156. Schuerwegh AJ, Stevens WJ, Bridts CH, De Clerck LS. Evaluation of monensin and brefeldin A for flow cytometric determination of interleukin-1 beta, interleukin-6, and tumor necrosis factor-alpha in monocytes. *Cytometry*. 2001;46(3):172-176.
157. Eberlein J, Nguyen TT, Victorino F, Golden-Mason L, Rosen HR, Homann D. Comprehensive assessment of chemokine expression profiles by flow cytometry. *J Clin Invest*. 2010;120(3):907-923.
158. Kolios G, Wright KL, Jordan NJ, Leithead JB, Robertson DA, Westwick J. C-X-C and C-C chemokine expression and secretion by the human colonic epithelial cell line, HT-29: differential effect of T lymphocyte-derived cytokines. *Eur J Immunol*. 1999;29(2):530-536.
159. Fitzgerald W, Freeman ML, Lederman MM, Vasilieva E, Romero R, Margolis L. A System of Cytokines Encapsulated in ExtraCellular Vesicles. *Sci Rep*. 2018;8(1):8973.
160. Lacy P. Editorial: secretion of cytokines and chemokines by innate immune cells. *Front Immunol*. 2015;6:190.
161. Rajput A, Dominguez San Martin I, Rose R, et al. Characterization of HCT116 human colon cancer cells in an orthotopic model. *J Surg Res*. 2008;147(2):276-281.
162. Edin S, Wikberg ML, Dahlin AM, et al. The distribution of macrophages with a M1 or M2 phenotype in relation to prognosis and the molecular characteristics of colorectal cancer. *PLoS One*. 2012;7(10):e47045.
163. Qian BZ, Pollard JW. Macrophage diversity enhances tumor progression and metastasis. *Cell*. 2010;141(1):39-51.
164. Wang M, Zhao J, Zhang L, et al. Role of tumor microenvironment in tumorigenesis. *J Cancer*. 2017;8(5):761-773.

165. Murdoch C, Muthana M, Coffelt SB, Lewis CE. The role of myeloid cells in the promotion of tumour angiogenesis. *Nat Rev Cancer*. 2008;8(8):618-631.
166. Schwarz M, Wahl M, Resch K, Radeke HH. IFN γ induces functional chemokine receptor expression in human mesangial cells. *Clin Exp Immunol*. 2002;128(2):285-294.
167. Helbig G, Christopherson KW, 2nd, Bhat-Nakshatri P, et al. NF-kappaB promotes breast cancer cell migration and metastasis by inducing the expression of the chemokine receptor CXCR4. *J Biol Chem*. 2003;278(24):21631-21638.
168. Liu Y, Beyer A, Aebbersold R. On the Dependency of Cellular Protein Levels on mRNA Abundance. *Cell*. 2016;165(3):535-550.
169. Roblek M, Protsyuk D, Becker PF, et al. CCL2 Is a Vascular Permeability Factor Inducing CCR2-Dependent Endothelial Retraction during Lung Metastasis. *Mol Cancer Res*. 2019;17(3):783-793.
170. Laurence AD. Location, movement and survival: the role of chemokines in haematopoiesis and malignancy. *Br J Haematol*. 2006;132(3):255-267.
171. Yamaguchi M, Okamura S, Yamaji T, et al. Plasma cytokine levels and the presence of colorectal cancer. *PLoS One*. 2019;14(3):e0213602.
172. Johdi NA, Mazlan L, Sagap I, Jamal R. Profiling of cytokines, chemokines and other soluble proteins as a potential biomarker in colorectal cancer and polyps. *Cytokine*. 2017;99:35-42.
173. Thomas JK, Mir H, Kapur N, Bae S, Singh S. CC chemokines are differentially expressed in Breast Cancer and are associated with disparity in overall survival. *Sci Rep*. 2019;9(1):4014.
174. Vilgelm AE, Richmond A. Chemokines Modulate Immune Surveillance in Tumorigenesis, Metastasis, and Response to Immunotherapy. *Front Immunol*. 2019;10:333.
175. Matsubara J, Honda K, Ono M, et al. Reduced plasma level of CXC chemokine ligand 7 in patients with pancreatic cancer. *Cancer Epidemiol Biomarkers Prev*. 2011;20(1):160-171.
176. Svensson S, Abrahamsson A, Rodriguez GV, et al. CCL2 and CCL5 Are Novel Therapeutic Targets for Estrogen-Dependent Breast Cancer. *Clin Cancer Res*. 2015;21(16):3794-3805.
177. Roy I, Evans DB, Dwinell MB. Chemokines and chemokine receptors: update on utility and challenges for the clinician. *Surgery*. 2014;155(6):961-973.
178. Dell'Agnola C, Biragyn A. Clinical utilization of chemokines to combat cancer: the double-edged sword. *Expert Rev Vaccines*. 2007;6(2):267-283.
179. Lubowicka E, Przyłipiak A, Zajkowska M, et al. Plasma Chemokine CCL2 and Its Receptor CCR2 Concentrations as Diagnostic Biomarkers for Breast Cancer Patients. *Biomed Res Int*. 2018;2018:2124390.
180. Niwa Y, Akamatsu H, Niwa H, Sumi H, Ozaki Y, Abe A. Correlation of tissue and plasma RANTES levels with disease course in patients with breast or cervical cancer. *Clin Cancer Res*. 2001;7(2):285-289.
181. De la Fuente Lopez M, Landskron G, Parada D, et al. The relationship between chemokines CCL2, CCL3, and CCL4 with the tumor microenvironment and tumor-associated macrophage markers in colorectal cancer. *Tumour Biol*. 2018;40(11):1010428318810059.

182. Brand T, Anderson GM. The measurement of platelet-poor plasma serotonin: a systematic review of prior reports and recommendations for improved analysis. *Clin Chem*. 2011;57(10):1376-1386.
183. Tormey CA, Stack G. Use of a cytokine-release assay to demonstrate loss of platelet secretory capacity during blood bank processing and storage. *Arch Pathol Lab Med*. 2014;138(11):1481-1487.
184. Del Conde I, Cruz MA, Zhang H, Lopez JA, Afshar-Kharghan V. Platelet activation leads to activation and propagation of the complement system. *J Exp Med*. 2005;201(6):871-879.
185. Alsaif M, Guest PC, Schwarz E, et al. Analysis of serum and plasma identifies differences in molecular coverage, measurement variability, and candidate biomarker selection. *Proteomics Clin Appl*. 2012;6(5-6):297-303.
186. Biancotto A, Feng X, Langweiler M, Young NS, McCoy JP. Effect of anticoagulants on multiplexed measurement of cytokine/chemokines in healthy subjects. *Cytokine*. 2012;60(2):438-446.
187. Agalliu I, Xue X, Cushman M, et al. Detectability and reproducibility of plasma levels of chemokines and soluble receptors. *Results Immunol*. 2013;3:79-84.
188. Jin WJ, Xu JM, Xu WL, Gu DH, Li PW. Diagnostic value of interleukin-8 in colorectal cancer: a case-control study and meta-analysis. *World J Gastroenterol*. 2014;20(43):16334-16342.
189. Shantha Kumara HMC, Sutton E, Bellini GA, et al. Plasma interleukin-8 levels are persistently elevated for 1 month after minimally invasive colorectal resection for colorectal cancer. *Mol Clin Oncol*. 2018;8(3):471-476.
190. Kantola T, Klintrup K, Vayrynen JP, et al. Stage-dependent alterations of the serum cytokine pattern in colorectal carcinoma. *Br J Cancer*. 2012;107(10):1729-1736.
191. Jono H, Ando Y. Midkine: a novel prognostic biomarker for cancer. *Cancers (Basel)*. 2010;2(2):624-641.
192. Tian W, Shen J, Chen W. Suppression of midkine gene promotes the antitumoral effect of cisplatin on human gastric cancer cell line AGS in vitro and in vivo via the modulation of Notch signaling pathway. *Oncol Rep*. 2017;38(2):745-754.
193. Krzystek-Korpacka M, Gorska S, Diakowska D, et al. Midkine is up-regulated in both cancerous and inflamed bowel, reflecting lymph node metastasis in colorectal cancer and clinical activity of ulcerative colitis. *Cytokine*. 2017;89:68-75.
194. Ibusuki M, Fujimori H, Yamamoto Y, et al. Midkine in plasma as a novel breast cancer marker. *Cancer Sci*. 2009;100(9):1735-1739.
195. Garver RI, Jr., Radford DM, Donis-Keller H, Wick MR, Milner PG. Midkine and pleiotrophin expression in normal and malignant breast tissue. *Cancer*. 1994;74(5):1584-1590.
196. Ye C, Qi M, Fan QW, et al. Expression of midkine in the early stage of carcinogenesis in human colorectal cancer. *Br J Cancer*. 1999;79(1):179-184.
197. Jones DR. Measuring midkine: the utility of midkine as a biomarker in cancer and other diseases. *Br J Pharmacol*. 2014;171(12):2925-2939.
198. Dominguez-Vigil IG, Moreno-Martinez AK, Wang JY, Roehrl MHA, Barrera-Saldana HA. The dawn of the liquid biopsy in the fight against cancer. *Oncotarget*. 2018;9(2):2912-2922.

199. Palmirotta R, Lovero D, Cafforio P, et al. Liquid biopsy of cancer: a multimodal diagnostic tool in clinical oncology. *Ther Adv Med Oncol*. 2018;10:1758835918794630.
200. Ashworth TR. A Case of Cancer in Which Cells Similar to Those in the Tumours Were Seen in the Blood after Death. *The Medical Journal of Australia*. 1869(14):146-147.
201. Patel H, Le Marer N, Wharton RQ, et al. Clearance of circulating tumor cells after excision of primary colorectal cancer. *Ann Surg*. 2002;235(2):226-231.
202. Lowes LE, Allan AL. Recent advances in the molecular characterization of circulating tumor cells. *Cancers (Basel)*. 2014;6(1):595-624.
203. Ferreira MM, Ramani VC, Jeffrey SS. Circulating tumor cell technologies. *Mol Oncol*. 2016;10(3):374-394.
204. Banko P, Lee SY, Nagygyorgy V, et al. Technologies for circulating tumor cell separation from whole blood. *J Hematol Oncol*. 2019;12(1):48.
205. Meunier A, Hernandez-Castro JA, Turner K, Li K, Veres T, Juncker D. Combination of Mechanical and Molecular Filtration for Enhanced Enrichment of Circulating Tumor Cells. *Anal Chem*. 2016;88(17):8510-8517.
206. Di Trapani M, Manaresi N, Medoro G. DEPArray system: An automatic image-based sorter for isolation of pure circulating tumor cells. *Cytometry A*. 2018;93(12):1260-1266.
207. Allan AL, Keeney M. Circulating tumor cell analysis: technical and statistical considerations for application to the clinic. *J Oncol*. 2010;2010:426218.
208. Hayes DF, Paoletti C. Circulating tumour cells: insights into tumour heterogeneity. *J Intern Med*. 2013;274(2):137-143.
209. Hayes DF, Cristofanilli M, Budd GT, et al. Circulating tumor cells at each follow-up time point during therapy of metastatic breast cancer patients predict progression-free and overall survival. *Clin Cancer Res*. 2006;12(14 Pt 1):4218-4224.
210. Tol J, Koopman M, Miller MC, et al. Circulating tumour cells early predict progression-free and overall survival in advanced colorectal cancer patients treated with chemotherapy and targeted agents. *Ann Oncol*. 2010;21(5):1006-1012.
211. Krebs MG, Renehan AG, Backen A, et al. Circulating Tumor Cell Enumeration in a Phase II Trial of a Four-Drug Regimen in Advanced Colorectal Cancer. *Clin Colorectal Cancer*. 2015;14(2):115-122 e111-112.
212. Gabriel MT, Calleja LR, Chalopin A, Ory B, Heymann D. Circulating Tumor Cells: A Review of Non-EpCAM-Based Approaches for Cell Enrichment and Isolation. *Clin Chem*. 2016;62(4):571-581.
213. Kalluri R, Weinberg RA. The basics of epithelial-mesenchymal transition. *J Clin Invest*. 2009;119(6):1420-1428.
214. Tannock I, Harrington L, Bristow R, Hill RP. The basic science of oncology. In: *McGraw-Hill international editions*. 5th edition. ed. New York: McGraw-Hill; 2013: <http://lib.myilibrary.com?id=513867>.
215. Mani SA, Guo W, Liao MJ, et al. The epithelial-mesenchymal transition generates cells with properties of stem cells. *Cell*. 2008;133(4):704-715.
216. Yu M, Bardia A, Wittner BS, et al. Circulating breast tumor cells exhibit dynamic changes in epithelial and mesenchymal composition. *Science*. 2013;339(6119):580-584.

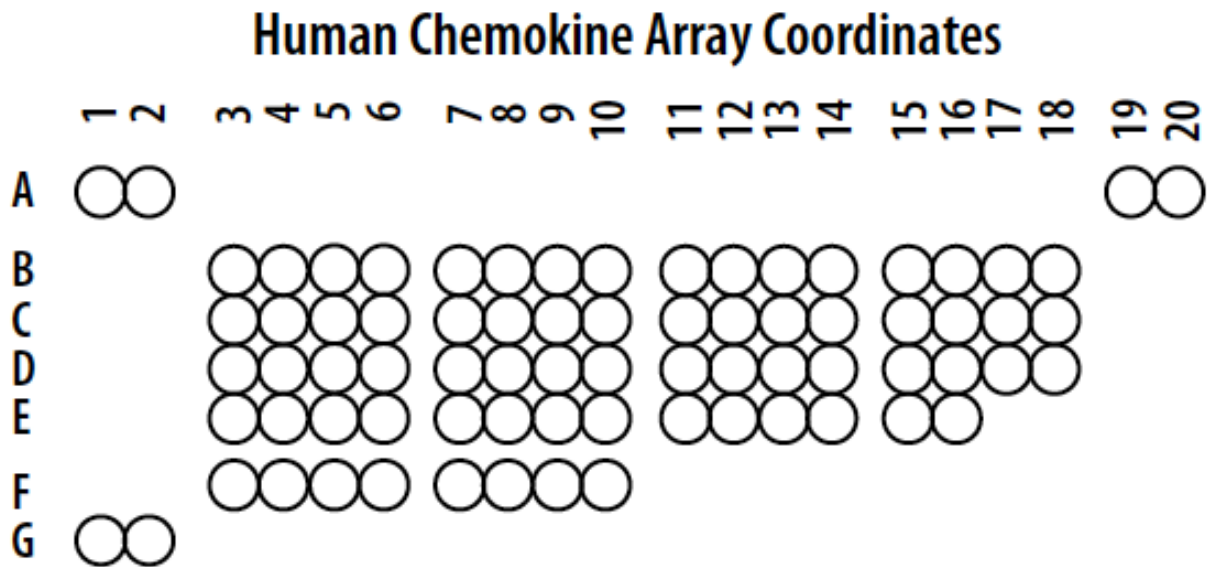
217. Jain S, Zuka M, Liu J, et al. Platelet glycoprotein Ib alpha supports experimental lung metastasis. *Proc Natl Acad Sci U S A*. 2007;104(21):9024-9028.
218. HumanCells. Naive Cynomolgus Peripheral Blood Mononuclear cells (Cynomolgus PBMCs). <https://humancellsbio.com/products/naive-cynomolgus-peripheral-blood-mononuclear-cells-pbmcs>. Published 2019. Accessed.
219. Henriksen KK, M.A. Biochemistry of Collagens, Laminins and Elastin. In: ScienceDirect; 2016:1-11.
220. Gakhar G, Navarro VN, Jurish M, et al. Circulating tumor cells from prostate cancer patients interact with E-selectin under physiologic blood flow. *PLoS One*. 2013;8(12):e85143.
221. Nastaly P, Ruf C, Becker P, et al. Circulating tumor cells in patients with testicular germ cell tumors. *Clin Cancer Res*. 2014;20(14):3830-3841.
222. Geislinger TM, Chan S, Moll K, Wixforth A, Wahlgren M, Franke T. Label-free microfluidic enrichment of ring-stage Plasmodium falciparum-infected red blood cells using non-inertial hydrodynamic lift. *Malar J*. 2014;13:375.
223. Barak V, Goike H, Panaretakis KW, Einarsson R. Clinical utility of cytokeratins as tumor markers. *Clin Biochem*. 2004;37(7):529-540.
224. Satelli A, Mitra A, Brownlee Z, et al. Epithelial-mesenchymal transitioned circulating tumor cells capture for detecting tumor progression. *Clin Cancer Res*. 2015;21(4):899-906.
225. Grover PK, Cummins AG, Price TJ, Roberts-Thomson IC, Hardingham JE. Circulating tumour cells: the evolving concept and the inadequacy of their enrichment by EpCAM-based methodology for basic and clinical cancer research. *Ann Oncol*. 2014;25(8):1506-1516.
226. Tan X, Patil R, Bartosik P, Runnels JM, Lin CP, Niedre M. In Vivo Flow Cytometry of Extremely Rare Circulating Cells. *Sci Rep*. 2019;9(1):3366.
227. Bahnassy AA, Saber MM, Mahmoud MG, et al. The role of circulating tumor cells in metastatic breast cancer: prognostic and predictive value. *Mol Biol Rep*. 2018;45(6):2025-2035.
228. Kang H, Kim J, Cho H, Han KH. Evaluation of Positive and Negative Methods for Isolation of Circulating Tumor Cells by Lateral Magnetophoresis. *Micromachines (Basel)*. 2019;10(6).
229. Yu M, Stott S, Toner M, Maheswaran S, Haber DA. Circulating tumor cells: approaches to isolation and characterization. *J Cell Biol*. 2011;192(3):373-382.
230. Lovitt CJ, Shelper TB, Avery VM. Doxorubicin resistance in breast cancer cells is mediated by extracellular matrix proteins. *BMC Cancer*. 2018;18(1):41.
231. Pelillo C, Bergamo A, Mollica H, Bestagno M, Sava G. Colorectal Cancer Metastases Settle in the Hepatic Microenvironment Through alpha5beta1 Integrin. *J Cell Biochem*. 2015;116(10):2385-2396.
232. Vihinen P, Riikonen T, Laine A, Heino J. Integrin alpha 2 beta 1 in tumorigenic human osteosarcoma cell lines regulates cell adhesion, migration, and invasion by interaction with type I collagen. *Cell Growth Differ*. 1996;7(4):439-447.
233. Cioce V, Castronovo V, Shmookler BM, et al. Increased expression of the laminin receptor in human colon cancer. *J Natl Cancer Inst*. 1991;83(1):29-36.
234. Hsiao CT, Cheng HW, Huang CM, et al. Fibronectin in cell adhesion and migration via N-glycosylation. *Oncotarget*. 2017;8(41):70653-70668.

235. Marchetti A, Del Grammastro M, Felicioni L, et al. Assessment of EGFR mutations in circulating tumor cell preparations from NSCLC patients by next generation sequencing: toward a real-time liquid biopsy for treatment. *PLoS One*. 2014;9(8):e103883.
236. Somlo G, Lau SK, Frankel P, et al. Multiple biomarker expression on circulating tumor cells in comparison to tumor tissues from primary and metastatic sites in patients with locally advanced/inflammatory, and stage IV breast cancer, using a novel detection technology. *Breast Cancer Res Treat*. 2011;128(1):155-163.
237. Pearl ML, Zhao Q, Yang J, et al. Prognostic analysis of invasive circulating tumor cells (iCTCs) in epithelial ovarian cancer. *Gynecol Oncol*. 2014;134(3):581-590.
238. Tulley S, Zhao Q, Dong H, Pearl ML, Chen WT. Vita-Assay Method of Enrichment and Identification of Circulating Cancer Cells/Circulating Tumor Cells (CTCs). *Methods Mol Biol*. 2016;1406:107-119.
239. Schneck H, Gierke B, Uppenkamp F, et al. EpCAM-Independent Enrichment of Circulating Tumor Cells in Metastatic Breast Cancer. *PLoS One*. 2015;10(12):e0144535.
240. Gerges N, Rak J, Jabado N. New technologies for the detection of circulating tumour cells. *Br Med Bull*. 2010;94:49-64.
241. Kallergi G, Politaki E, Alkahtani S, Stournaras C, Georgoulas V. Evaluation of Isolation Methods for Circulating Tumor Cells (CTCs). *Cell Physiol Biochem*. 2016;40(3-4):411-419.
242. Duffy MJ, McDermott EW, Crown J. Blood-based biomarkers in breast cancer: From proteins to circulating tumor cells to circulating tumor DNA. *Tumour Biol*. 2018;40(5):1010428318776169.
243. Economopoulou P, Kotsantis I, Kyrodimos E, Lianidou ES, Psyrris A. Liquid biopsy: An emerging prognostic and predictive tool in Head and Neck Squamous Cell Carcinoma (HNSCC). Focus on Circulating Tumor Cells (CTCs). *Oral Oncol*. 2017;74:83-89.
244. Fusi A, Liu Z, Kummerlen V, Nonnemacher A, Jeske J, Keilholz U. Expression of chemokine receptors on circulating tumor cells in patients with solid tumors. *J Transl Med*. 2012;10:52.
245. Bulfoni M, Turetta M, Del Ben F, Di Loreto C, Beltrami AP, Cesselli D. Dissecting the Heterogeneity of Circulating Tumor Cells in Metastatic Breast Cancer: Going Far Beyond the Needle in the Haystack. *Int J Mol Sci*. 2016;17(10).
246. Connor AA, McNamara K, Al-Sukhni E, et al. Central, But Not Peripheral, Circulating Tumor Cells are Prognostic in Patients Undergoing Resection of Colorectal Cancer Liver Metastases. *Ann Surg Oncol*. 2016;23(7):2168-2175.
247. de Bono JS, Scher HI, Montgomery RB, et al. Circulating tumor cells predict survival benefit from treatment in metastatic castration-resistant prostate cancer. *Clin Cancer Res*. 2008;14(19):6302-6309.
248. Cheng YH, Chen YC, Lin E, et al. Hydro-Seq enables contamination-free high-throughput single-cell RNA-sequencing for circulating tumor cells. *Nat Commun*. 2019;10(1):2163.
249. D'Avola D, Villacorta-Martin C, Martins-Filho SN, et al. High-density single cell mRNA sequencing to characterize circulating tumor cells in hepatocellular carcinoma. *Sci Rep*. 2018;8(1):11570.

250. Fior R, Pova V, Mendes RV, et al. Single-cell functional and chemosensitive profiling of combinatorial colorectal therapy in zebrafish xenografts. *Proc Natl Acad Sci U S A*. 2017;114(39):E8234-E8243.
251. Dhar M, Lam JN, Walser T, Dubinett SM, Rettig MB, Di Carlo D. Functional profiling of circulating tumor cells with an integrated vortex capture and single-cell protease activity assay. *Proc Natl Acad Sci U S A*. 2018;115(40):9986-9991.
252. Heymann D, Tellez-Gabriel M. Circulating Tumor Cells: The Importance of Single Cell Analysis. *Adv Exp Med Biol*. 2018;1068:45-58.
253. Budnik B, Levy E, Harmange G, Slavov N. SCoPE-MS: mass spectrometry of single mammalian cells quantifies proteome heterogeneity during cell differentiation. *Genome Biol*. 2018;19(1):161.
254. Thiele JA, Pitule P, Hicks J, Kuhn P. Single-Cell Analysis of Circulating Tumor Cells. *Methods Mol Biol*. 2019;1908:243-264.
255. Fernandez SV, Bingham C, Fittipaldi P, et al. TP53 mutations detected in circulating tumor cells present in the blood of metastatic triple negative breast cancer patients. *Breast Cancer Res*. 2014;16(5):445.
256. Pestrin M, Salvianti F, Galardi F, et al. Heterogeneity of PIK3CA mutational status at the single cell level in circulating tumor cells from metastatic breast cancer patients. *Mol Oncol*. 2015;9(4):749-757.
257. Kryczka J, Stasiak M, Dziki L, Mik M, Dziki A, Cierniewski C. Matrix metalloproteinase-2 cleavage of the beta1 integrin ectodomain facilitates colon cancer cell motility. *J Biol Chem*. 2012;287(43):36556-36566.
258. Maity G, Sen T, Chatterjee A. Laminin induces matrix metalloproteinase-9 expression and activation in human cervical cancer cell line (SiHa). *J Cancer Res Clin Oncol*. 2011;137(2):347-357.

7. Appendices

Appendix IA: Coordinates and names of chemokines for the ARY017 – human chemokine array kit ARY017.



Note: this image is taken from the R&D systems catalogue for their product #ARY017.

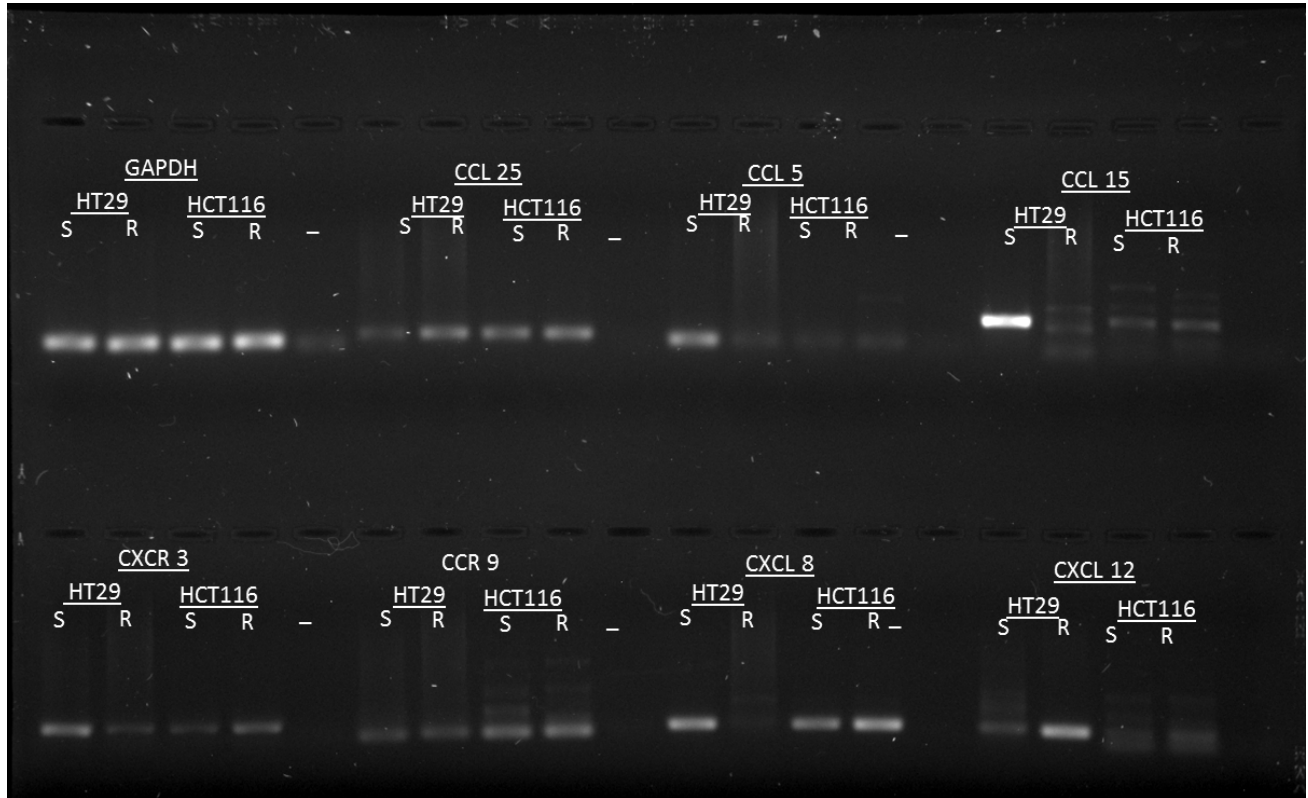
Appendix IB: Coordinate Guide for chemokine array kit ARY017 – R&D Systems.

| Coordinate | Analyte/Control | Alternate Nomenclature |
|------------------|--------------------------|------------------------------------|
| A1, A2, A19, A20 | Reference Spots | — |
| B3, B4 | 6Ckine | CCL21, Exodus-2 |
| B5, B6 | CCL28 | MEC |
| B7, B8 | CXCL16 | SRPSOX |
| B9, B10 | Chemerin | TIG-2, RARRES2 |
| B11, B12 | ENA-78 | CXCL5 |
| B13, B14 | Eotaxin-3 | CCL26 |
| B15, B16 | Fractalkine | CX3CL1, Neurotactin |
| B17, B18 | GRO α | CXCL1 |
| C3, C4 | HCC-1 | CCL14, HCC-3 |
| C5, C6 | I-309 | CCL1, TCA3 |
| C7, C8 | IL-8 | CXCL8 |
| C9, C10 | IL-16 | LCF |
| C11, C12 | IP-10 | CXCL10 |
| C13, C14 | I-TAC | CXCL11 |
| C15, C16 | Lymphotactin | XCL1, Lptn, ATAC, SCM-1 α |
| C17, C18 | MCP-1 | CCL2, MCAF |
| D3, D4 | MCP-3 | CCL7 |
| D5, D6 | MDC | CCL22, STCP-1, ABCD-1 |
| D7, D8 | Midkine | — |
| D9, D10 | MIG | CXCL9 |
| D11, D12 | MIP-1 α / β | CCL3, CCL4 |
| D13, D14 | MIP-1 δ | CCL15, Leukotactin 1, MIP-5, HCC-2 |
| D15, D16 | MIP-3 α | CCL20, LARC, Exodus-1 |
| D17, D18 | MIP-3 β | CCL19, ELC, Exodus-3 |
| E3, E4 | NAP-2 | CXCL7, CTAP III |
| E5, E6 | PARC | CCL18, MIP-4, AMAC-1 |
| E7, E8 | PF4 | CXCL4 |
| E9, E10 | RANTES | CCL5, SIS δ |
| E11, E12 | SDF-1 | CXCL12, PBSF |
| E13, E14 | TARC | CCL17 |
| E15, E16 | VCC-1 | CXCL17, DMC |

| Coordinate | Analyte/Control | Alternate Nomenclature |
|------------|--------------------------------|------------------------|
| F3, F4 | Fibrinogen (Sample Control) | — |
| F5, F6 | gp130 (Sample Control) | IL6ST, CD130 |
| F7, F8 | Transferrin R (Sample Control) | TfR, CD71 |
| F9, F10 | Negative Control | Control (-) |
| G1, G2 | Reference Spots | — |

Appendix II: Raw images of the RT-PCR results

2016-02-10 P19



S: HT29 or HCT116 cDNA (100 ng); R: HT29-S or HCT116-S cDNA (100 ng) –: H₂O

Reaction Date: 2016-02-08

cDNA Collection:

HT29/HT29-S:

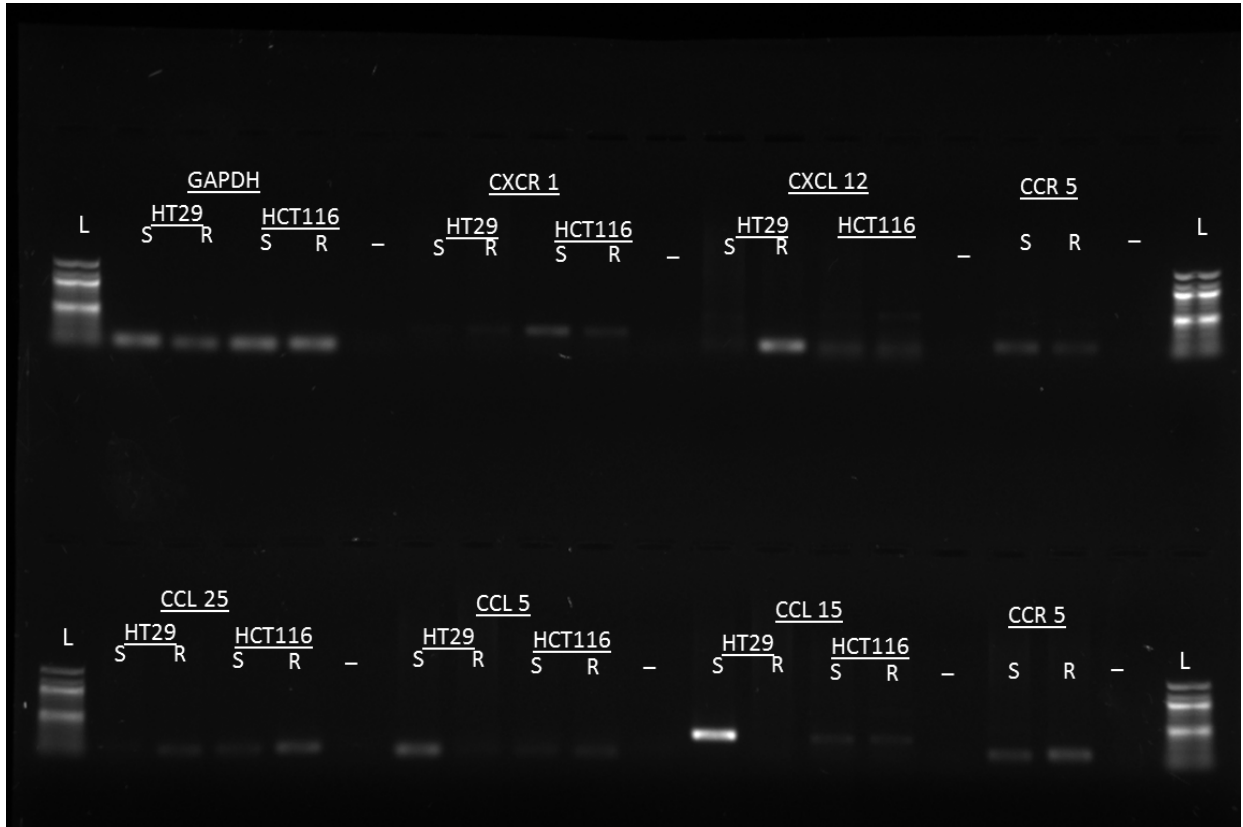
2015-05-13

HCT116/HCT116-S: 2015-02-02

Gel ran at 95 V

For 28 mins

2016-01-20 DP16
Six Chemokine markers



L- 1µL 100 bp DNA ladder (NEB)

S: HT29 or HCT116 cDNA 100ng; R: HT29-S or HCT116-S cDNA 100ng; -: H₂O

cDNA Collection:

HT29/HT29-S: 2014-04-29

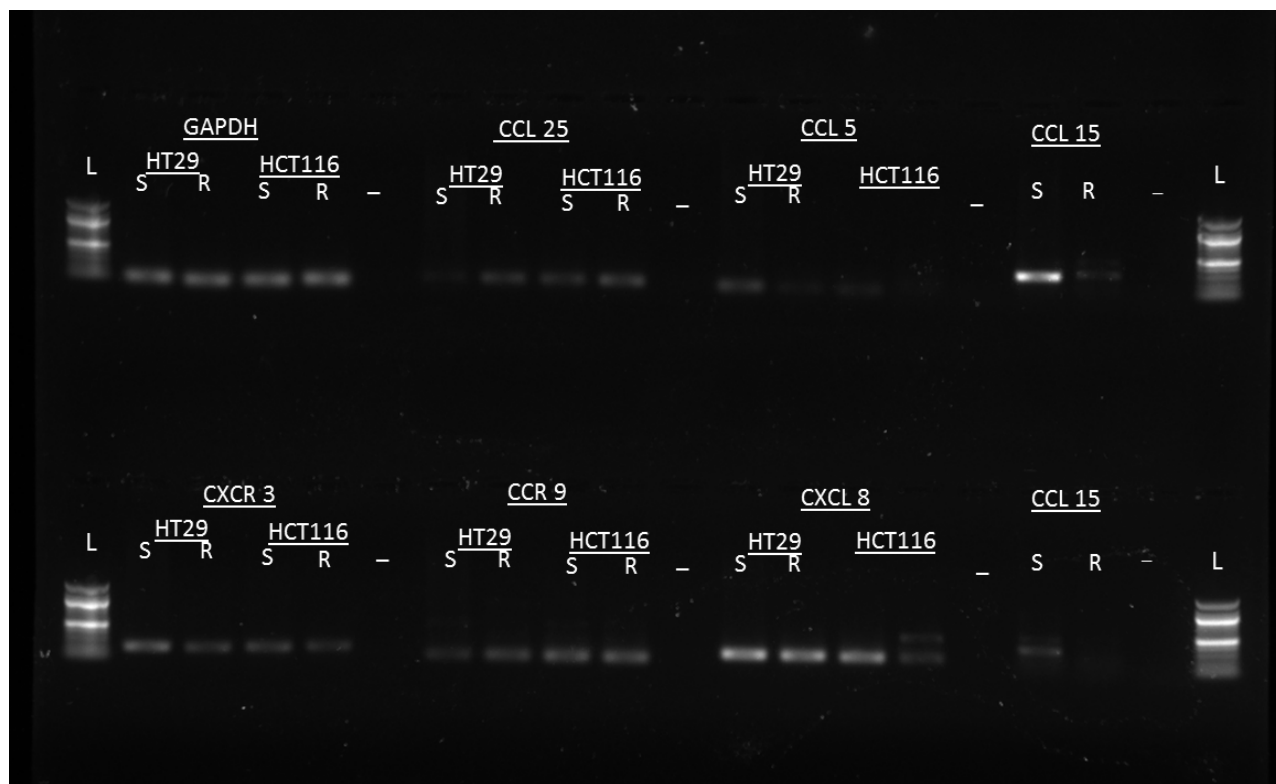
HCT116/HCT116-S: 2014-10-24

Gel ran at 95 V

For 30 mins

Note: HT29-S GAPDH sample – when loading, a very small faint droplet leaked out of the second well

2016-01-14 DP15



L- 1 μ L 100 bp DNA ladder (NEB)

S: HT29 or HCT116 cDNA (100 ng); R: HT29-S or HCT116-S cDNA (100 ng); -: H₂O

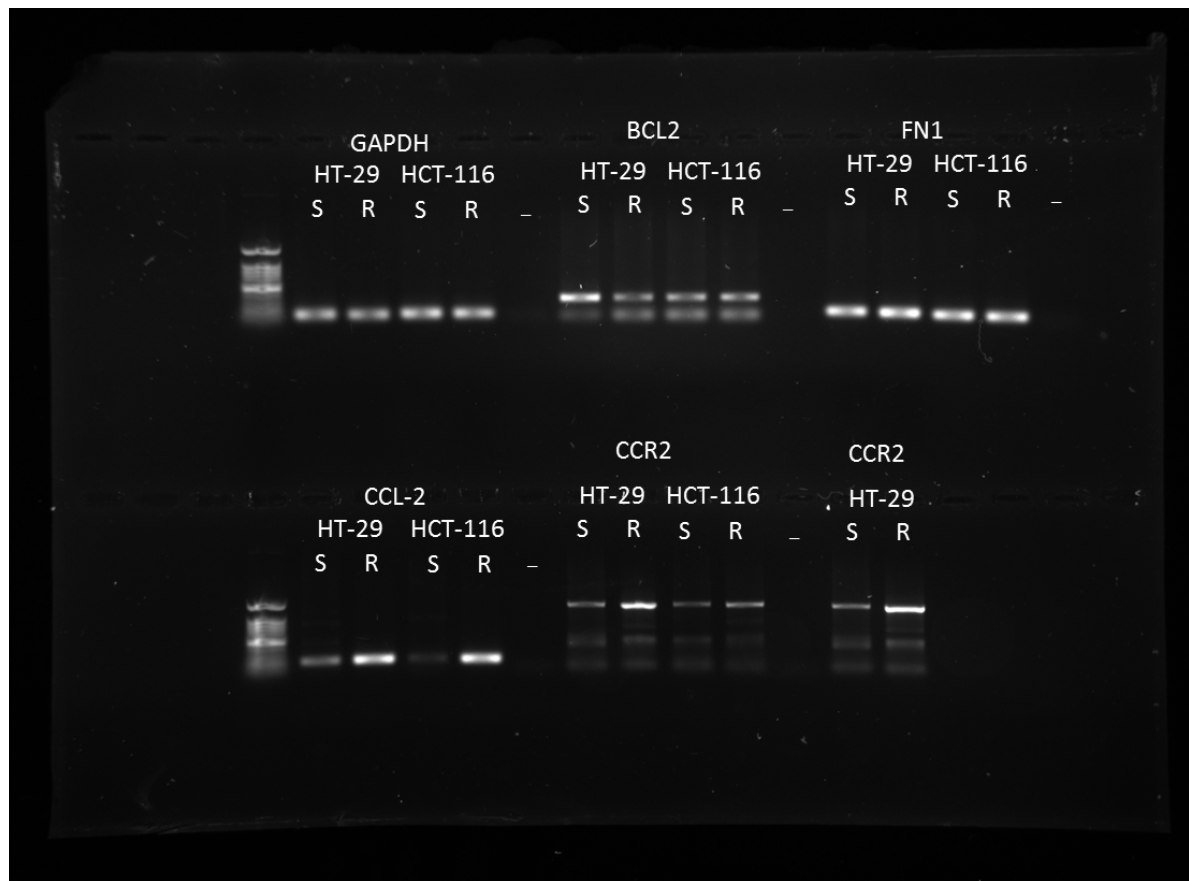
cDNA Collection:

2015-03-27

Gel ran at 95 V

For 25 mins

2015-05-14 DP-12

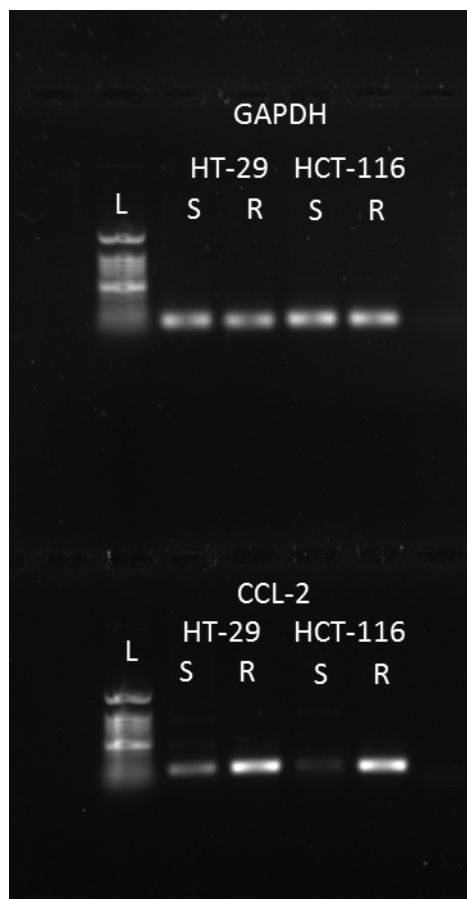


L- 5 μ L 100 bp DNA ladder (Promega)

HT29: 100 ng cDNA; HT29-S: 100 ng cDNA; -: H₂O

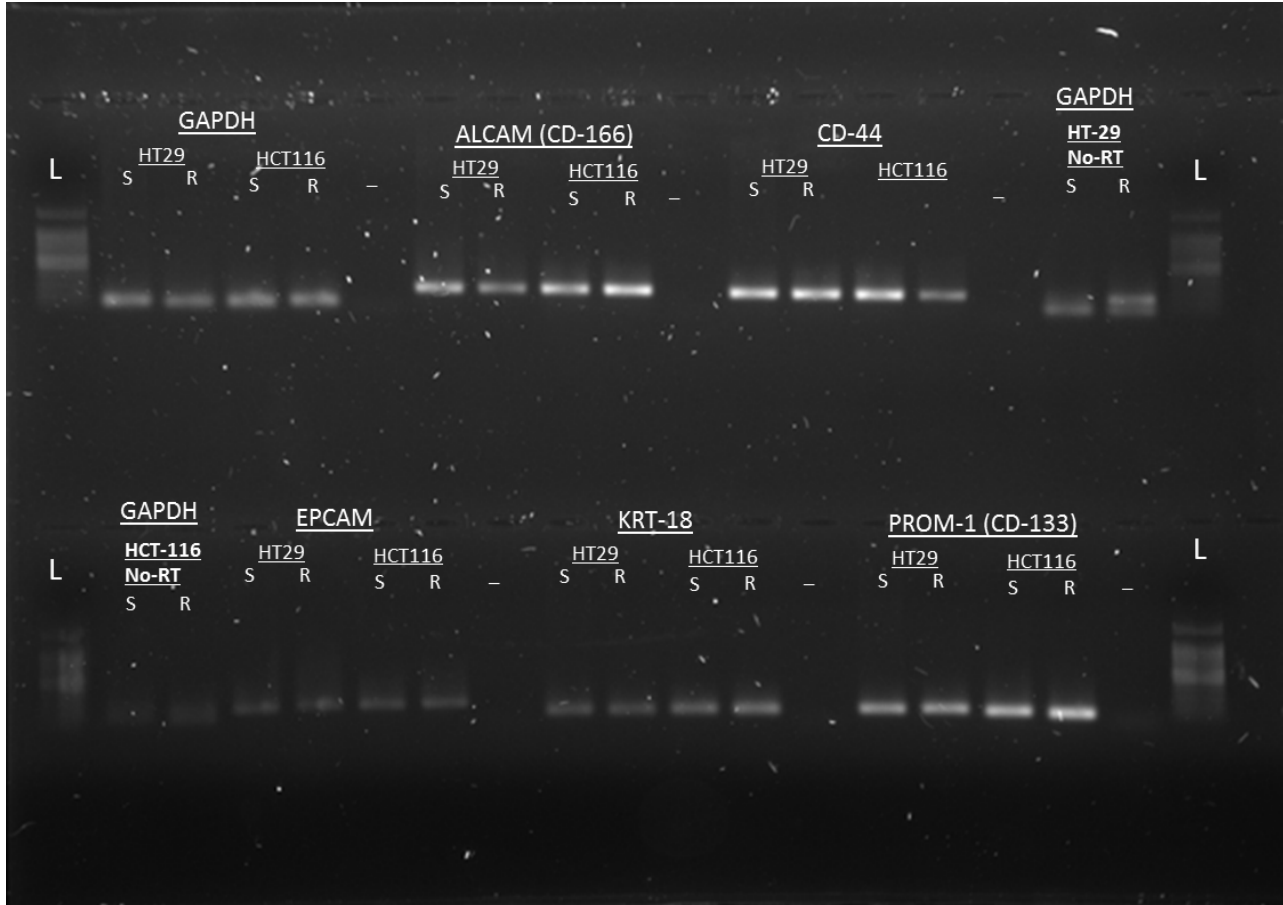
cDNA Collection:
2015-02-01
Gel ran at 95 V
For 25 mins

Experiment: DP-12
2015-05-14



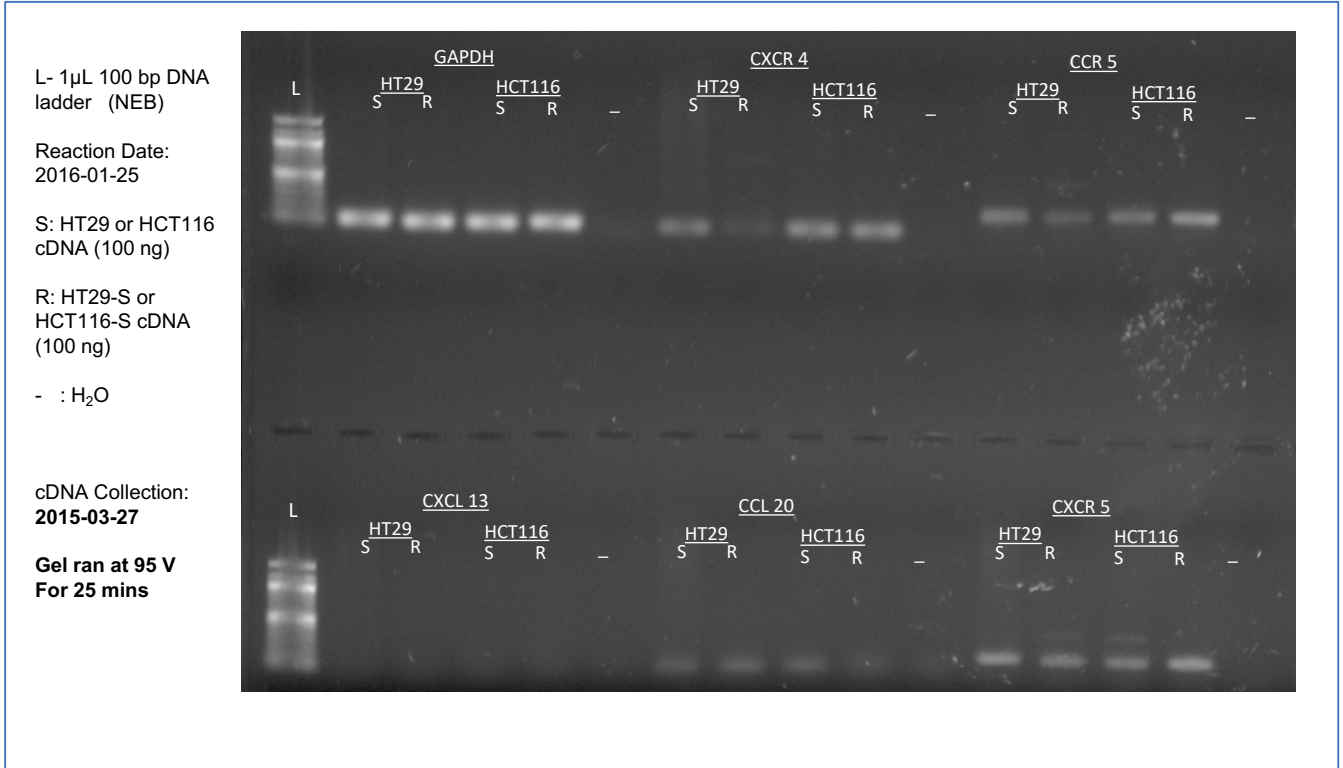
L- 5 μ L 100 bp DNA ladder (Promega)
HT-29 , HCT116
S = sensitive
R= Resistant
Amount : 100 ng cDNA
-: H₂O
cDNA collection: 2015-02-01

Blay Lab – DP8
2015-03-31



L- 5µL 100 bp DNA ladder (Promega)
 S: HT29 or HCT116 cDNA (100 ng)
 R: HT29-S or HCT116-S cDNA (100 ng)
 – : H₂O
 N/A : duplicate of HT-29 sample under CD-44 primer
 KRT-18 : Cytokeratin 18
 HT29,HT29-S = 2015-03-27 collection
 HT116, HT116-S
 2015-03-27 collection

DP17
2016-01-28



S: HT29 or HCT116 cDNA (100 ng)

R: HT29-S or HCT116-S cDNA (100 ng)

L- 1 μ L 100 bp DNA ladder (NEB)

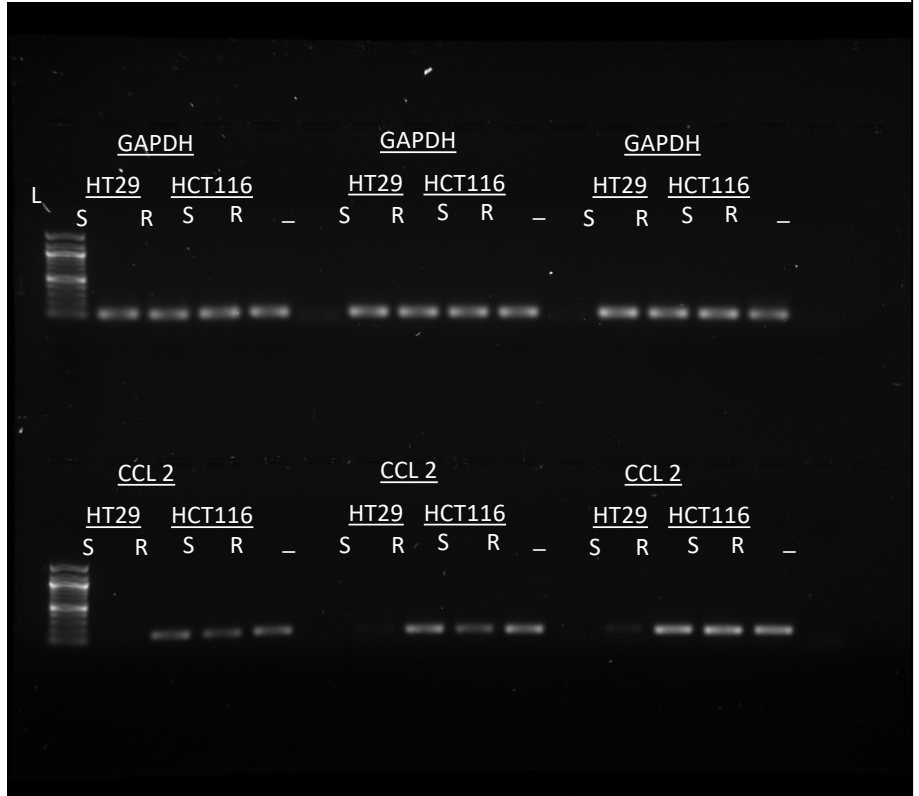
CCL2

cDNA Collection 1:
2016-03-02

cDNA Collection 2:
2016-03-05

cDNA Collection 3:
2016-03-10

- : H₂O control



CCL2 PRIMER SEQUENCE: 5'-3': GCTGTGATCTTCAAGACCATTG
3'-5': AACAGGGTGTCTGGGGAAAG

S: HT29 or HCT116 cDNA (100 ng)

CCL 5 (paper)

R: HT29-S or HCT116-S cDNA (100 ng)

L- 1µL 100 bp DNA ladder (NEB)

cDNA Collection 1:

2016-03-02

cDNA Collection 2:

2016-03-05

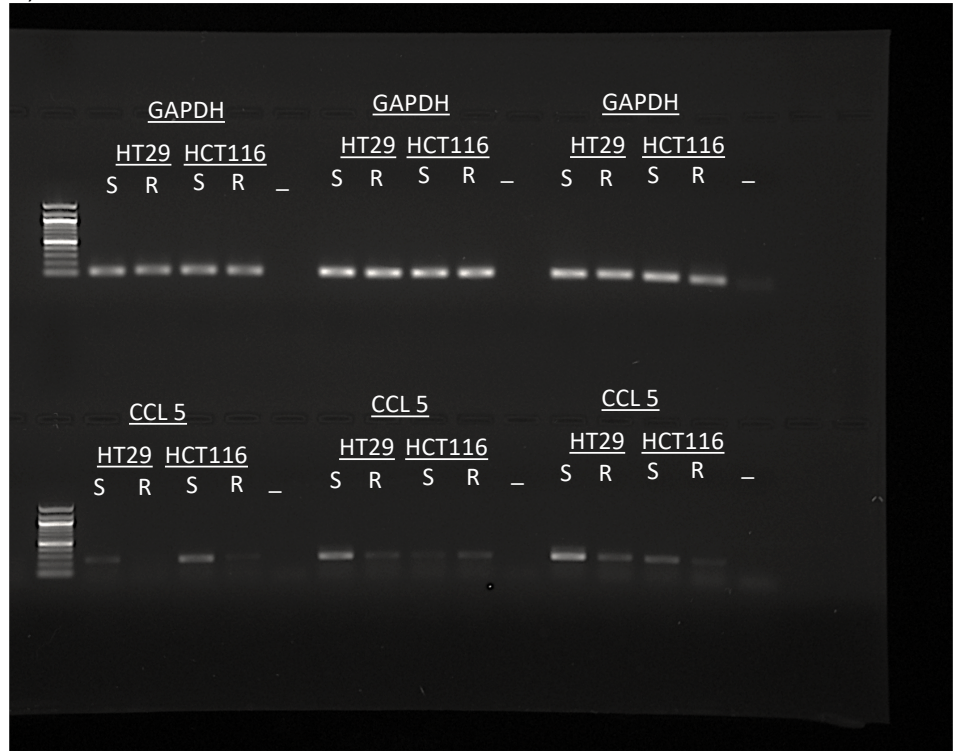
cDNA Collection 3:

2016-03-10

- : H₂O control

Primer source:

Vaday GG, Peehl DM, Kadam PA, Lawrence DM. Expression of CCL5 (RANTES) and CCR5 in prostate cancer. *The Prostate*. 2006. doi:10.1002/pros.20306.



CCL5 PRIMER SEQUENCE: 5'-3': CTCATTGCTACTGCCCTCTGC
3'-5': GCTCATCTCCAAAGAGTTGAT

S: HT29 or HCT116 cDNA (100 ng)

CCL 15

R: HT29-S or HCT116-S cDNA (100 ng)

L- 1 μ L 100 bp DNA ladder (NEB)

cDNA Collection 1:
2016-03-02

cDNA Collection 2:
2016-03-05

cDNA Collection 3:
2016-03-10

- : H₂O control



PRIMER SEQUENCE: 5'-3': CCAAGCCAGGTGTCATATTCC
3'-5': TCAGACCAAGAAACTCACAGGA

S: HT29 or HCT116 cDNA (100 ng)

CXCL 8

R: HT29-S or HCT116-S cDNA (100 ng)

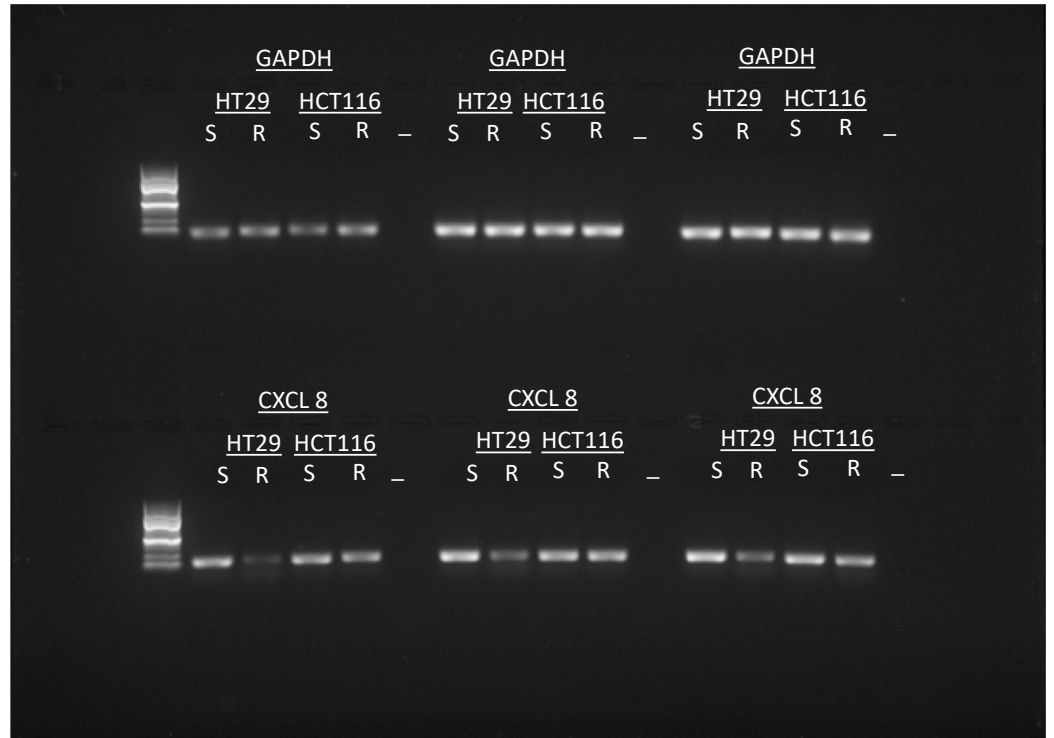
L- 1 μ L 100 bp DNA ladder (NEB)

cDNA Collection 1:
2016-03-02

cDNA Collection 2:
2016-03-05

cDNA Collection 3:
2016-03-10

- : H₂O control



PRIMER SEQUENCE: 5'-3': TCAGAGACAGCAGAGCACAC
3'-5': CCAGTTTTCCTTGGGGTCCAGA

S: HT29 or HCT116 cDNA (100 ng)

CCL 20

R: HT29-S or HCT116-S cDNA (100 ng)

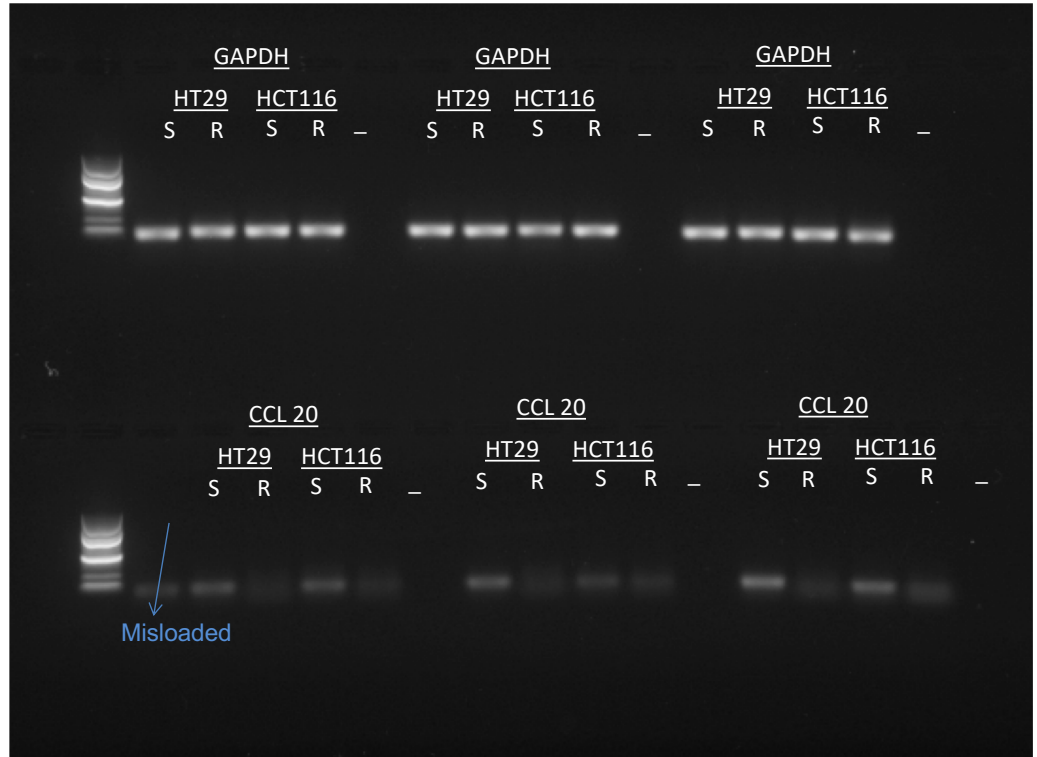
L- 1 μ L 100 bp DNA ladder (NEB)

cDNA Collection 1:
2016-03-02

cDNA Collection 2:
2016-03-05

cDNA Collection 3:
2016-03-10

- : H₂O control



PRIMER SEQUENCE: 5'-3': TTTGCTCCTGGCTGCTTTGAT
3'-5': AGTTGCTTGCTGCTTCTGATTTCG

S: HT29 or HCT116 cDNA (100 ng)

CXCR 4

R: HT29-S or HCT116-S cDNA (100 ng)

L- 1 μ L 100 bp DNA ladder (NEB)

cDNA Collection 1:

2016-03-02

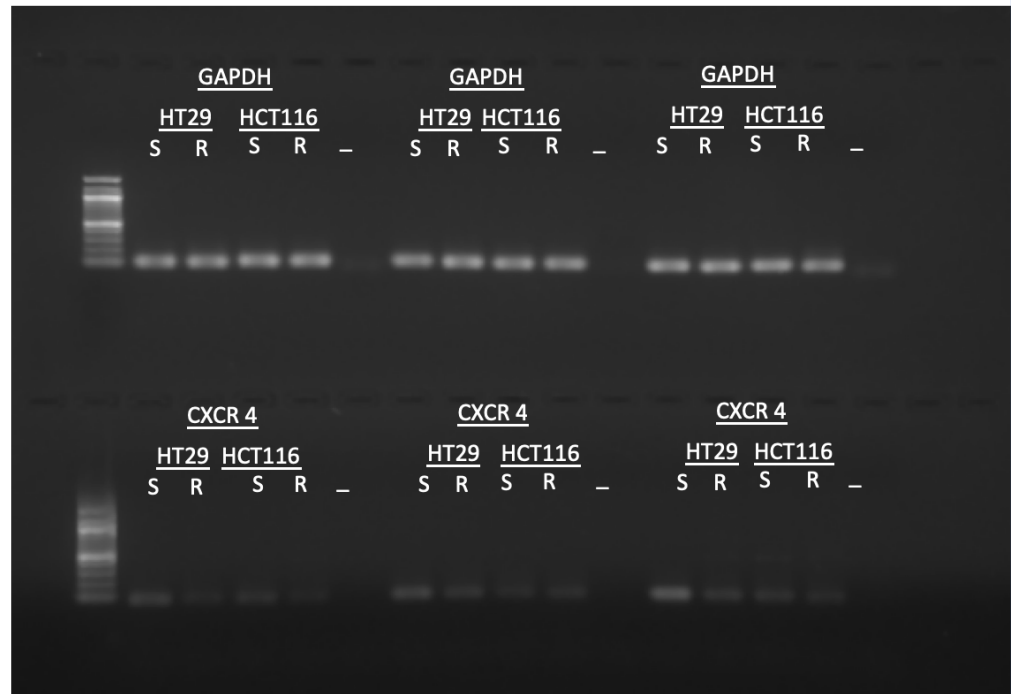
cDNA Collection 2:

2016-03-05

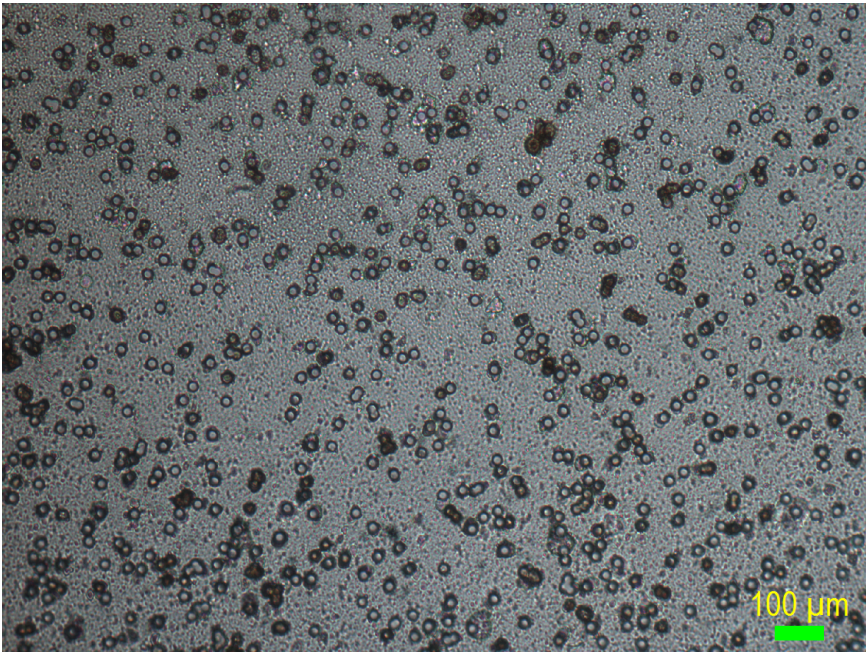
cDNA Collection 3:

2016-03-10

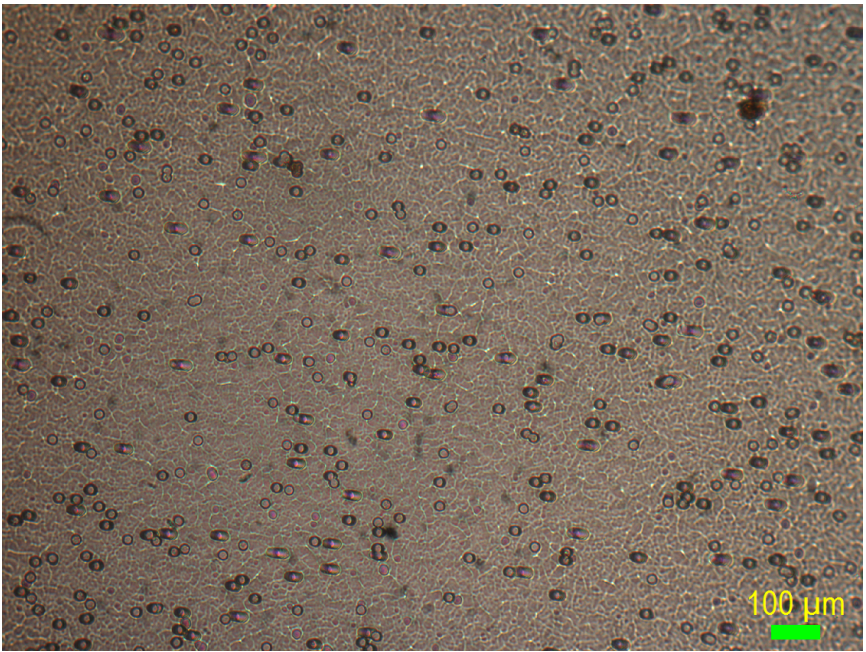
- : H₂O control



Appendix III: Comparison of different Transwell Chambers



Granier

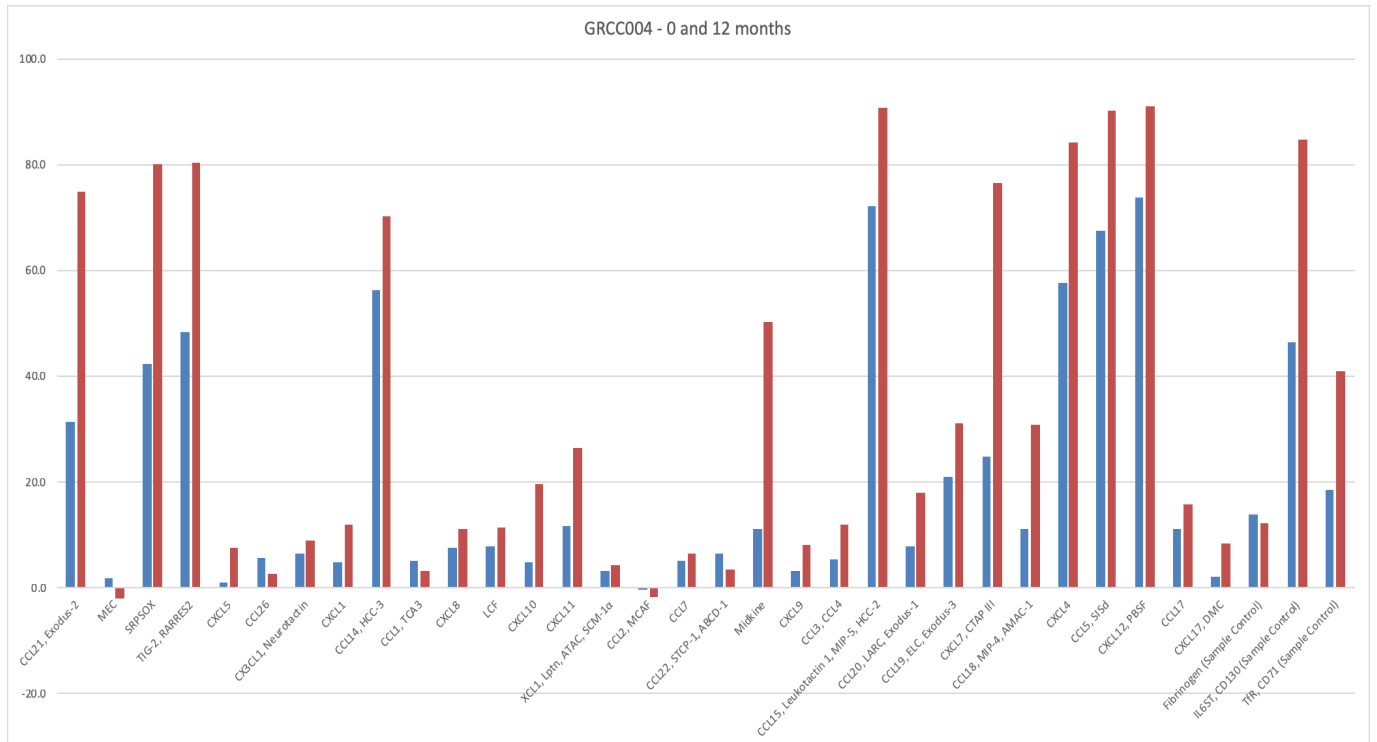
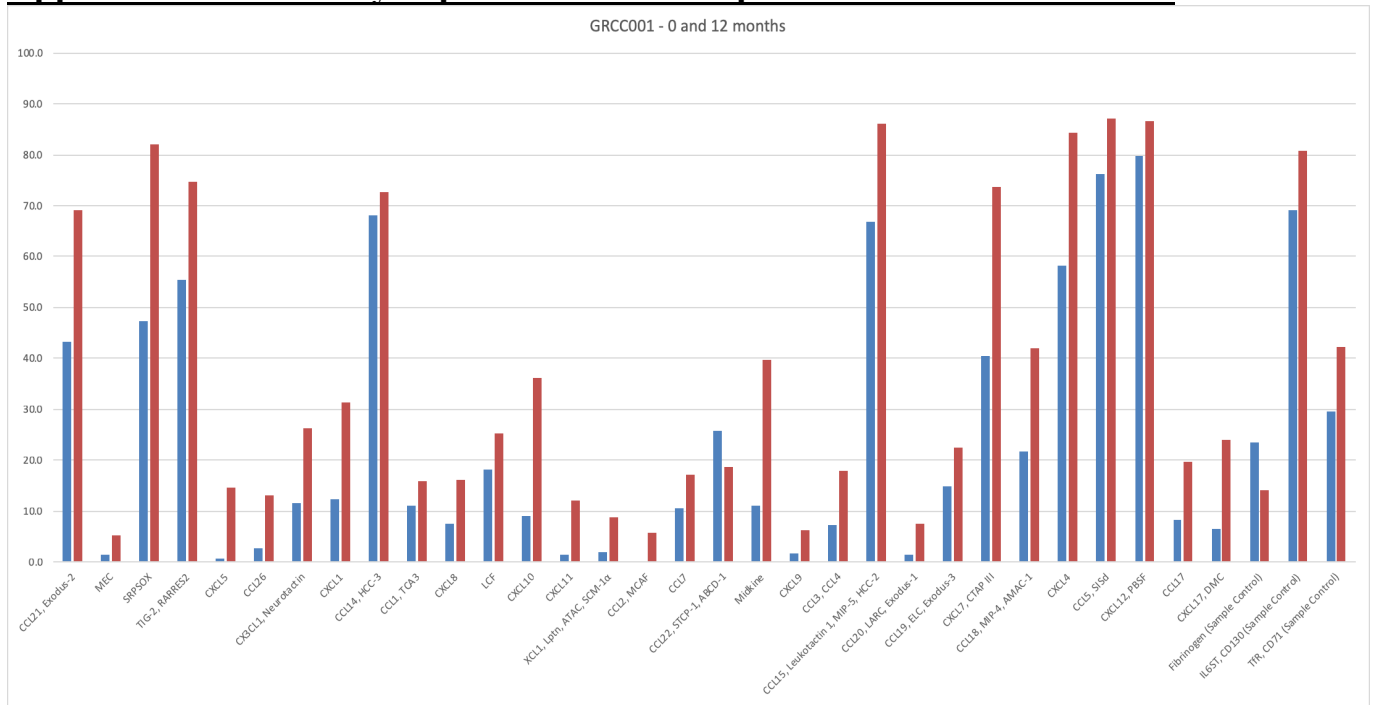


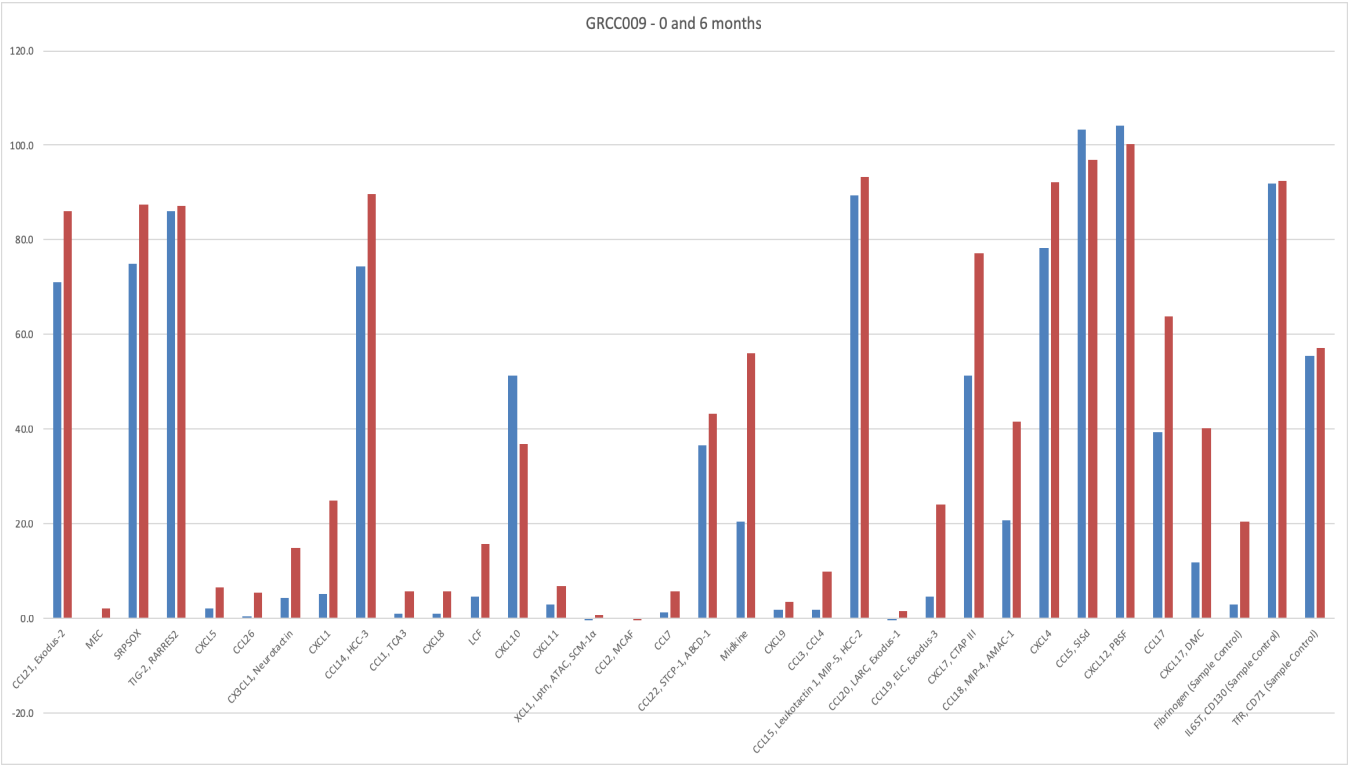
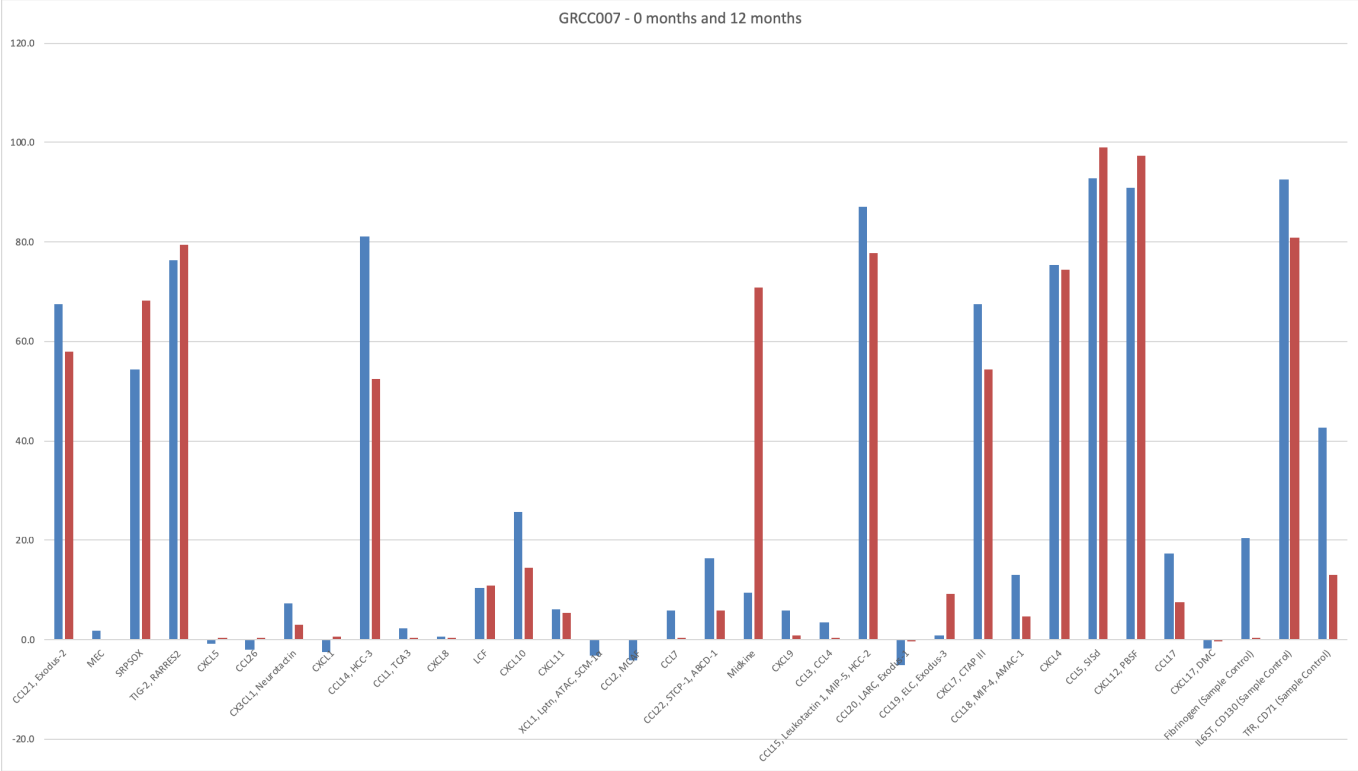
VWR

Appendix IV: Tracking for chemokine array samples





| Sample # | Date Received | Patient | Chemokine Array |
|-----------------|----------------------|----------------|------------------------|
| Sample 1 | 29-Aug-16 | GRCC001 | Completed |
| Sample 2 | 15-Sep-16 | GRCC002 | Completed |
| Sample 3 | 23-Sep-16 | GRCC003 | Completed |
| Sample 4 | 21-Oct-16 | GRCC004 | Completed |
| Sample 5 | 30-Nov-16 | GRCC005 | Completed |
| Sample 6 | 30-Nov-16 | GRCC006 | Completed |
| Sample 7 | 01-Dec-16 | GRCC007 | Completed |
| Sample 8 | 21-Dec-16 | GRCC008 | Completed |
| Sample 9 | 18-Jan-17 | GRCC009 | Completed |
| Sample 10 | 19-Jan-17 | GRCC010 | Completed |
| Sample 11 | 28-Mar-17 | GRCC001 | Completed |
| Sample 12 | 25-Apr-17 | GRCC004 | Completed |
| Sample 13 | 10-May-17 | GRCC011 | Completed |
| Sample 14 | 15-Jun-17 | GRCC005 | Completed |
| Sample 15 | 28-Jun-17 | GRCC007 | Completed |
| Sample 16 | 13-Jul-17 | GRCC009 | Completed |
| Sample 17 | 04-Aug-17 | GRCC012 | Completed |
| Sample 18 | 15-Aug-17 | GRCC001 | |
| Sample 19 | 06-Sep-17 | GRCC013 | Completed |
| Sample 20 | 15-Sep-17 | GRCC014 | Completed |
| Sample 21 | 19-Oct-17 | GRCC015 | Completed |
| Sample 22 | 06-Nov-17 | GRCC011 | Completed |
| Sample 23 | 24-Nov-17 | GRCC004 | Completed |
| Sample 24 | 11-Jan-18 | GRCC016 | Completed |
| Sample 25 | 23-Jan-18 | GRCC007 | Completed |
| Sample 26 | 21-Feb-18 | GRCC009 | Completed |
| Sample 27 | 18-Apr-18 | GRCC017 | Completed |
| Sample 28 | 01-Jun-18 | GRCC018 | Completed |
| Sample 29 | 05-Jul-18 | GRCC019 | Completed |
| Sample 30 | 09-Jul-18 | GRCC020 | Completed |
| Sample 31 | 09-Jul-18 | GRCC021 | Completed |
| Sample 32 | 10-Aug-18 | GRCC016 | Completed |
| Sample 33 | 31-Oct-18 | GRCC017 | Completed |
| Sample 34 | 14-Nov-18 | GRCC023 | |
| Sample 35 | 05-Nov-18 | GRCC022 | |
| Sample 36 | 28-Nov-18 | GRCC024 | Completed |
| Sample 37 | 03-Dec-18 | GRCC025 | |
| Sample 38 | 11-Dec-18 | GRCC026 | |
| Sample 39 | 04-Jan-18 | GRCC019 | Completed |
| Sample 40 | 15-Jan-18 | GRCC021 | |
| Sample 41 | 27-Mar-19 | GRCC020 | Completed |

Appendix V: Raw analysis plots of individual patients at 0 and 12 months





Appendix VI: Copy of the approved ethics protocol confirmations

| | | |
|---|---|---|
|  |  |  |
| <p align="center">TRI-HOSPITAL RESEARCH ETHICS BOARD (THREB)</p> | | |
| <p align="center">(A shared service for Cambridge Memorial Hospital, Grand River Hospital and St. Mary's General Hospital) Grand River Hospital, Rm. 615, Kaufman Building, 835 King Street West, Kitchener, Ontario, N2G 1G3 Tel: (519) 749-4300 ext. 5367 Fax: (519) 749-4250</p> | | |
| <p>Tri-Hospital Research Ethics Board Membership</p> <p>Michael Coughlin, PhD Chair, Tri-Hospital Research Ethics Board</p> <p>Narayan Abhishek, MD CCFP (COE) Medicine</p> <p>Edmond Chouinard, MD Oncologist</p> <p>Sherri Ferguson, CHRL VP, People, Quality & Performance</p> <p>Carla Girolametto, MA, CCRP Director, Research, Innovation and Clinical Trials</p> <p>Sandra Hett, MN, BScN, BaS VP Clinical Programs & Chief Nursing Executive</p> <p>Robert Howe, MBA Performance Management</p> <p>Tina Mah, PKhD, BScOT, MBS, VP Research and Innovation</p> <p>Paul Motz, BSc Community Member</p> <p>Trishana Nayjager, MSc(HRM), CCRA Community Member, Research Methods</p> <p>Amy Stahlke, BA, LLB, Community Member, Law</p> <p>Anthony Wassef, MD, Cardiology</p> <p>The Tri-Hospital Research Ethics Board operates in compliance with the Tri-Council Policy Statement: Ethical Conduct for Research Involving Humans (2010), the ICH Good Clinical Practice Guidelines and Division 5 Health Canada Food and Drug Regulations.</p> | <p>February 6, 2019</p> <p align="right">THREB #2016-0586</p> <p>Dr. Mario Valdes Grand River Hospital 835 King St. W. Kitchener, Ontario, N2G 1 G3</p> <p>Dear Dr Mario Valdes, THREB# 2016-0586 Predicting aggressive behaviours of cancer cells from the general blood circulation. Dr. Mario Valdes MD GRH Co.UW</p> <hr/> <p>Study Identification Number: THREB #2016-0586 Initial Approval Date: March 21, 2016 Anniversary for Renewal: March 21, 2020</p> | |
| | <p>Thank you for your Annual Status Report requesting continuation of the above study for another year.</p> | |
| | <p>The Annual Status Report and request for renewal for the above study was reviewed at a full board meeting of the Tri-Hospital Research Ethics Board on February 6, 2019 and is considered acceptable for a one year continuation. The study will be reviewed prior to the Anniversary for Renewal indicated above by the Tri-Hospital Research Ethics Board.</p> | |
| | <p>Sincerely,</p>  <p>Michael D. Coughlin, Ph.D. Chair, Tri-Hospital Research Ethics Board</p> <p>Cc: Carla Girolametto, Carol Ballantyne</p> | |

From: **Kuali Notifications** no-reply@kuali.co
Subject: **Renewed application # 30755 has ethics clearance**
Date: **February 25, 2019 at 3:19 PM**
To: j3blay@uwaterloo.ca



Dear Jonathan Blay and other members of the research team:

Your application has been reviewed by CREC. We are pleased to inform you the **Renewed application for 30755 Predicting aggressive behaviours of cancer cells from the general blood circulation** has been given ethics clearance.

This research must be conducted in accordance with the most recent version of the application in the research ethics system and the most recent versions of all supporting materials.

Ethics clearance for this study is valid until Sunday, March 22nd 2020.

The research team is responsible for obtaining any additional institutional approvals that might be required to complete this Full Board study.

University of Waterloo Research Ethics Committees operate in compliance with the institution's guidelines for research with human participants, the [Tri-Council Policy Statement for the Ethical Conduct for Research Involving Humans](#) (TCPS, 2nd edition), [Internalization Conference on Harmonization: Good Clinical Practice](#) (ICH-GCP), the [Ontario Personal Health Information Protection Act](#) (PHIPA), and the applicable laws and regulations of the province of Ontario. Both Committees are registered with the [U.S. Department of Health and Human Services](#) under the [Federal Wide Assurance](#), FWA00021410, and IRB registration number IRB00002419 (Human Research Ethics Committee) and IRB00007409 (Clinical Research Ethics Committee).

Renewal: Multi-year research must be renewed at least once every 12 months unless a more frequent review has been specified on the notification of ethics clearance. This is a requirement as outlined in Article 6.14 of the [Tri-Council Policy Statement for the Ethical Conduct for Research Involving Humans](#) (TCPS2, 2014). The annual renewal report/application must receive ethics clearance before Thursday, February 27th 2020. Failure to receive ethics clearance for a study renewal will result in suspension of ethics clearance and the researchers must cease conducting the study. Research Finance will be notified ethics clearance is no longer valid.

Amendment: Changes to this study are to be submitted by initiating the amendment procedure in the research ethics system and may only be implemented once the proposed changes have received ethics clearance.

Adverse event: Events that adversely affect a study participant must be reported as soon as possible, but no later than 24 hours following the event, by contacting the Director, Research Ethics. Submission of an [adverse event form](#) is to follow the next business day.

Deviation: Unanticipated deviations from the approved study protocol or approved documentation or procedures are to be reported within 7 days of the occurrence using a [protocol deviation form](#).

Incidental finding: Anticipated or unanticipated incidental findings are to be reported as soon as possible by contacting the Director, Research Ethics. Submission of the [incidental findings form](#) is to follow within 3 days of learning of the finding. Participants may not be contacted regarding incidental findings until after clearance has been received from a Research Ethics Committee to contact participants to disclose these findings.

Study closure: Report the end of this study by submitting a study closure report through the research ethics system.

Coordinated Reviews: If your application was reviewed in conjunction with Wilfrid Laurier University, Conestoga College, Western University or the Tri-Hospital Research Ethics Board, note the following: 1) Amendments must receive prior ethics clearance through both REBs before the changes are put in place, 2) PI must submit the required annual renewal report to both REBs and failure to complete the necessary annual reporting requirements may result in Research Finance being notified at both institutions, 3) In the event that there is an unanticipated event involving a participant that adversely affects them, the PI must report this to both REBs within 24 hours of the event taking place and any unanticipated or unintentional changes which may impact the research protocol shall be reported within seven days of the deviation to both REBs.

Initial application ethics clearance notification: Your clearance notification will be added to the record within 24 hours. Go to "View Admin Attachments" in the research ethics system (right-hand side) to print a copy of the initial application ethics clearance notification.

Best wishes for success with this study.

If you have any questions concerning this notification, please contact the [Research Ethics Office](#) or email researchethics@uwaterloo.ca.

From: **Kuali Notifications** no-reply@kuali.co 
Subject: **Renewed application # 31549 has ethics clearance**
Date: **January 29, 2019 at 10:16 AM**
To: **j3blay@uwaterloo.ca**



Dear Jonathan Blay and other members of the research team:

Your application has been reviewed by CREC. We are pleased to inform you the **Renewed application for 31549 Normal human blood for control studies relating to human cancer cell research** has been given ethics clearance.

This research must be conducted in accordance with the most recent version of the application in the research ethics system and the most recent versions of all supporting materials.

Ethics clearance for this study is valid until Sunday, February 16th 2020.

The research team is responsible for obtaining any additional institutional approvals that might be required to complete this Full Board study.

University of Waterloo Research Ethics Committees operate in compliance with the institution's guidelines for research with human participants, the [Tri-Council Policy Statement for the Ethical Conduct for Research Involving Humans](#) (TCPS, 2nd edition), [Internalization Conference on Harmonization: Good Clinical Practice](#) (ICH-GCP), the [Ontario Personal Health Information Protection Act](#) (PHIPA), and the applicable laws and regulations of the province of Ontario. Both Committees are registered with the [U.S. Department of Health and Human Services](#) under the [Federal Wide Assurance](#), FWA00021410, and IRB registration number IRB00002419 (Human Research Ethics Committee) and IRB00007409 (Clinical Research Ethics Committee).

Renewal: Multi-year research must be renewed at least once every 12 months unless a more frequent review has been specified on the notification of ethics clearance. This is a requirement as outlined in Article 6.14 of the [Tri-Council Policy Statement for the Ethical Conduct for Research Involving Humans](#) (TCPS2, 2014). The annual renewal report/application must receive ethics clearance before Saturday, January 25th 2020. Failure to receive ethics clearance for a study renewal will result in suspension of ethics clearance and the researchers must cease conducting the study. Research Finance will be notified ethics clearance is no longer valid.

Amendment: Changes to this study are to be submitted by initiating the amendment procedure in the research ethics system and may only be implemented once the proposed changes have received ethics clearance.

Adverse event: Events that adversely affect a study participant must be reported as soon as possible, but no later than 24 hours following the event, by contacting the Director, Research Ethics. Submission of an [adverse event form](#) is to follow the next business day.

Deviation: Unanticipated deviations from the approved study protocol or approved documentation or procedures are to be reported within 7 days of the occurrence using a [protocol deviation form](#).

Incidental finding: Anticipated or unanticipated incidental findings are to be reported as soon as possible by contacting the Director, Research Ethics. Submission of the [incidental findings form](#) is to follow within 3 days of learning of the finding. Participants may not be contacted regarding incidental findings until after clearance has been received from a Research Ethics Committee to contact participants to disclose these findings.

Study closure: Report the end of this study by submitting a study closure report through the research ethics system.

Coordinated Reviews: If your application was reviewed in conjunction with Wilfrid Laurier University, Conestoga College, Western University or the Tri-Hospital Research Ethics Board, note the following: 1) Amendments must receive prior ethics clearance through both REBs before the changes are put in place, 2) PI must submit the required annual renewal report to both REBs and failure to complete the necessary annual reporting requirements may result in Research Finance being notified at both institutions, 3) In the event that there is an unanticipated event involving a participant that adversely affects them, the PI must report this to both REBs within 24 hours of the event taking place and any unanticipated or unintentional changes which may impact the research protocol shall be reported within seven days of the deviation to both REBs.

Initial application ethics clearance notification: Your clearance notification will be added to the record within 24 hours. Go to "View Admin Attachments" in the research ethics system (right-hand side) to print a copy of the initial application ethics clearance notification.

Best wishes for success with this study.

If you have any questions concerning this notification, please contact the [Research Ethics Office](#) or email researchethics@uwaterloo.ca.
